DEVELOPMENT OF A TSUNAMI FORECAST MODEL FOR ATLANTIC CITY, NEW JERSEY (DRAFT)

Yong Wei

June, 2011

Abstract

As part of NOAA's tsunami forecast, this study addresses the development, validation, and stability tests of the tsunami forecast model for Atlantic City, New Jersey. Based on the Method of Splitting Tsunami (MOST), the tsunami forecast model is constructed at a spatial resolution of 2 arcsec, in the finest grid, to accomplish 4-hour simulation of wave inundation onto dry land within 12 minutes of CPU time. A reference inundation model is developed in parallel using grids of higher resolution up to eight meters to provide modeling references for the forecast model. The present study also conducted sensitivity tests to optimize grid coverage and grid resolution by comparing results between the forecast model and the reference model. Due to lack of historical tsunami data, the Atlantic City forecast model was carefully evaluated using the 1755 Lisbon earthquake. The model validations show excellent agreement between the forecast model and reference model, meaning the forecast model is qualified to provide quantitative estimation of the inundation, runup and computed maximum values for potential threats of future tsunamis. The stability of the forecast model is further evaluated based on eight synthetic scenarios generated in Puerto Rico Trench, Hispaniola Trench, Cayman Trough, Los Muertos Trough and South Sandwich Island at different levels of M_w 9.3, M_w 7.5 and M_w 6.4.

1. Background and Objectives

The National Oceanic and Atmospheric Administration (NOAA) Center for Tsunami, Research (NCTR) at the NOAA Pacific Marine Environmental Laboratory (PMEL) has developed a tsunami forecasting capability for operational use by NOAA's two Tsunami Warning Centers located in Hawaii and Alaska (Titov *et al.*, 2005a). The system is designed to efficiently provide basin-wide warning of approaching tsunami waves accurately and quickly. The system, termed Short-term Inundation Forecast of Tsunamis (SIFT), combines real-time tsunami event data with numerical models to produce estimates of tsunami wave arrival times and amplitudes at a coastal community of interest. The SIFT system integrates several key components: deep-ocean observations of tsunamis in real time, a basin-wide pre-computed propagation database of water level and flow velocities based on potential seismic unit sources, an inversion algorithm to refine the tsunami source based on deep-ocean observations during an event, and high-resolution tsunami forecast models.

Located at the oceanfront of New Jersey, Atlantic City's major attractions are featured with tourism and casino resorts (Figure 1). Aside from 40,000 residents, Atlantic City attracts nearly three million visitors every year, and most visitors are residing in the oceanfront hotels throughout their visits. Although the threat is rare compared to the US

West Coast, a tsunami that developed hundreds of miles at sea or an ocean away could have potential impact on the shores of Atlantic City. However, the potential tsunami impact on the coast of Atlantic City is significantly understudied, probably due to uncommon tsunami activities in the Atlantic and lack of historical tsunami data. Atlantic City has experienced tsunami induced water level increase during the 2004 Indian Ocean tsunami that was generated thousands of miles away. A similar earthquake from any seismically active region in the Atlantic, even though the possibility is believed to be low, will pose catastrophic hazards to Atlantic City. The landslide sources along the U.S. Atlantic margin may cause even more severe damage to Atlantic City since these sources are usually much closer to the coastline and give much less time to prepare. Most of the populated areas of Atlantic City are located on Absecon Island, and as is common of such barrier islands, is connected inland by bridges and highways, which will slow the evacuation during a tsunami event due to congested traffic through these narrow exits. It is therefore vital to prepare a populated area like Atlantic City for short- and long-term tsunami hazard assessment.

The objective of this present work is to develop an operational forecast model to be used in near real time to protect the community of Atlantic, New Jersey, from the potential impact posed by a tsunami if generated. Titov et al. (2009) employed high-resolution tsunami inundation forecast models to assess the potential tsunami hazards for coastal communities on the U.S. Atlantic coast due to distant earthquake- and landslide-generated tsunamis in the Atlantic.. The development of Atlantic City tsunami forecast model and high-resolution inundation model is a valuable supplement to this assessment, and more importantly another essential contribution to the existing NOAA's tsunami forecasting system in the Atlantic.

2. Forecast Methodology

A high-resolution inundation model was used as the basis for development of a tsunami forecast model to operationally provide an estimate of wave arrival time, wave height, and inundation at Atlantic City, New Jersey following tsunami generation. All tsunami forecast models are run in real time while a tsunami is propagating across the open ocean. The Atlantic City model was designed and tested to perform under stringent time constraints given that time is generally the single limiting factor in saving lives and property. The goal of this work is to maximize the length of time that the community of Atlantic City has to react to a tsunami threat by providing accurate information quickly to emergency managers and other officials responsible for the community and infrastructure.

The general tsunami forecast model, based on the Method of Splitting Tsunami (MOST), is used in the tsunami inundation and forecasting system to provide real-time tsunami forecasts at selected coastal communities. The model runs in minutes while employing high-resolution grids constructed by the National Geophysical Data Center. MOST is a suite of numerical simulation codes capable of simulating three processes of tsunami evolution: earthquake, transoceanic propagation, and inundation of dry land. The MOST model has been extensively tested against a number of laboratory experiments and

benchmarks (Synolakis *et al.*, 2008) and was successfully used for simulations of many historical tsunami events. The main objective of a forecast model is to provide an accurate, yet rapid, estimate of wave arrival time, wave height, and inundation in the minutes following a tsunami event. Titov and González (1997) describe the technical aspects of forecast model development, stability, testing, and robustness, and Tang *et al*. (2009) provide detailed forecast methodology.

A basin-wide database of pre-computed water elevations and flow velocities for unit sources covering worldwide subduction zones has been generated to expedite forecasts (Gica *et al.*, 2008). As the tsunami wave propagates across the ocean and successively reaches tsunameter observation sites, recorded sea level is ingested into the tsunami forecast application in near real-time and incorporated into an inversion algorithm to produce an improved estimate of the tsunami source. A linear combination of the pre-computed database is then performed based on this tsunami source, now reflecting the transfer of energy to the fluid body, to produce synthetic boundary conditions of water elevation and flow velocities to initiate the forecast model computation.

Accurate forecasting of the tsunami impact on a coastal community largely relies on the accuracies of bathymetry and topography and the numerical computation. The high spatial and temporal grid resolution necessary for modeling accuracy poses a challenge in the run-time requirement for real-time forecasts. Each forecast model consists of three telescoped grids with increasing spatial resolution in the finest grid, and temporal resolution for simulation of wave inundation onto dry land. The forecast model utilizes the most recent bathymetry and topography available to reproduce the correct wave dynamics during the inundation computation. Forecast models, including the Atlantic City model, are constructed for at-risk populous coastal communities in the Pacific and Atlantic Oceans. Previous and present development of forecast models in the Pacific (Titov *et al*., 2005; Titov, 2009; Tang *et al*., 2008; Wei *et al*., 2008) have validated the accuracy and efficiency of each forecast model currently implemented in the real-time tsunami forecast system. Models are tested when the opportunity arises and are used for scientific research. Tang *et al*. (2009) provide forecast methodology details.

3. Model development

The general methodology for modeling at-risk coastal communities is to develop a set of three nested grids, referred to as A, B, and C-grids, each of which becomes successively finer in resolution as they telescope into the population and economic center of the community of interest. The offshore area is covered by the largest and lowest resolution A-grid while the near-shore details are resolved within the finest scale C-grid to the point that tide gauge observations recorded during historical tsunamis are resolved within expected accuracy limits. The procedure is to begin development with large spatial extent merged bathymetric topographic grids at high resolution, and then optimize these grids by sub sampling to coarsen the resolution and shrink the overall grid dimensions to achieve a 4 to 10 hr simulation of modeled tsunami waves within the required time period of 10 min of wall-clock time. The basis for these grids is a high-resolution digital elevation model constructed by the National Geophysical Data Center and NCTR using all available bathymetric, topographic, and shoreline data to reproduce the wave dynamics during the inundation computation for an at-risk community. For each

community, data are compiled from a variety of sources to produce a digital elevation model referenced to Mean High Water in the vertical and to the World Geodetic System 1984 in the horizontal (http://ngdc.noaa.gov/mgg/inundation/tsunami/inundation.html). From these digital elevation models, a set of three high-resolution, "reference" elevation grids are constructed for development of a high-resolution reference model from which an 'optimized' model is constructed to run in an operationally specified period of time. The operationally developed model is referred to as the optimized tsunami forecast model or forecast model for brevity.

3.1 Forecast area

Atlantic City is a coastal city in the south New Jersey with its economy mostly relying on gambling, conventions and leisure. Atlantic City today has a year-round population of 40,517, and is within easy driving distance of a third of the population of the United States. Being the capital city of gambling and amusement in the northeast of U.S., Atlantic City is an attraction of real estate and a potential resort town for developers. However, the entire city was built on low land, less than 3 m above sea level, between barrier islands and marshlands, and it makes the city particularly vulnerable to potential tsunami generated in the Atlantic.

Barrier islands are dynamic landforms, subject to storm-surge flooding and sand transport processes. These coastal features are particularly vulnerable areas for human habitation, since they extend seaward of the mainland and are composed entirely of loose sediment (Leatherman, 1982). The oceanfront of Absecon Island has historically been one of the hardest hit of all the New Jersey barrier islands during the coastal storms (http://www.nap.usace.army.mil/cenap-dp/projects/absecon/absecon.htm). It is well known that barrier islands in Atlantic experience serious beach erosion problems in the storm season. Along Absecon Island, the predominant transport of sand by waves is to the southwest. Beach nourishment has needed to be done periodically to the beach in Atlantic City, over the past half-century in order to stabilize the shoreline location at Ventnor, Margate, and Longport. These beachfills have moved the shoreline seaward more than a street block since 1899 (Figure 2). Atlantic City has had several large beachfills to maintain a beach along its northern end, and has had a series of groins installed to help stabilize the shoreline. The dynamic shoreline may make Atlantic City more vulnerable to tsunami impact as the wave shoaling will occur in a shorter distance and the wave height can grow more dramatically when the waves hit the shoreline. The communities of Ventnor and Margate have low-elevation beaches that are prone to oceanside flooding despite the presence of bulkheads. At Longport, shore protection is provided by concrete seawall and timber bulkhead, and the latter has had failures in the past that resulted in significant property damage during coastal storms.

The NOS Atlantic City tide station is located on a steel pier (Taj Mahal Pier) at the waterfront of Atlantic City without any harbor sheltering (**Figure 3**), so the measurements at this tide station are a direct indication of wave impact on the shoreline. The water depth at the tide gage location is about 5 m (Mean High Water). This National Ocean Service (NOS) station was established on 5 June 1978, and upgraded to its present installation on 17 November 1997. The local mean tide range is about 0.65 m, and the diurnal range is 0.76 m. Like many coastlines in Atlantic, Atlantic City, with over 90

years of tide records, shows increasing sea level change, and the 4 mm/yr rate gives rise to a 0.4 m increase in 100 years.

3.2 Historical events and data

National Geophysical Data Center (NGDC)'s tsunami runup database (http://www.ngdc.noaa.gov/hazard/tsu.shtml) shows that there have been a number of historical tsunamis affecting the coasts of Virginia, Maryland, Delaware, New Jersey and New York (**Figure 4** and **Table 1**). Four of them were measured by the Atlantic City tide station.

The 1929 Grand Banks tsunami is notable for a number of reasons: this event is Canada's most tragic earthquake (M_w 7.2) with 28 lives lost (Ruffman, 1996); it was one of the very few catastrophic tsunamis, up to 27 m tsunami runup, to occur in the Atlantic; and it was one of the very few transoceanic tsunamis generated by a landslide (Pasad et al., 2009). Natural Resources Canada (2006) reported that "the earthquake triggered a large submarine slump (an estimated volume of 200 cubic kilometers of material was moved on the Laurentian slope), which ruptured 12 transatlantic cables in multiple places, and generated a tsunami. The tsunami was recorded along the eastern seaboard as far south as South Carolina and across the Atlantic Ocean in Portugal." Lockridge et al. (2002) reported that the Atlantic City tide gage recorded a change of approximately 0.68 m. Tide gage records showed that it was also recorded at Ocean City, Maryland and Charleston, South Carolina.

Tsunami waves, that have affected the coasts from Virginia to New York, have complex triggering mechanisms including earthquake, landslide or meteorological events (**Table 1**). In some of these cases, shortly after the local earthquakes occurred, unusual tsunami-like waves were reported in the coasts within 200-kilometers of the earthquake location. Such earthquakes are the 1817 Philadelphia, 1840 Philadelphia, 1871 New York, 1884 New York, and 1895 New Jersey. Some of the distant tsunamis that have impacted the Virginia-New York coast were triggered by earthquakes in Puerto Rico Trench or Hispaniola Trench in northeast of Caribbean, such as the 1973 Mona Passage, 4 August 1946 Dominican Republic, and 8 August 1946 Dominican Republic. Except for the 1929 Grand Banks, the trans-Atlantic tsunami that may have had an impact on Atlantic City is the 1755 Lisbon tsunami due to an M_w 8.5 – 9.0 earthquake (Barkan et al., 2009; Roger et al., 2009; Muir-Wood and Mignan, 2009). Runup reports from the 1755 Lisbon tsunami were documented in the Caribbean, Brazil and Newfoundland (Canada), and no reports were documented along the U.S. East Coast (Barkan et al., 2009). A model simulation of the Lisbon tsunami (see section 4.1 of this report) showed that the computed maximum wave amplitudes are about 2 m along the Atlantic City's shoreline and about 1.9 m at the tide gage. The global reach of the catastrophic 26 December 2004 Indian tsunami was also recorded on the U.S. East Coast, 0.11 m at Atlantic City, NJ and 0.06 m at Cape May, NJ (Titov et al., 2005). It is worth noting that large tsunamis can propagate substantial and damaging wave energy to distant coasts, even different oceans, through a combination of source focusing and topographic waveguides. Local resonant effects may also amplify the arriving waves (Titov et al., 2005).

ten Brink et al. (2008) evaluated the tsunami sources with the potential to impact the U.S. Atlantic and Gulf Coasts. Their report indicated that earthquake sources located west of Gibraltar and in Puerto Rick Trench are capable of generating trans-oceanic tsunamis. A large tsunamigenic earthquake taking place in the Puerto Rico trench may be destructive to many parts of the U.S. East Coast, although the ability of this plate boundary to generate earthquakes is still in debate. ten Brink et al. (2008) also speculated that landslides along the U.S. Atlantic margin have the potential to cause tsunami locally. For instance, the Currituck Slide, 300 km southeast of Atlantic City, is one of the major mass movements on the Atlantic continental margin over the last 100,000 years (Prior et al., 1986) and could have caused a damaging tsunami to the East Coast of United States. The landslide modeling results of Geist et al. (2009) showed that the failure of Currituck landslide could trigger tsunami waves of 3 m amplitude on the shelf offshore of Ocean City, Maryland.

Other than earthquake-generated tsunamis, tsunami-like waves were also recorded at tide gages on the U.S. East Coast with unclear generation mechanism. Some of them were associated with passing hurricanes or meteorological pressure changes. For instances, tsunami-like waves were observed in Virginia when a category 4 hurricane moved over on 3 September 1821. When "heavy tides" up to 3 m were observed in Atlantic City on 10 June of 1913, no one could link them to neither storms nor earthquakes (Lockridge et al., 2002). These types of waves were frequently seen on the coast of New Jersey and New York in 1923, 1924, 1931, 1932, 1938, 1944, and 1964. Some of them were attributed to either submarine landslides or abnormal weather events.

3.3 Model setup

3.3.1 Grid boundary and resolution

The wide continental shelf on the U.S. East Coast complicates the tsunami waves approaching the shoreline. When a tsunami reaches continental shelf and begins to shoal, it will slow down and increase in height while introducing model diffusion and dispersion. Burwell et al. (2007) studied the diffusion and dispersion characterization of MOST model, and concluded that the nature of the scheme at all resolvable wave numbers, in particular, that the scheme is diffusive and dispersive for $\beta = (gd)^{1/2}\Delta t/\Delta x \neq 1$, where Δt is the temporal step and Δx is the space step. Diffusive effects are stronger for poorly resolved waves (large space step compared to wave length), while diffusive effects go down but dispersive effects continue to increase as β reduces. Thus, numerical dispersion can be an issue closer to shore, but can be controlled to some level over the choice of β, in other words, the ratio between Δt and Δx. The tsunami propagation database (Gica et al., 2008) was developed at a grid spacing of 4-arc-minute (about 7.2 km at the equator) and saved at 16-arc-minute (about 28.8 km at the equator) resolution. This resolution may introduce enormous model diffusion effects if applied directly to the continental shelf where water depth is generally less than 100 m. The telescoped grids adopted in MOST model are thus critical for wave transformation over the continental shelf, and eventually critical for the inundation modeling at the coastline. Ideally, manipulation of β value will reduce the effects of diffusion and mimic the real-world dispersion through numerical dispersion.

3.3.2 Digital Elevation Model of Atlantic City, New Jersey

The bathymetry and topography used in the development of this forecast model was based on a digital elevation model provided by the National Geophysical Data Center and the author considers it to be an adequate representation of the local topography/bathymetry. As new digital elevation models become available, forecast models will be updated and report updates will be posted at http://nctr.pmel.noaa.gov/forecast_reports/.

Taylor et al. (2007) at the National Geophysical Data Center (NGDC) developed a 1/3-arc-sec (~ 8 m at latitude 39.35 degree) digital elevation model of Atlantic City, New Jersey. The bathymetry was developed base on the hydrographic survey data from NGDC's NOS Hydrographic Survey Database, US Army Corps of Engineers (USACE) hydrographic surveys, NOS shallow water multibeam survey, Office of Coast Survey electronic navigational chart extracted soundings, and digital intracoastal waterway. The topography in NGDC's DEM was based on USGS 1/3 arcsec NED DEM and the Coastal Service Center (CSC) LiDAR survey data. The CSC bathymetric-topographic LiDAR dataset CSC) provided full coverage of the entire length of the Atlantic Ocean shoreline.

Taylor et al. (2007) provided a detailed description of how these datasets were implemented in the DEM development for Atlantic City. They also speculated that the CSC bathymetric and topographic LiDAR data was not processed to bare earth. The hydrographic and LiDAR surveys for nearshore areas especially in bays, estuaries and coastal marshes need to be completed in order to further improve the Atlantic City DEM.

3.3.3 Development of model grids

Development of an optimized tsunami forecast model for Atlantic City began with the spatial extent merged bathymetric/topographic grids shown in **Figure 5 to 9**. Grid dimension extension and additional information were updated as needed and appropriate. A significant portion of the modeled tsunami waves, typically 4 to 10 hr of modeled tsunami time, pass through the model domain without appreciable signal degradation. **Table 2** provides specific details of both reference and tsunami forecast model grids, including extents and complete input parameter information for the model runs is provided in **Appendix 1**.

Figure 5 shows the coverage of A grid with a space resolution of 30 arc seconds (~ 715 m at latitude 39.5 degree), which was employed by both the optimized tsunami forecast model and the reference model. This grid is obtained from the General Bathymetric Chart of Oceans (GEBCO) 30-sec global database. For the reasons that were laid out in section 3.3.1, the eastern boundary of A grid is specified at 71°W, where the water depth ranges from 1,000 m to more than 4,000 m. It's recommended that the ocean boundary of A grid be placed at a water depth greater than 1,500 m to allow a smooth transition from the 4 arcmin tsunami propagation database where the waves are assumed to be linear. One can see the abrupt depth change, from 2,000 m to less then 100 m, along the continental slope. The continental shelf extends more than 100 km offshore off the coastline, typically with water depth of less than 100 m and 60% of the shelf is even shallower than

50 m. This grid covers almost the entire coastline of New Jersey between Delaware Bay to the south and Lower Bay to the north.

Figure 6 and **Figure 7** show the bathymetry and topography of B grid for the optimized forecast model and the reference model. The two grids have the same model extent (Table 2) with different grid resolutions, 6 arc second (~ 140 m at latitude 39.5 degree) for the forecast model and 3 arc second (~ 72 m at latitude 39.5 degree) for the reference model. Both grids were obtained from the Atlantic City 1/3-arc-sec DEM developed by NGDC (Taylor et al., 2007). The eastern boundary of the B grid is located about 40 km offshore of Atlantic City coastline with a maximum water depth of 40 m. Atlantic City is placed at the center of B grid to minimize the numerical errors introduced by the connecting boundary between grids A and B. The long and slim barrier islands in the south and central part of New Jersey coastlines are covered by B grid. The high grid resolution clearly shows the sand ripples offshore, caused by the long-term longshore sediment transport, which may be important bathymetric features affecting tsunami propagation on the shelf.

To satisfy the model computing time requirement, the C grid of the optimized forecast model was developed at a 2-arcsec grid resolution (~ 48 m at latitude 39.5 degree, **Figure 8**), while a 1/3-arc-sec (~ 8 m at latitude 39.5 degree) resolution was used in the reference model covering the same area (**Figure 9**). In order to provide model forecast for populated areas, the Atlantic City C grid covers the entire coastline of Atlantic County, New Jersey, including the most populated area in Atlantic City and four other coastal cities (Longport, Margate, Ventnor and Brigantine). Both grids were built from the Atlantic City 1/3-arc-sec DEM developed by NGDC (Taylor et al., 2007) with the maximum water depth of 15 m located at the southeastern boundary. As the CSC LiDAR dataset was not processed to bald earth, a stripe of dense building structures can be clearly identified, especially in the reference model grid. The forecast model C grid has been processed to widen the harbor entrance and the marina to avoid the forming enclosed water bodies due to the 2-arcsec grid resolution.

4. Results and Discussion

4.1 Model validation

Lack of tsunami measurements in the Atlantic has been a major issue of model validation for the tsunami forecast models developed for U.S. East Coast and Caribbean. An alternative approach is the model-to-model comparison between different models. Unfortunately, other than this study, tsunami modeling for Atlantic City has not been available from any tsunami modeling or research group. Another crude validation is to test the model with a historical case, for which the tsunami impact is well known at the modeling site or its vicinity, and consider the model is validated if this model gives no "surprising" results. The 1755 Lisbon tsunami is a representative case for such a model validation for Atlantic City.

The earthquake source of the 1755 Lisbon tsunami has not been fully understood. Previous studies have proposed a few source mechanisms that may have potentially produced this basin-wide tsunami. The magnitude of the proposed earthquake ranges

from 8.0 to 9.0 (Barkan et al., 2009; Muir-Wood and Mignan, 2009; Titov et al., 2009; Roger et al., 2009), while the rupture area varies between 6,000 km^2 and 480,000 km^2. Titov et al. (2009) has compared five tsunami scenarios due to different earthquake sources and they all indicated that the tsunami impact on U.S. East Coast was minor, as a tsunami not reported or documented anywhere in United States. The preferred scenario of Barkan et al. (2009) reported very similar result after comparing the tsunami records at many places in the Atlantic, particularly in the Caribbean (**Figure 10**).

This report uses the 1755 Lisbon tsunami as a "validation" case study, for which we adopted earthquake rupture parameters from Barkan et al. (2009), and an earthquake magnitude 9.0 from Muir-Wood and Mignan (2009). This scenario represents a "worst case" scenario of the 1755 Lisbon tsunami, which can explain the tsunami runup heights and overwash observed in the British Virgin Islands and Lesser Antilles (Wei et al., 2011). **Figure 11** shows the computed time series at the tide gage location of Atlantic City. One can see that the maximum wave amplitude is about 1.9 m, and the maximum wave height is about 2.9 m. Such a tsunami wave, having a 15- to 20-minute wave period may have produced noticeable coastal impact in Atlantic City. The models indicate minor tsunami inundation at the waterfront of Atlantic City and Ventnor City (**Figure 12**). The computational results show high-speed current up to 4 m/s (about 8 knots) along the coastline where tsunami flooding occurs. The tsunami-induced current in the Absecon Inlet is about 1.5 m/s (about 3 knots) in the middle of the inlet, and 3.0 m/s (about 6 knots) on the east bank of the inlet. **Figure 12** also shows high waves and fast currents in the inlet and marinas connecting the open ocean, with energy decay after the tsunami passed through the narrow channels, and entered the marshy area behind the barrier islands.

The results from the forecast model and the reference model show high analogy in wave amplitude, wave period, arrival time, and current speed. The computed time series at the tide gage (**Figure 11**) are almost identical, which further confirms the forecast model developed at 2 arcsec is able to achieve the same computational accuracy as the reference model, but can save computational resources by 50 times. This makes the forecast model a very powerful tool to provide rapid and accurate tsunami forecast in real time.

4.2 Model stability testing using synthetic scenarios

Model stability testing using synthetic scenarios provides important case studies to test the robustness, durability, and efficiency of the developed models from different perspectives:

1. Synthetic scenarios examine the developed models with mega tsunamis to guarantee model stability. These model tests ensure the efficiency of the forecast model during a catastrophic event.

2. Synthetic scenarios also examine the developed models with medium tsunamis to guarantee model stability under smaller wave conditions. These model tests ensure the efficiency of the forecast model during a moderate event.

3. Synthetic scenarios examine the developed models with negligible tsunami waves to guarantee the modeling results are not interfered by the numerical noises.

4. The synthetic scenarios were selected in such way that at least one from each potential tsunami source zone is tested. These cases are used to examine the reliability of the developed models in response to the directionality of tsunami waves.

Table 3 summarized all the synthetic scenarios (plotted in **Figure 13**) used in the present model testing. Except for the 1755 Lisbon (used as a model validation in section 4.1), other scenarios were artificially constructed from the combination of the unit sources, shown as black boxes. Table 3 gives the details of unit source and the coefficients for a total of eight scenarios, six with magnitude 9.3, one with magnitude 7.5 and one no-wave. Five of the magnitude-9.3 cases were selected in the Puerto Rico Trench and Hispaniola Trench since they are considered as the most dangerous tsunamigenic earthquake zones in the Atlantic (ten Brink et al., 2007). The earthquake zones between the Caribbean plate and South America have been relatively inactive, and the tsunami waves generated there have minor impacts on the U.S. East Coast based on the tsunami hazard assessment study by Titov et al. (2009, Chapter 2). Therefore, no synthetic scenarios were selected from this area. The magnitude-9.3 scenario from South Sandwich source zone was used for modeling stability test in response to different tsunami directionalities.

The synthetic scenario ATSZ 48-57, generated by a 2004-Indian-Ocean-type M_w 9.3 earthquake from Puerto Rico Trench, causes catastrophic impact to Atlantic City and its vicinity. The modeling results in **Figure 14** show that such an event, if arriving at high tide, will wipe out most of the waterfront on Absecon Island, Ventor, Margate and Longport, by waves up to 6.8 m high. The flooding water will penetrate inland up to 2 km from the shoreline with strong current, speeds up to 7 m/s (about 14 knots), between the fourth and fifth hours after the tsunami generation. Similarly, severe flooding will also occur on the 9-km-long Brigantine Island. The waves entering the Absecon Inlet will reach 4 to 5 m above mean high water, which results in flooding on the west and east banks of the inlet. Located on the west bank of the Absecon Inlet, the harbor of Atlantic City will have waves up to 2 m in the basin, along with up to 5 m/s currents in the harbor channels. These wave conditions and currents are very hazardous to harbor facilities and boats resting in the harbor, and they should be taken into serious account when planning local emergency management plans for harbor evacuation during a tsunami event. The time series in **Figure 15** indicates a dominant first wave up to 5 m above mean high water at the tide gage followed by a series of smaller waves with a maximum trough of 3 ms. The time series computed by the reference model and forecast model are nearly identical, which again reflects the high accuracy of forecast model under extreme wave conditions. The 24-hour run of forecast model shows no instability, meaning the model will stay stable under large waves.

The only difference between the forecast model and reference model probably lies in the water elevation and flow velocities over the barrier islands when the tsunami flooding occurs – forecast model shows relatively smaller values than those in reference model. This is attributed to different grid resolution implemented in the two models, where the

reference model at 1/3 arcsec can describe the ocean-front building structures better than forecast model at 2 arcsec. These fine features are mostly smoothed into coarser details in the forecast model, and therefore create a smoother land elevation in the forecast model. It is worth noting that this difference does not affect the inundation limit computed by the two models, and the flooding areas are almost the same in both.

However, the same magnitude, from the synthetic scenario ATSZ 38-47, causes minor flooding on the coastline of Atlantic City with maximum wave amplitude of up to 3 m. Similar to scenario ATSZ 48-57, the highest water elevation occurs along at the water front, and the shoreline of Atlantic City showed minor flooding. Flooding also occurs at the Atlantic City harbor, where the water is pushed into the harbor through the narrow entrance channel at current speeds of up to 4 m/s. The tsunami waves enter the Absecon Inlet with wave amplitude up to 2 m. The current speed is about 2.5 m/s (about 5 knots) on the west of channel, but is up to 4 m/s (8 knots) on the east of the channel (**Figure 16**). Both models show an excellent agreement at the tide gage location (**Figure 17**) with a maximum wave amplitude of 2.5 m (4 m in wave height).

With similar fault orientation and location, the synthetic scenarios ATSZ 58-67 and ATSZ 82-91 give analogous computational results at Atlantic City. Both scenarios showed no inundation on Absecon Island and Brigantine Island. The color pattern in **Figure 18** and **Figure 20** show that, in both scenarios, waves are up to 1.3 m in amplitude with current flow of up to 0.5 m/s along the Atlantic City coastline. The narrow opening at the inlet entrance sped up the flow to about 1 m/s (about 2 knots), which then reaches 2 m/s (about 4 knots) in the harbor channel. This flow speed is still considered to be hazardous to the facilities and boats in the harbor.

A notable feature of the time series at the tide gage, in both scenarios (**Figure 19** and **Figure 21**), is the leading depression N-waves (Tadepalli and Synolakis, 1994), which was propagating from the tsunami source. Different than the Puerto Rico Trench and the Hispaniola Trench, where the North America plate is subducting southwesterly beneath the Caribbean plate, the geological setting at ATSZ 58-67 and ATSZ 82-91 is featured with submarine troughs – Cayman Trough at ATSZ 58-67 and Los Muertos Trough at ATSZ 82-91. Cayman Trough is a complex transform fault zone bounded by strike-slip faults, while Los Muertos trough is an indication of northerly dipping Caribbean Plate and associated seismic zones, in contrast to the south-dipping Puerto Rico – Lesser Antilles subduction zone (LaForge and McCann, 2005). The northerly dipping of the Los Muertos Trough results in an uplift at its southern extent but a subsidence at the north that corresponds to the leading depression when the tsunami waves propagate. ATSZ 58-67 in the Cayman Trough disturbs the water surface in a similar, but more conservative, way by simulating these faults using a subducting mechanism rather than a strike-slip mechanism.

The synthetic scenario of ATSZ 68-77 is a special case that highlights two important characteristics of tsunami waves: wave period and late waves. The computed time series at the Atlantic City tide gage shows that the wave period of the ATSZ 68-77 scenario, about one and half hours to two hours, is unusually long. The wave amplitude did not

reach its maximum until almost 21 hours after the tsunami was generated, while the first wave arrived about at six hours. When comparing the modeling results between the forecast model and the reference model for the first nine hours, one sees an excellent agreement in computed wave amplitude, flow speed, and time series at the tide gage (**Figure 22** and **Figure 23**. The synthetic scenario of ATSZ 68-77 stresses the need of retaining the tsunami warning or watch for more than 24 hours for the coasts of Atlantic City during a real tsunami event.

Excellent agreement was also found between the forecast model and reference model for the synthetic scenario of SSSZ 1-10 (**Figure 24** and **Figure 25**) that represents a Mw 9.3 earthquake-generated tsunami waves from South Sandwich source zone. The model results show that maximal water elevation of 1.2 m is along the coastline while the flow speed in the inlet is about 1 m/s (2 knots), and up to 3 m/s (6 knots) in the Atlantic City harbor. The maximum wave amplitude at the tide gage is about 70 cm with limited impact to the coastline. Similar to ATSZ 68-77, the largest wave arrives about five hours later than the first wave probably due to reflected waves from Africa.

The synthetic scenario of magnitude 7.5, ATSZ b52, introduces up to 0.15 m wave amplitude along the shoreline of Atlantic City, and 0.12 m at the tide gage. Both the forecast model and reference model show good model consistency and stability in terms of maximum wave amplitudes, flow speed (**Figure 26**) and the time series at the tide gage (**Figure 27**). The micro scenario ATSZ b11 is very useful in testing the model stability under the conditions of negligible wave. From the computed maximum wave amplitude (Figure 27), one can see that the water elevation at the oceanfront is only on the order of 10^{-4} m, and the computed time series from both models have excellent match. The two models show small difference mostly in the marshy area and narrow marinas, where the reference model describes many more local bathymetric and topographic features that result in more wave dynamics, which, on the other hand, may also introduce some numerical abnormality to the model. This issue is being further investigated.

5. Summary and conclusions

Atlantic City, New Jersey is a coastal community built on barrier islands in the Atlantic. A popular tourist attraction, attracting tourists from all over the world, Atlantic City is also known of its vulnerability to potential coastal hazards such as beach erosion, sea level change, storm surge and tsunamis. These pose challenging, yet long-standing, questions for the coastal communities on how to protect their lives and properties. Previous studies show that Atlantic City has developed methodologies and procedures to protect their coastline from beach erosion, sea level change, and storm surge. Tsunami forecast and hazard assessment in Atlantic City, however, remains significantly understudied, probably due to the minor impact and infrequent occurrence of tsunamis in Atlantic City's history, as well as in the Atlantic.

A tsunami forecast model is presently developed for the community of Atlantic City, New Jersey. The developed model is being implemented into NOAA's Short-term Inundation Forecast of Tsunamis (SIFT) to provide real-time modeling forecasts of tsunami wave characteristics, runup and inundation along Atlantic City's coastline. Discussion of the details of each individual components of the forecast model, including

the bathymetry and topography, the basic model setup, and the model parameters are provided in the report. The forecast model employs grids as fine as 48 m and can accomplish a four-hour simulation, after tsunami arrival, in 12 minutes of computer CPU time. In parallel, a reference model was developed, using grids as fine as 8 m, to provide reference results basis for performance evaluation of the forecast model.

Due to lack of historical tsunami records, the 1755 Lisbon tsunami is used as a model validation case to show the Atlantic City models did not produce "surprising" results. Based on Barkan et al. (2009) and Miur-Wood and Mignan (2009) sources of the 1755 tsunami, the modeling results showed a 2.9 m maximum wave amplitude in the nearshore of Atlantic City and 1.9 m at the tide gage. Minor tsunami inundationwas shown at the waterfront of Atlantic City with a maximum current speed of 4 m/sec. The current speed in the Absecon Inlet ranges from 1.5 m/s to 3.0 m/s, which is hazardous to ship navigation in the inlet and the harbor. It is noted that the modeling of 1755 Lisbon tsunami in Atlantic City was based on its present bathymetric and topographic features instead of those at that time. The results from both the forecast model and the reference model showed excellent agreement in wave amplitude, wave period, arrival time, and current speed.

A total of nine synthetic scenarios, including six catastrophic, one small-size, and one micro-size earthquake-generated, were used to examine the stability of the developed forecast model and reference model for Atlantic City. The synthetic scenarios were selected in such way that at least one from each of the Puerto Rico Trench, Hispaniola Trench and South Sandwich source zone is tested. Both the forecast model and reference model give stable, yet consistent between the two models, results for all synthetic scenarios representing tsunami waves from different source locations and different directionalities. Other than testing the model stability, these synthetic scenarios are also useful to summarize some common the characteristics of tsunami waves generated from these source zones.

1. A magnitude of 9.3 earthquake in Puerto Rico Trench, represented by ATSZ 48-57 in this report, may generate a catastrophic tsunami for many communities in the Atlantic coast of United States. The modeling results show such a tsunami inundated most of the barrier islands, where Atlantic City and four other cities were build on, with approximately 7 m wave amplitude along the coastline and 7 m/s flow current on land.

2. Scenarios ATSZ 38-47 caused minor flooding at the waterfront of Atlantic City, and current speed up to 4 m/s along the coastline and in the Absecon Inlet. Other scenarios are considered as less threatening, but may still cause damages to the harbor facilities and boats resting in the harbor with high-speed currents in the Absecon inlet and Atlatic City Harbor.

3. Tsunamis generated from the submarine trough are featured with a leading depression when propagating in the Atlantic toward U.S. East Coast. The northerly dipping of the Los Muertos Trough (scenario ATSZ 82-91) results in an uplift at its south, but a subsidence at the north that corresponds to the leading depression when the tsunami waves propagate in the Atlantic. The faults in

Cayman Trough (scenario ATSZ 68-77) were simulated using a subducting mechanism rather than a strike-slip mechanism.

4. For tsunamis generated in the Cayman trough or in South Sandwich source zone, the model simulations show the late waves are higher than the first waves and may pose larger impact to Atlantic City's coastline. Along with these waves are longer wave period up to one and half hours. This lays emphasis on the need of retaining the tsunami warning or watch for more than 24 hours for the coasts of Atlantic City during a real tsunami event.

All model validation and stability tests demonstrated that the developed tsunami forecast model and reference model for Atlantic City, New Jersey, are robust and efficient for their implementation into both the short-term real-time tsunami forecast system and long-term tsunami inundation investigations, although the model accuracy still requires validation through real events in future. The optimized forecast model developed for Atlantic City provides a four-hour forecast of first wave arrival, amplitudes, and inundation within 12 minutes based on testing with available historical and synthetic events as presented in this report.

6. Acknowledgement

The author wish to thank Edison Gica and Jean Newman for their work in the propagation database, Burak Uslu for providing propagation database tabular unit source information and graphics, and the entire modeling group of NCTR for helpful suggestions and discussion. The author especially acknowledges and thanks Marie C. Eble and Sandra Bigley for providing invaluable technical assistance and for editorial review. Collaborative contribution of the National Weather Service, the National Geophysical Data Center, and the National Data Buoy Center were invaluable.

Funding for this publication and all work leading to development of a tsunami forecast model for Atlantic City, New Jersey was provided by the National Oceanic and Atmospheric Administration. This publication was partially funded by the Joint Institute for the Study of the Atmosphere and Ocean (JISAO) under NOAA Cooperative Agreement NO. NA17RJ1232, JISAO Contribution No. ****. This is PMEL Contribution No. ****.

7. References:

Burwell, D., E. Tolkova, and A. Chawla (2007), Diffusion and dispersion characterization of a numerical tsunami model, *Ocean Modeling*, 19, 10-30.

Barkan, R., U.S. ten Brink, and J. Lin (2009), Far filed tsunami simulations of the 1755 Lisbon earthquake: implications for tsunami hazards to the U.S. East Coast and the Caribbean, *Marine Geology*, 264, 109-122, doi: 10.1016/j/margeo.2008.10.010.

Geist, E.L., P.J. Lynett and J.D. Chayton (2009), Hydrodynamic modeling of tsunamis from the Currituck landslide, *Marine Geology*, 264, 41-52.

Gica, E., M. Spillane, V.V. Titov, C. Chamberlin, and J.C. Newman (2008), Development of the forecast propagation database for NOAA's Short-term Inundation Forecast for Tsunamis (SIFT). NOAA Tech. Memo. OAR PMEL-139, 89 pp.

LaForge, R.C. and W.R. McCann (2005). A seismic source model for Puerto Rico, for use in probabilistic ground motion hazard analyses, Active Tectonics and Seismic Hazards of Puerto Rico, the Virgin Islands, and Offshore Areas, edited by P. Mann, The Geological Society of America special Paper 385, 223-248.

Leatherman, S.P. (1982). Barrier island handbook. College Park, Md.: University of Maryland, 109pp.

Lockridge, P.A., L.S. Whiteside, J.F. Lander (2002), Tsunamis and tsunami-like waves of the eastern United States, *Science of Tsunami Hazards*, 20(3), 120-157.

Muir-Wood, R. and A. Mignan (2009), A phenomenological reconstruction of the Mw9 Novermber 1st 1755 earthquake source, *The 1755 Lisbon Earthquake: Revisited*, *Geotechnical, Geological, and Earthquake Engineering*, 7, Part III, 121-146, doi: 10.1007/978-1-4020-8609-0_8.

Natural Resource Canada (2006), Earthquakes Canada; Canadian Hazard Information Service. Historic Earthquakes Web Pages, http://earthquakescanada.nrcan.gc.ca/

Pasad, R., E. Cunningham, and G. Bagchi (2009), Tsunami hazard assessment at nuclear power plant sites in the United States of America – Final Report, United States Nuclear Regulatory Commission, NUREG/CR-6966 and PNNL-17397, NRC Job Code J3301, Office of New Reactors, p84.

Prior, D.P., Doyle, E.H., and Neurauter, T. (1986), The Currituck Slide, Mid Atlantic continental slope-revisited, *Marine Geology*, V73, p25-4.

Roger, J., S. Allgeyer, H. Hebert, M.A. Baptista, A. Loevenbruck, F. Schindele (2009), The 1755 Lisbon tsunami in guadeloup Archipelago: source sensitivity and investigation of resonance effects, *The Open Oceanography Journal*, 3, 1-13.

Ruffman, A (1996). Tsunami runup mapping as an emergency preparedness planning tool: the 1929 tsunami in St. Lawrance, Newfoundland. *Geomarine Associates Ltd.*, Contract Report for Emergency Preparedness Canada (EPC), Office of the Senior Scientific Advisor, Ottawa, Ontario, V1 – Report, 107 pp.; V2 – Appendices and Enclosures, 281 pp.

Synolakis, C.E., E.N. Bernard, V.V. Titov, U. Kânoğlu, and F.I. González (2008): Validation and verification of tsunami numerical models. *Pure Appl. Geophys.*, *165*(11–12), 2197–2228.

Tadepalli, S. and C.E. Synolakis (1994). The run-up of N-waves on sloping beaches. Proc. R. Soc. A 445, 99-112.

Tang, L., V.V. Titov, Y. Wei, H.O. Mofjeld, M. Spillane, D. Arcas, E.N. Bernard, C. Chamberlin, E. Gica, and J. Newman (2008): Tsunami forecast analysis for the May 2006 Tonga tsunami. *J. Geophys. Res.*, *113*, C12015, doi: 10.1029/2008JC004922.

Tang, L., V. V. Titov, and C. D. Chamberlin (2009), Development, testing, and applications of site-specific tsunami inundation models for real-time forecasting, *J. Geophys. Res.*, 114, C12025, doi:10.1029/2009JC005476.

Taylor, L.A., B.W. Eakins, K.S. Carignan, R.R. Warnken, T. Sazonova, and D.C. Schoolcraft (2007): Digital elevation model for Atlantic City, New Jersey: procedue, data sources and analysis, prepared for the Pacific Marine Environmental Laboratory (PMEL) – NOAA Center for Tsunami Research, Cooperative Institute for Research in Environmental Sciences, Univeristy of Colorado at Boulder, and NOAA National Geophysical Data Center, Boulder, Colorado, 31p.

ten Brink, U., D. Twichell, E. Geist, J. Chaytor, J. Locat, H. Lee, B. Buczkowski, R. Barkan, A. Solow, B. Andrews, T. Parsons, P. Lynett, J. Lin, and M. Sansoucy (2008): Evaluation of tsunami sources with the potential to impact the U.S. Atlantic and Gulf coasts, *USGS Administrative report to the Nuclear Regulatory Commission*, 300pp.

Titov, V.V. (2009): Tsunami forecasting. Chapter 12 in *The Sea, Volume 15: Tsunamis*, Harvard University Press, Cambridge, MA and London, England, 371–400.

Titov, V.V, E. Gica, M. Spillane, Y. Wei, C. Moore, H. Zhou and R. Weiss (2009), Tsunami hazard assessment for the U.S. East Coast based on generation, propagation and inundation modeling, *NCTR Letter Report to the Nuclear Regulatory Commission*, 117pp.

Titov, V., and F.I. González (1997): Implementation and testing of the Method of Splitting Tsunami (MOST) model. NOAA Tech. Memo. ERL PMEL-112 (PB98-122773), NOAA/Pacific Marine Environmental Laboratory, Seattle, WA, 11 pp.

Titov, V.V., F.I. González, E.N. Bernard, M.C. Eble, H.O. Mofjeld, J.C. Newman, and A.J. Venturato (2005a): Real-time tsunami forecasting: Challenges and solutions. Nat. Hazards, 35(1), Special Issue, U.S. National Tsunami Hazard Mitigation Program, 41–58.

Titov, V.V., A.B. Rabinovich, H.O. Mofjeld, R.E. Thomson, and F.I. González (2005b), The global reach of the 26 December 2004 Sumatra Tsunami. *Science*. doi: 10.1126/science.1114576.

Wei, Y., E. Bernard, L. Tang, R. Weiss, V. Titov, C. Moore, M. Spillane, M. Hopkins, and U. Kânoğlu (2008): Real-time experimental forecast of the Peruvian tsunami of August 2007 for U.S. coastlines. *Geophys. Res. Lett.*, *35*, L04609, doi: 10.1029/2007GL032250.

Wei, Y., U.S. ten Brink, and B. Atwater (2011): Tsunami sources that might explain the catastrophic overwash of Anegada, British Virgin Islands, between 1650 and 1800. *Journal of Geophysical Research*, in preparation.

Figures:

Figure 1. (a) Aerial view from north of coastline of Atlantic City. (b) Aerial view from south of coastline of Atlantic City.

Figure 2. Historical shoreline changes at Ventnor City, New Jersey (Courtesy of United States Army Corps of Engineers).

Figure 3. Location of NOA Atlantic City tide station. (a) Google aerial view of Absecon Island, Absecon Inlet and Brigantine Island; (b) Location of the pier (Taj Mahal Pier) that hosts the NOS Atlantic City tide station; (c) Closer view of Taj Mahal Pier and the location of NOS Atlantic City tide station. (d) Outside appearance of the tide station (photo courtesy of http://tideandcurrents.noaa.gov).

Figure 4. Historical tsunami events that have affected central north of U.S. East Coast, where ● indicates the earthquake location and M represents the meteorological tsunamis. The black boxes are the tsunami propagation unit sources (Gica et al., 2008).

Figure 5. Grid A bathymetry and topography for both the forecast model and the reference model, where the black boxes indicate coverage of B grid and C grid and the red circle indicates the location of Atlantic City tide station.

Figure 6. B grid bathymetry and topography for the forecast model, where the black boxes indicate coverage of C grid in forecast model and the red circle indicates the location of Atlantic City tide station.

Figure 7. B grid bathymetry and topography for the reference model, where the black boxes indicate coverage of C grid in forecast model and the red circle indicates the location of Atlantic City tide station.

Figure 8. C grid bathymetry and topography for the forecast model, where the red circle indicates the location of Atlantic City tide station.

Figure 9. C grid bathymetry and topography for the reference model, where the red circle indicates the location of Atlantic City tide station.

Figure 10. Tsunami energy projection (or computed maximum wave amplitude) of the 1755 Lisbon tsunami (M 9.0 scenario) in the Atlantic.

Figure 11. Comparison of computed time series between forecast model and reference model at the Atlantic City tide station for 1755 Lisbon tsunami. The upper panel is a zoom-in view of eighth to 16th hours in the lower panel, which shows modeled time series of a 24-hour run after tsunami arrival.

Figure 12. Computed maximum wave amplitude and maximum current speed in C grid for the 1755 Lisbon tsunami (M 9.0 scenario). (a) Maximum wave amplitude in C grid computed with the reference model; (b) maximum current speed in C grid computed with the reference model; (c) maximum wave amplitude in C grid computed with the forecast model; (d) maximum current speed in C grid computed with the forecast model.

Figure 13. Model scenarios used in model validation and model stability testing, where the model scenarios are speculated in detail in Table 3.

Figure 14. Computed maximum wave amplitude and maximum current speed in C grid for ATSZ 48-57 scenario. (a) Maximum wave amplitude in C grid computed with the reference model; (b) maximum current speed in C grid computed with the reference model; (c) maximum wave amplitude in C grid computed with the forecast model; (d) maximum current speed in C grid computed with the forecast model.

Figure 15. Comparison of computed time series between forecast model and reference model at the Atlantic City tide station for ATSZ 48-57 scenario. The upper panel is a zoom-in view of fourth to 12th hours in the lower panel, which shows modeled time series of a 24-hour run after tsunami arrival.

Figure 16. Computed maximum wave amplitude and maximum current speed in C grid for ATSZ 38-47 scenario. (a) Maximum wave amplitude in C grid computed with the reference model; (b) maximum current speed in C grid computed with the reference model; (c) maximum wave amplitude in C grid computed with the forecast model; (d) maximum current speed in C grid computed with the forecast model.

Figure 17. Comparison of computed time series between forecast model and reference model at the Atlantic City tide station for ATSZ 38-47 scenario. The upper panel is a zoom-in view of fourth to 12th hours in the lower panel, which shows modeled time series of a 24-hour run after tsunami arrival.

Figure 18. Computed maximum wave amplitude and maximum current speed in C grid for ATSZ 58-67 scenario. (a) Maximum wave amplitude in C grid computed with the reference model; (b) maximum current speed in C grid computed with the reference model; (c) maximum wave amplitude in C grid computed with the forecast model; (d) maximum current speed in C grid computed with the forecast model.

Figure 19. Comparison of computed time series between forecast model and reference model at the Atlantic City tide station for ATSZ 58-67 scenario. The upper panel is a zoom-in view of fourth to 12th hours in the lower panel, which shows modeled time series of a 24-hour run after tsunami arrival.

Figure 20. Computed maximum wave amplitude and maximum current speed in C grid for ATSZ 82-91 scenario. (a) Maximum wave amplitude in C grid computed with the reference model; (b) maximum current speed in C grid computed with the reference model; (c) maximum wave amplitude in C grid computed with the forecast model; (d) maximum current speed in C grid computed with the forecast model.

Figure 21. Comparison of computed time series between forecast model and reference model at the Atlantic City tide station for ATSZ 82-91 scenario. The upper panel is a zoom-in view of fourth to 12th hours in the lower panel, which shows modeled time series of a 24-hour run after tsunami arrival.

Figure 22. Computed maximum wave amplitude and maximum current speed in C grid for ATSZ 68-77 scenario. (a) Maximum wave amplitude in C grid computed with the

reference model; (b) maximum current speed in C grid computed with the reference model; (c) maximum wave amplitude in C grid computed with the forecast model; (d) maximum current speed in C grid computed with the forecast model.

Figure 23. Comparison of computed time series between forecast model and reference model at the Atlantic City tide station for ATSZ 68-77 scenario. The upper panel is a zoom-in view of fourth to 12th hours in the lower panel, which shows modeled time series of a 24-hour run after tsunami arrival.

Figure 24. Computed maximum wave amplitude and maximum current speed in C grid for SSSZ 01-10 scenario. (a) Maximum wave amplitude in C grid computed with the reference model; (b) maximum current speed in C grid computed with the reference model; (c) maximum wave amplitude in C grid computed with the forecast model; (d) maximum current speed in C grid computed with the forecast model.

Figure 25. Comparison of computed time series between forecast model and reference model at the Atlantic City tide station for SSSZ 01-10 scenario. The upper panel is a zoom-in view of 17th to 25th hours in the lower panel, which shows modeled time series of a 24-hour run after tsunami arrival.

Figure 26. Computed maximum wave amplitude and maximum current speed in C grid for ATSZ b52 scenario. (a) Maximum wave amplitude in C grid computed with the reference model; (b) maximum current speed in C grid computed with the reference model; (c) maximum wave amplitude in C grid computed with the forecast model; (d) maximum current speed in C grid computed with the forecast model.

Figure 27. Comparison of computed time series between forecast model and reference model at the Atlantic City tide station for ATSZ b52 scenario. The upper panel is a zoom-in view of fourth to 12th hours in the lower panel, which shows modeled time series of a 24-hour run after tsunami arrival.

Figure 28. Computed maximum wave amplitude and maximum current speed in C grid for SSSZ b11scenario. (a) Maximum wave amplitude in C grid computed with the reference model; (b) maximum current speed in C grid computed with the reference model; (c) maximum wave amplitude in C grid computed with the forecast model; (d) maximum current speed in C grid computed with the forecast model.

Figure 29. Comparison of computed time series between forecast model and reference model at the Atlantic City tide station for SSSZ b11 scenario. The upper panel is a zoom-in view of 22th to 30th hours in the lower panel, which shows modeled time series of a 24-hour run after tsunami arrival.

TAJ MAHAL
SHOWBOAT
SHOWBOAT

© www.AerialPhotosofNJ.com

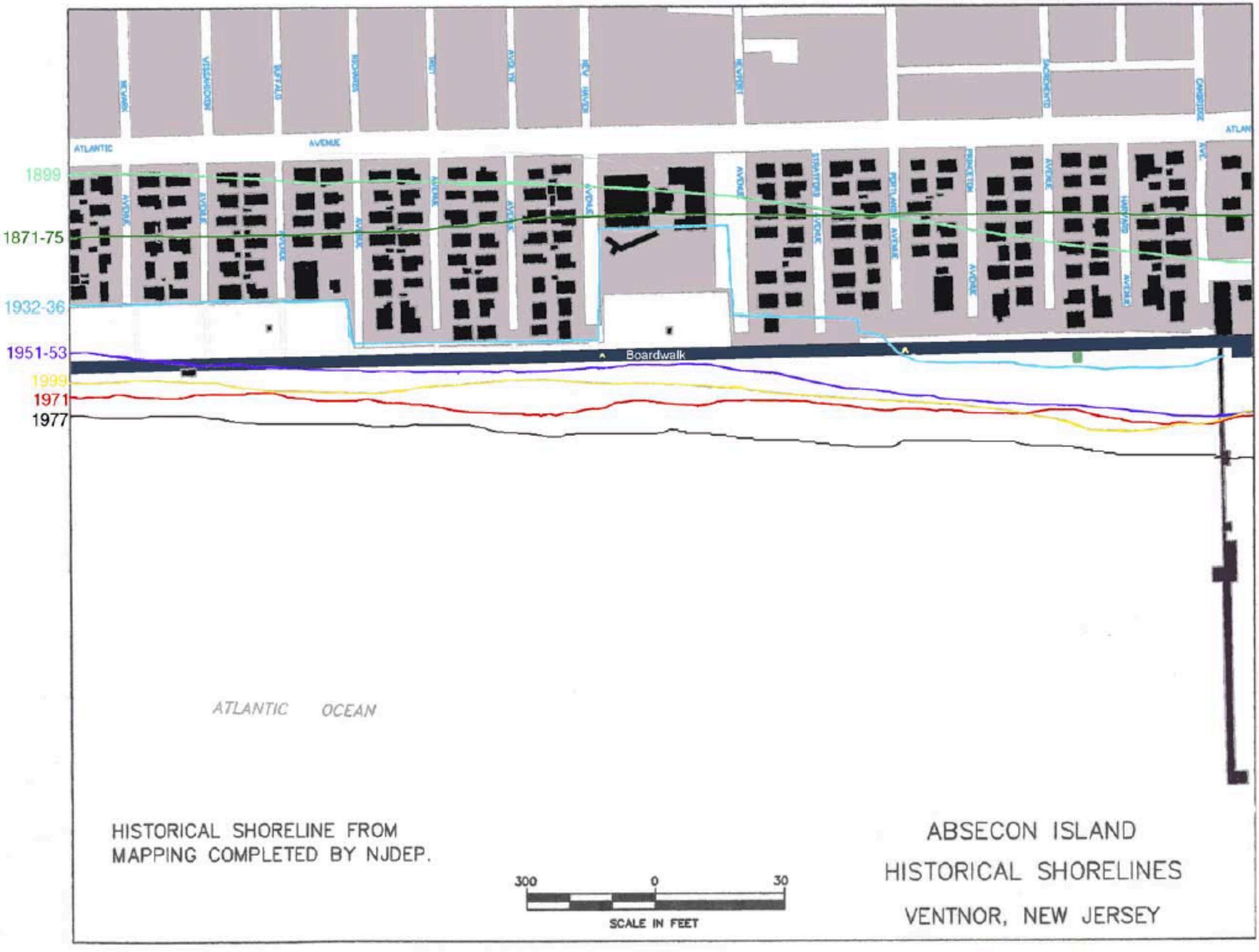

HISTORICAL SHORELINE FROM
MAPPING COMPLETED BY NJDEP.

ABSECON ISLAND
HISTORICAL SHORELINES
VENTNOR, NEW JERSEY

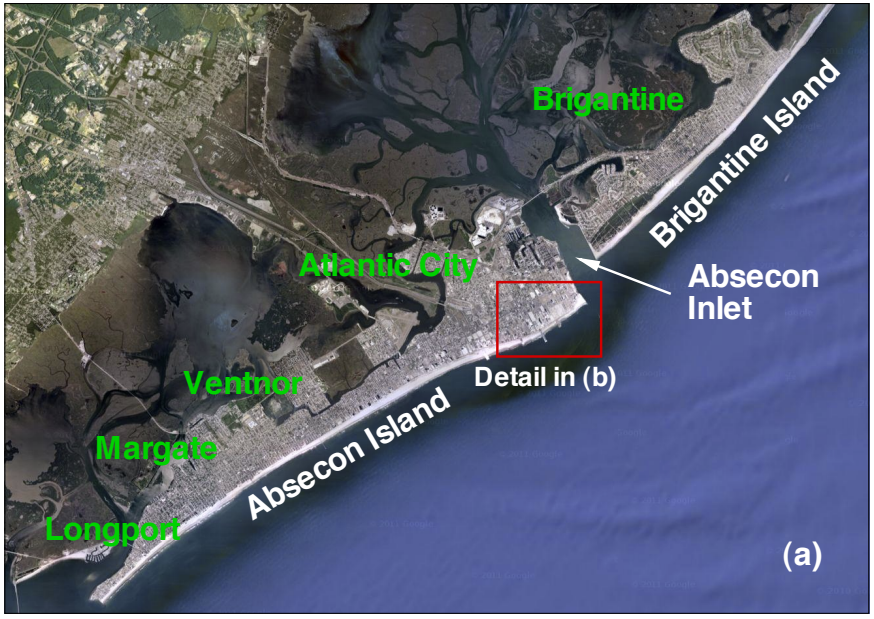
Brigantine
Brigantine Island
Atlantic City
Absecon
Inlet
Detail in (b)
Ventnor
Margate
Absecon Island
Longport
(a)

Absecon
Inlet
Atlantic City
Detail in (c)
(b)

Atlantic CIty
Tide Gage
Taj Mahal
Pier
(c)

(d)

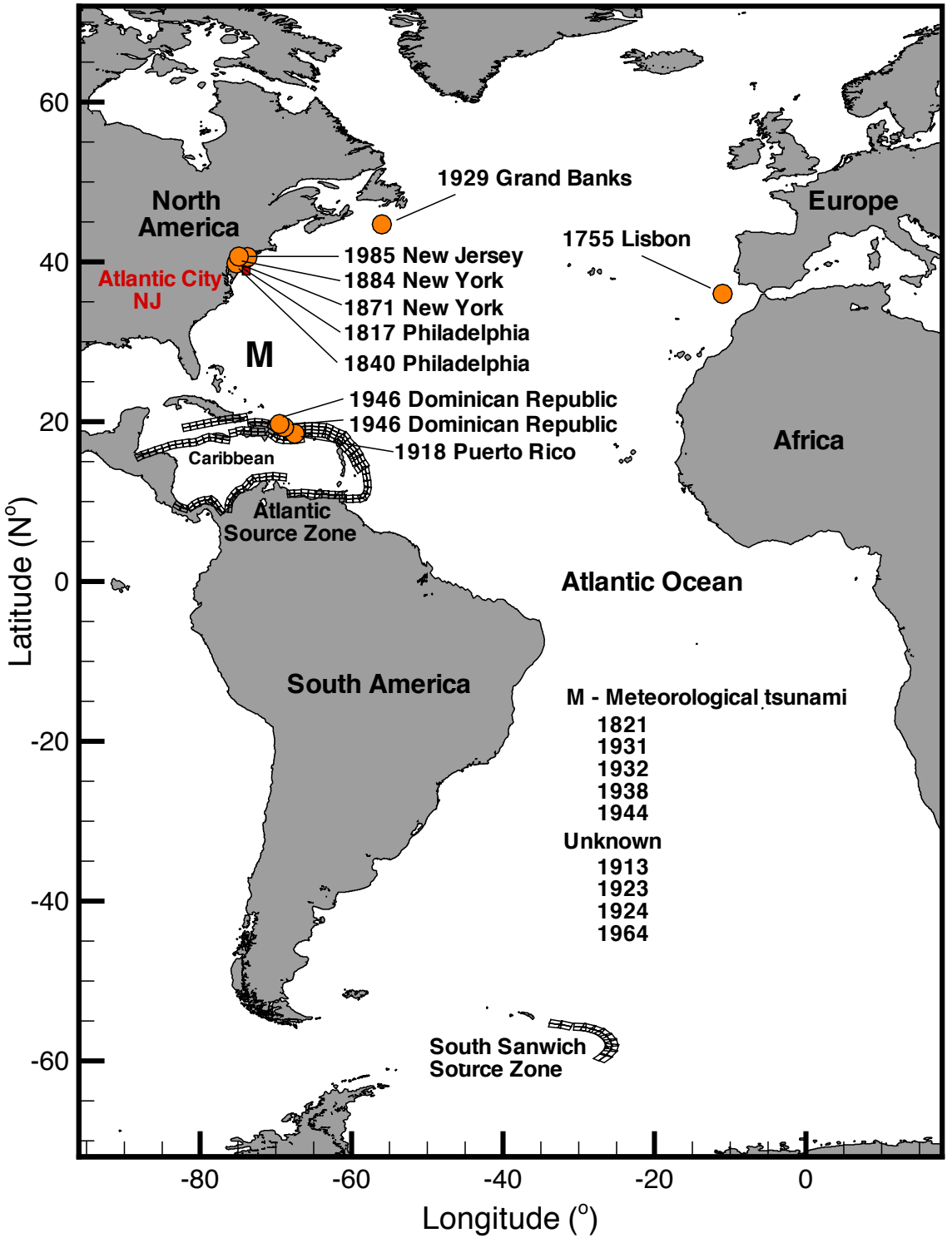
1929 Grand Banks
North America
Europe
1755 Lisbon
1985 New Jersey
Atlantic City NJ
1884 New York
1871 New York
1817 Philadelphia
M
1840 Philadelphia
1946 Dominican Republic
1946 Dominican Republic
1918 Puerto Rico
Africa
Caribbean
Atlantic Source Zone
Atlantic Ocean
South America
M - Meteorological tsunami
1821
1931
1932
1938
1944
Unknown
1913
1923
1924
1964
South Sanwich Source Zone
60
40
20
0
-20
-40
-60
Latitude (N°)
-80
-60
-40
-20
0
Longitude (°)

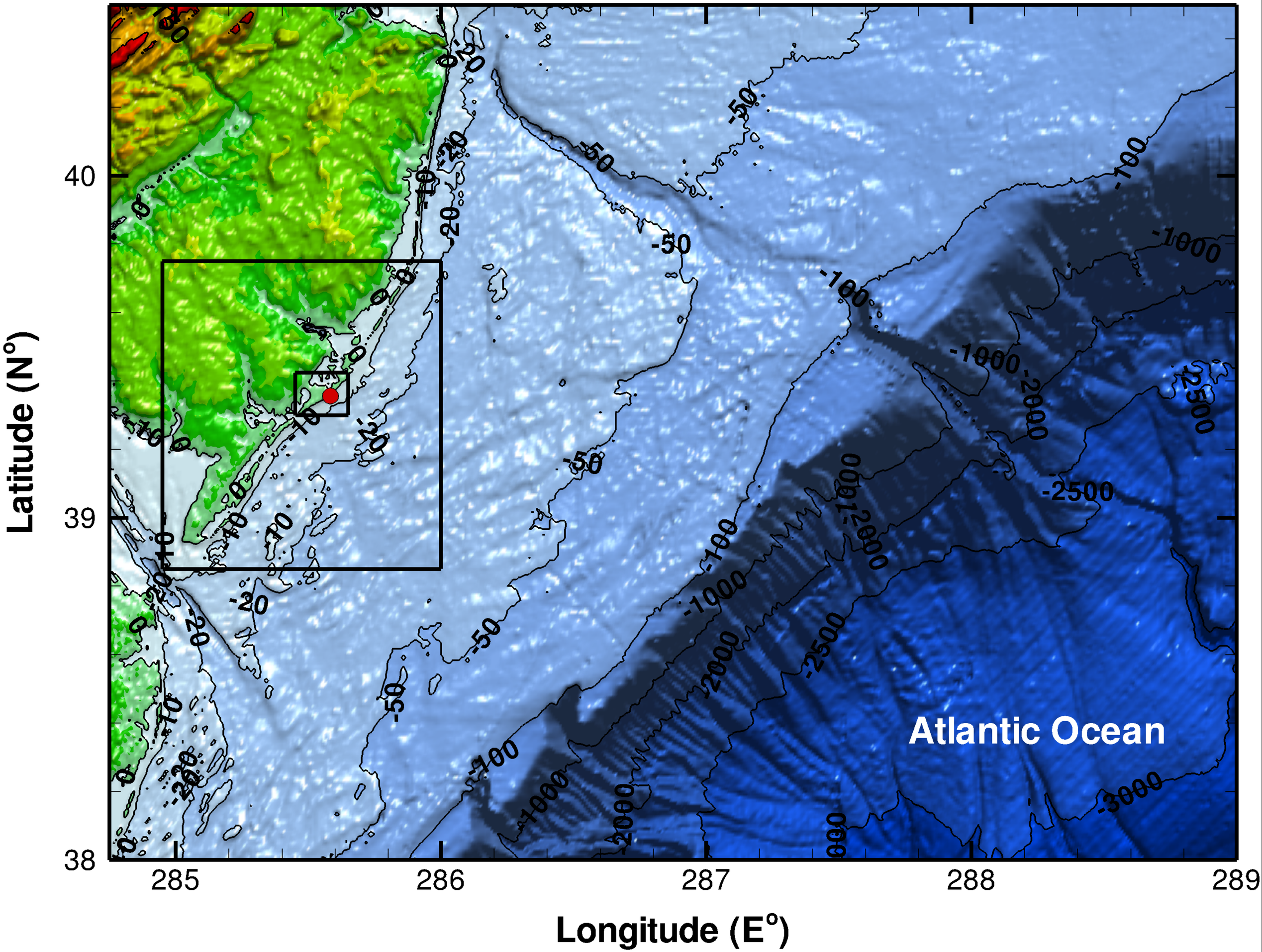
Atlantic Ocean
Latitude (N°)
Longitude (E°)
38
39
40
285
286
287
288
289
-50
-100
-1000
-2000
-2500
-3000

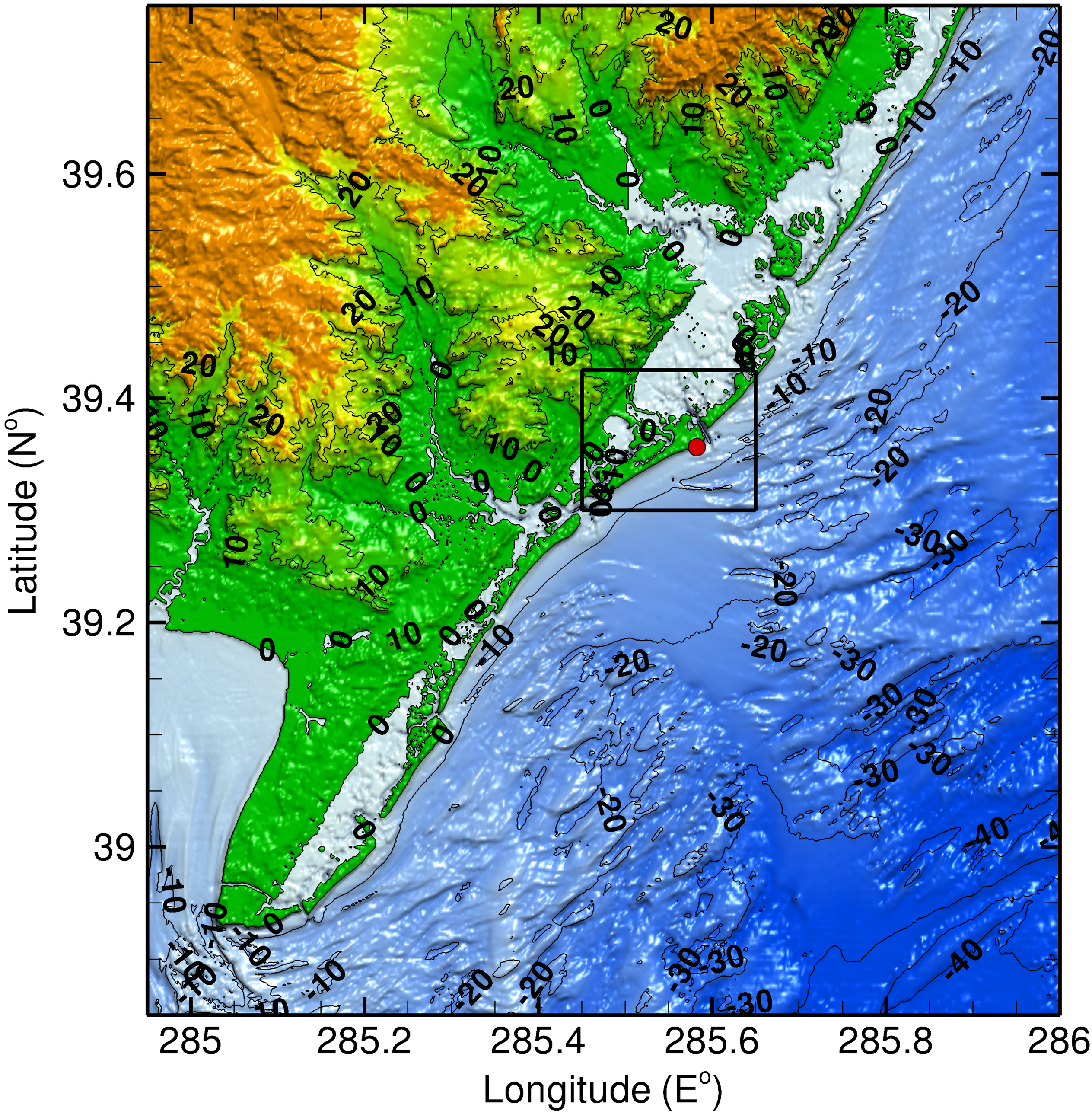
39.6
39.4
39.2
39
Latitude (N°)
285
285.2
285.4
285.6
285.8
286
Longitude (E°)

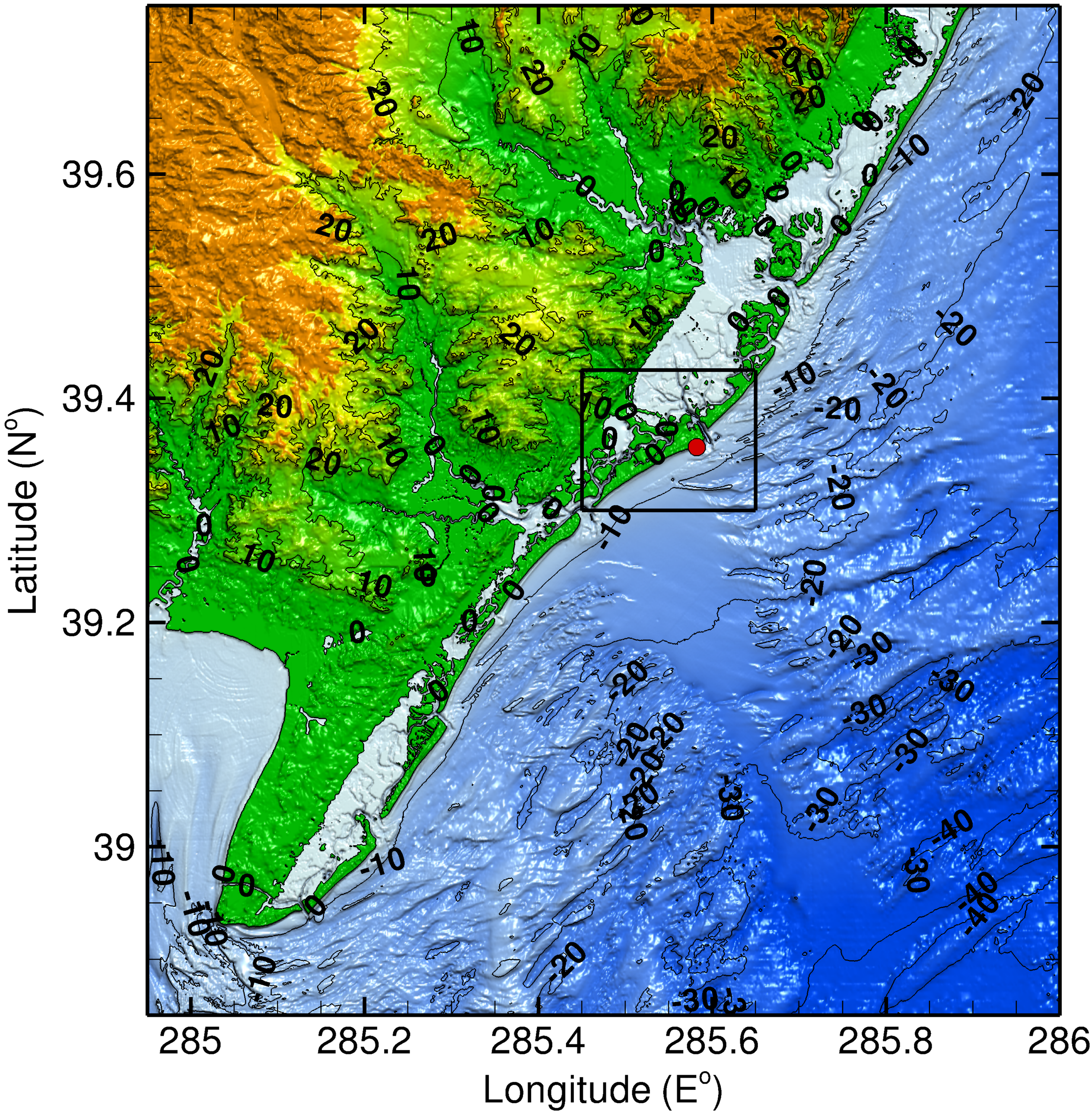
39.6
39.4
39.2
39
Latitude (N°)
285
285.2
285.4
285.6
285.8
286
Longitude (E°)

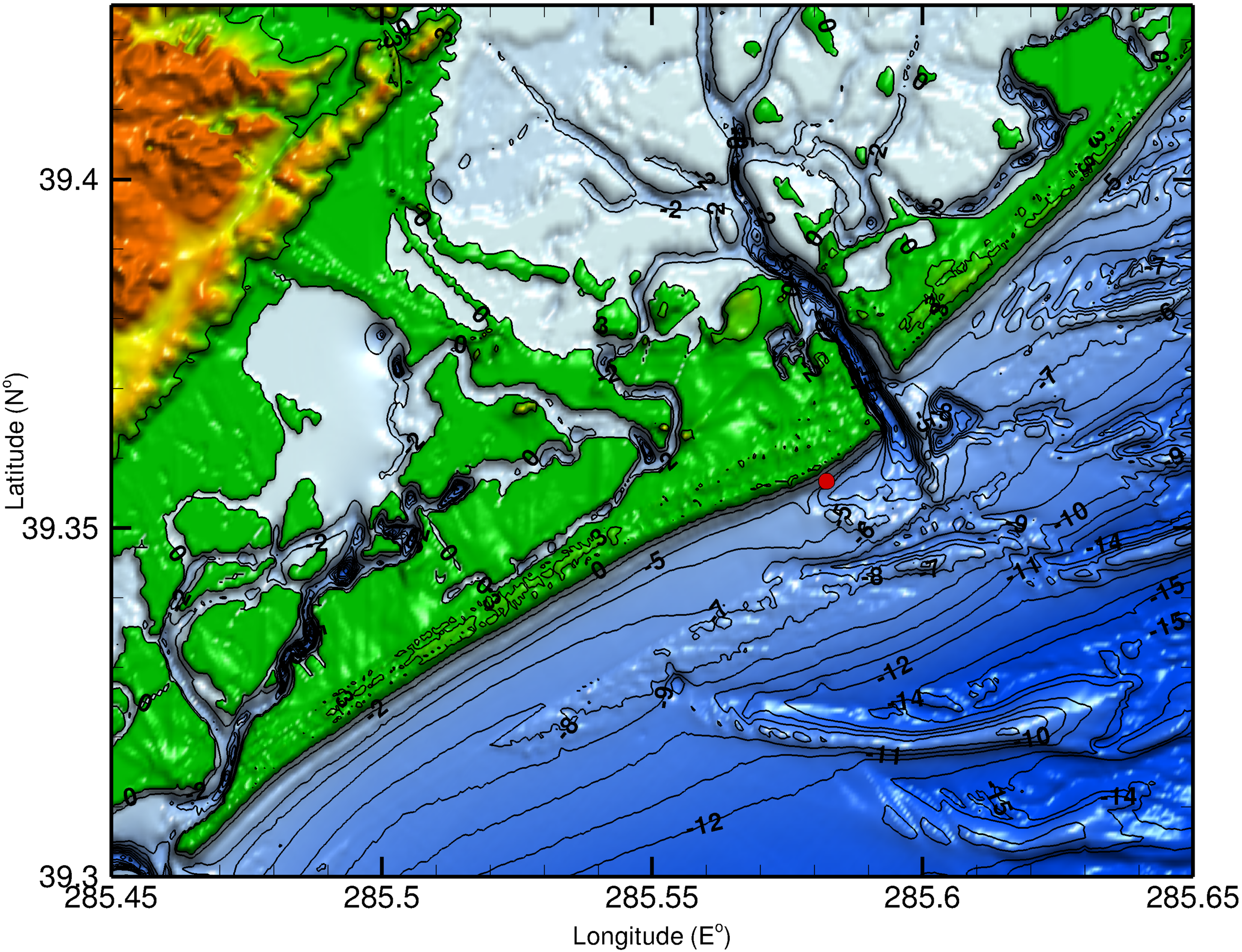
39.4
39.35
39.3
Latitude (N°)
285.45
285.5
285.55
285.6
285.65
Longitude (E°)

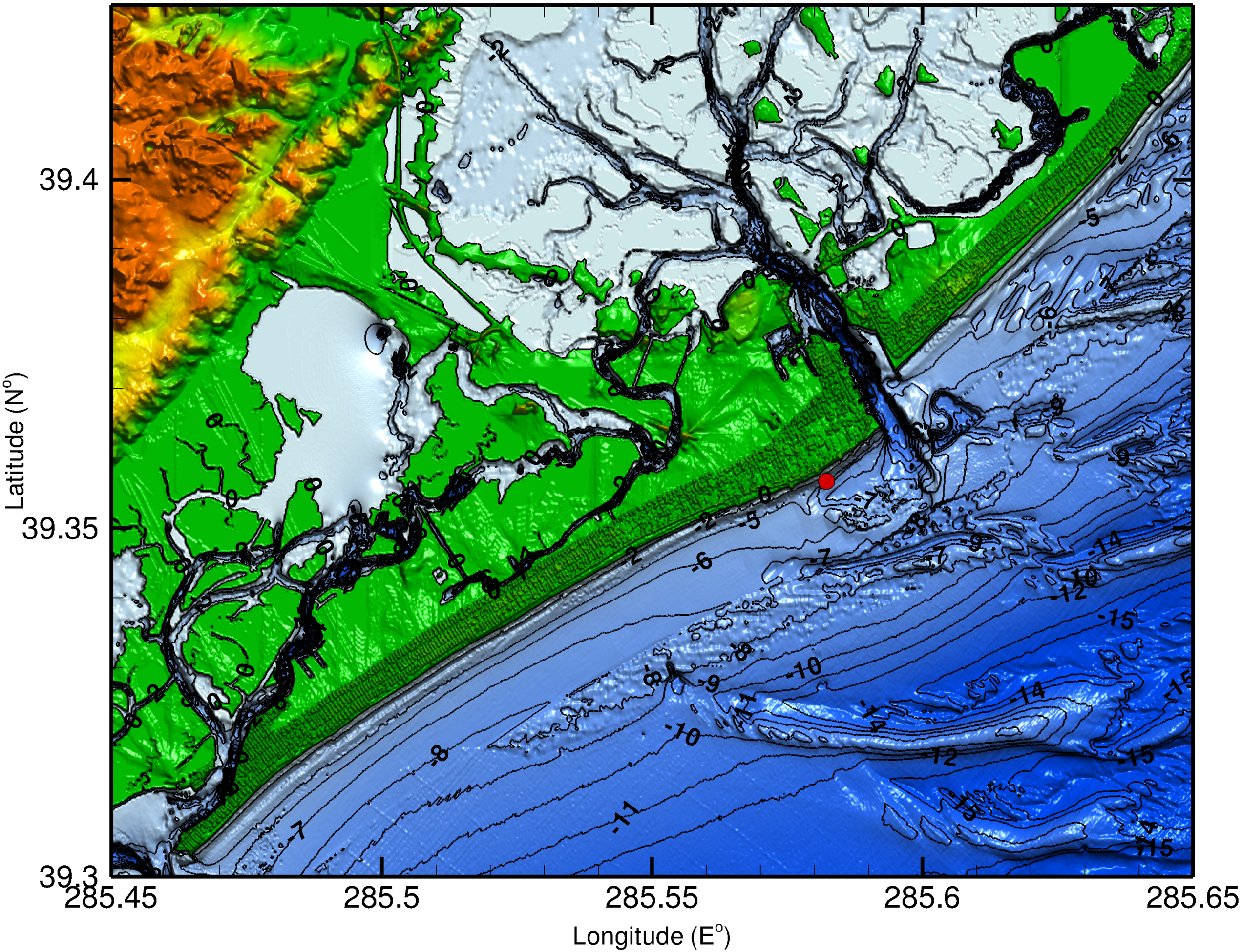
39.4
39.35
39.3
Latitude (N°)
285.45
285.5
285.55
285.6
285.65
Longitude (E°)

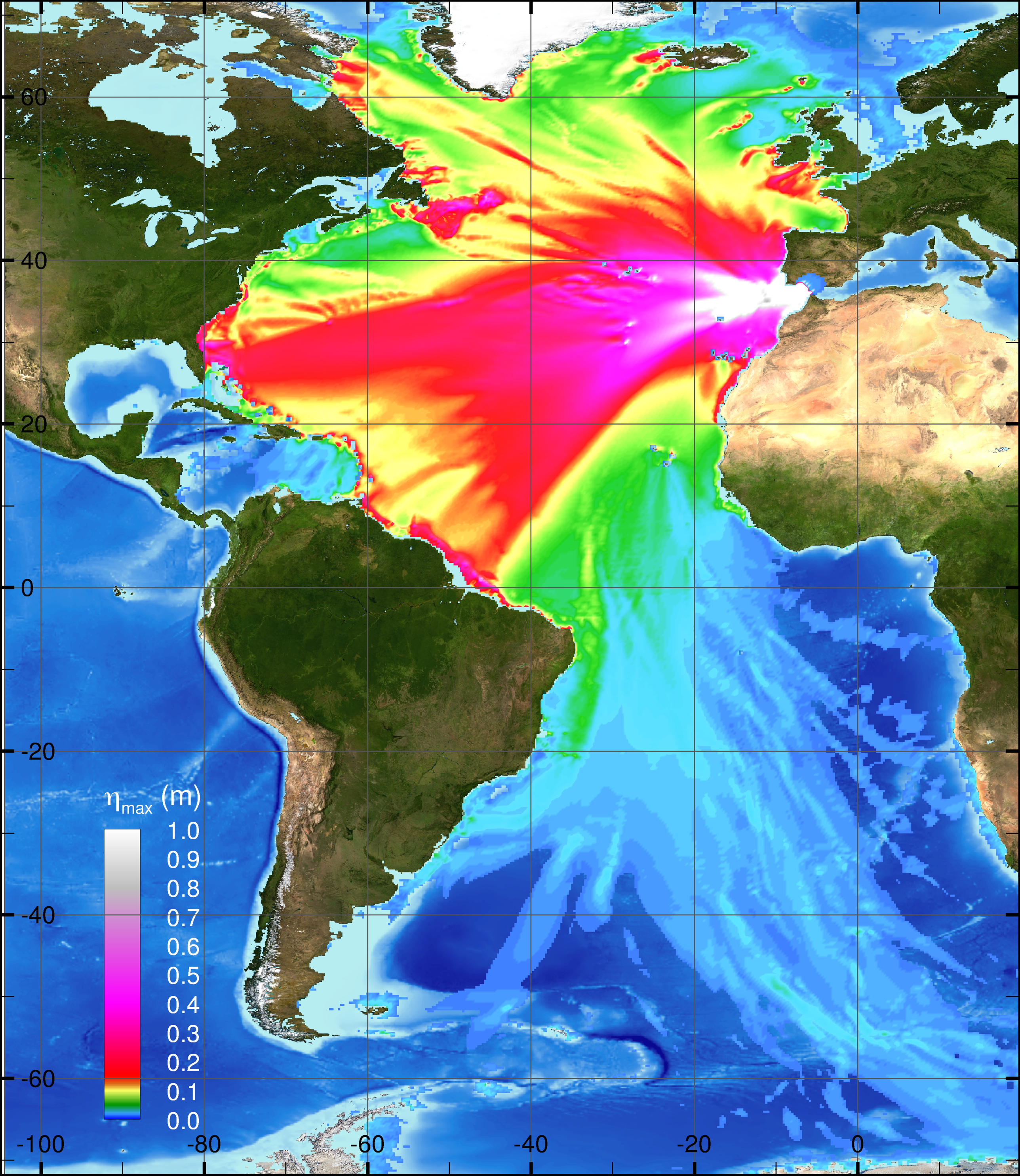
60
40
20
0
-20
-40
-60
-100
-80
-60
-40
-20
0
η_{max} (m)
1.0
0.9
0.8
0.7
0.6
0.5
0.4
0.3
0.2
0.1
0.0

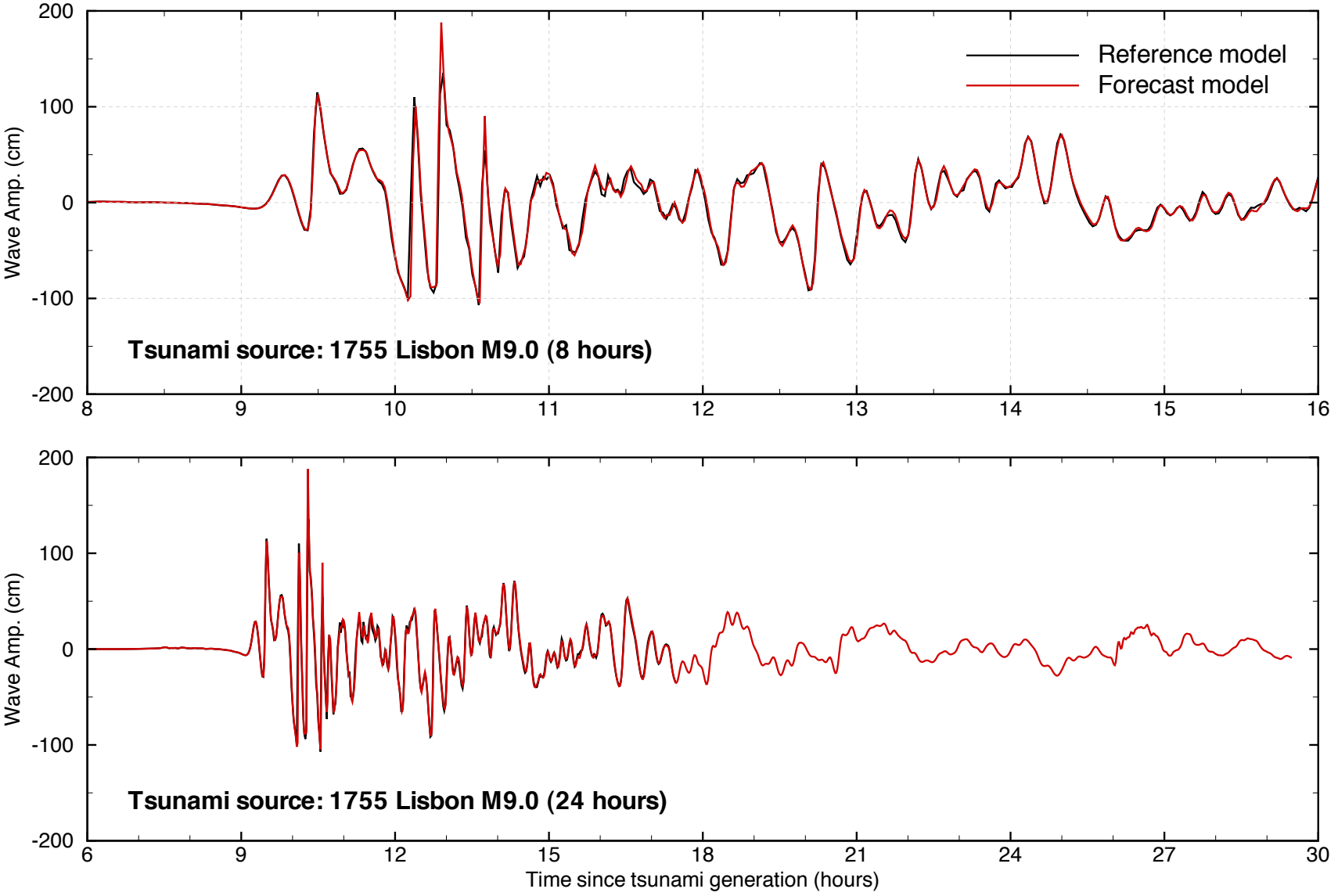
Reference model
Forecast model
Tsunami source: 1755 Lisbon M9.0 (8 hours)
Tsunami source: 1755 Lisbon M9.0 (24 hours)
Wave Amp. (cm)
Wave Amp. (cm)
Time since tsunami generation (hours)
200
100
0
-100
-200
8
9
10
11
12
13
14
15
16
6
9
12
15
18
21
24
27
30

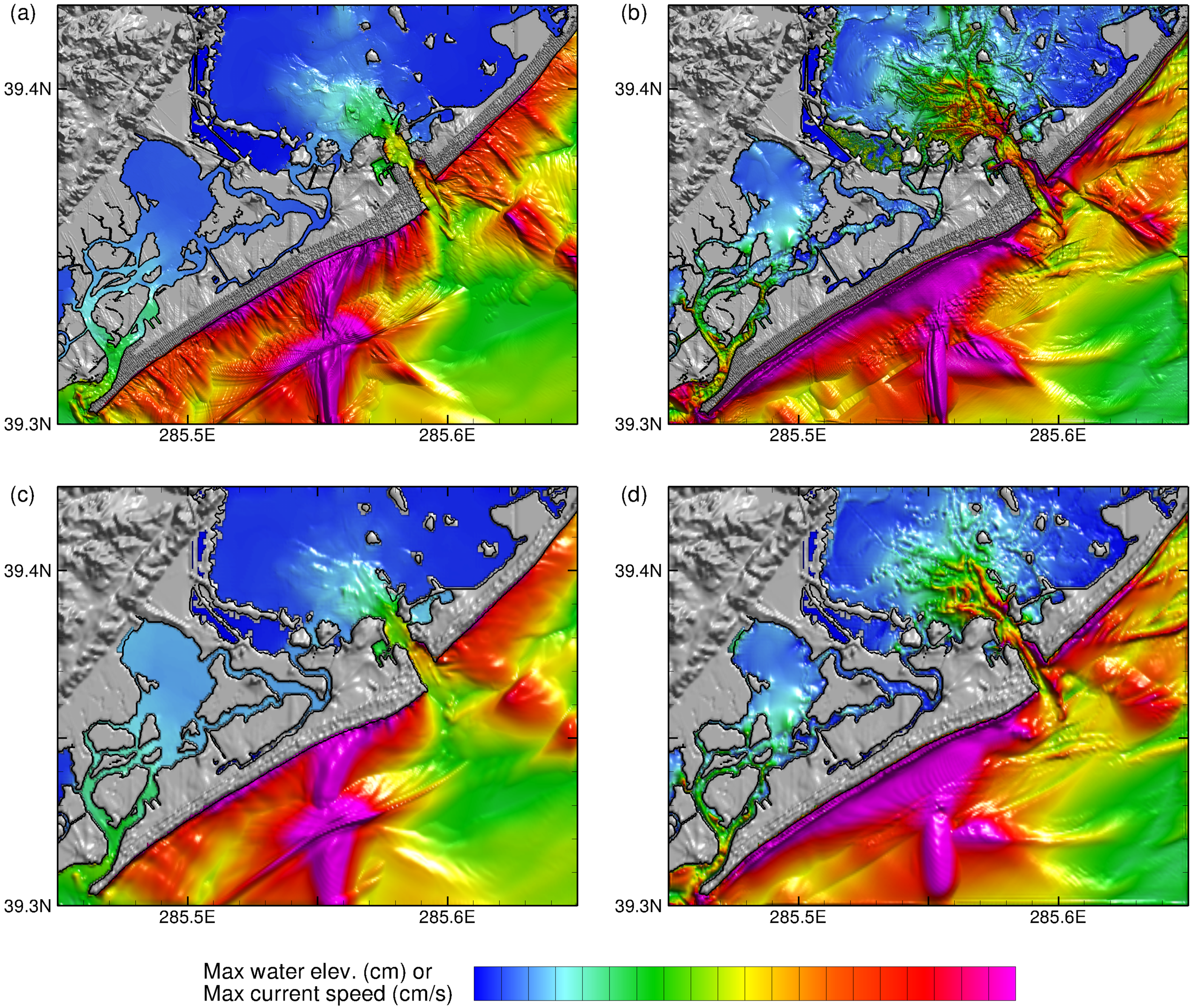
(a)
(b)
(c)
(d)
39.4N
39.3N
285.5E
285.6E
Max water elev. (cm) or
Max current speed (cm/s)
0
20
40
60
80
100
120
140
160
180
200

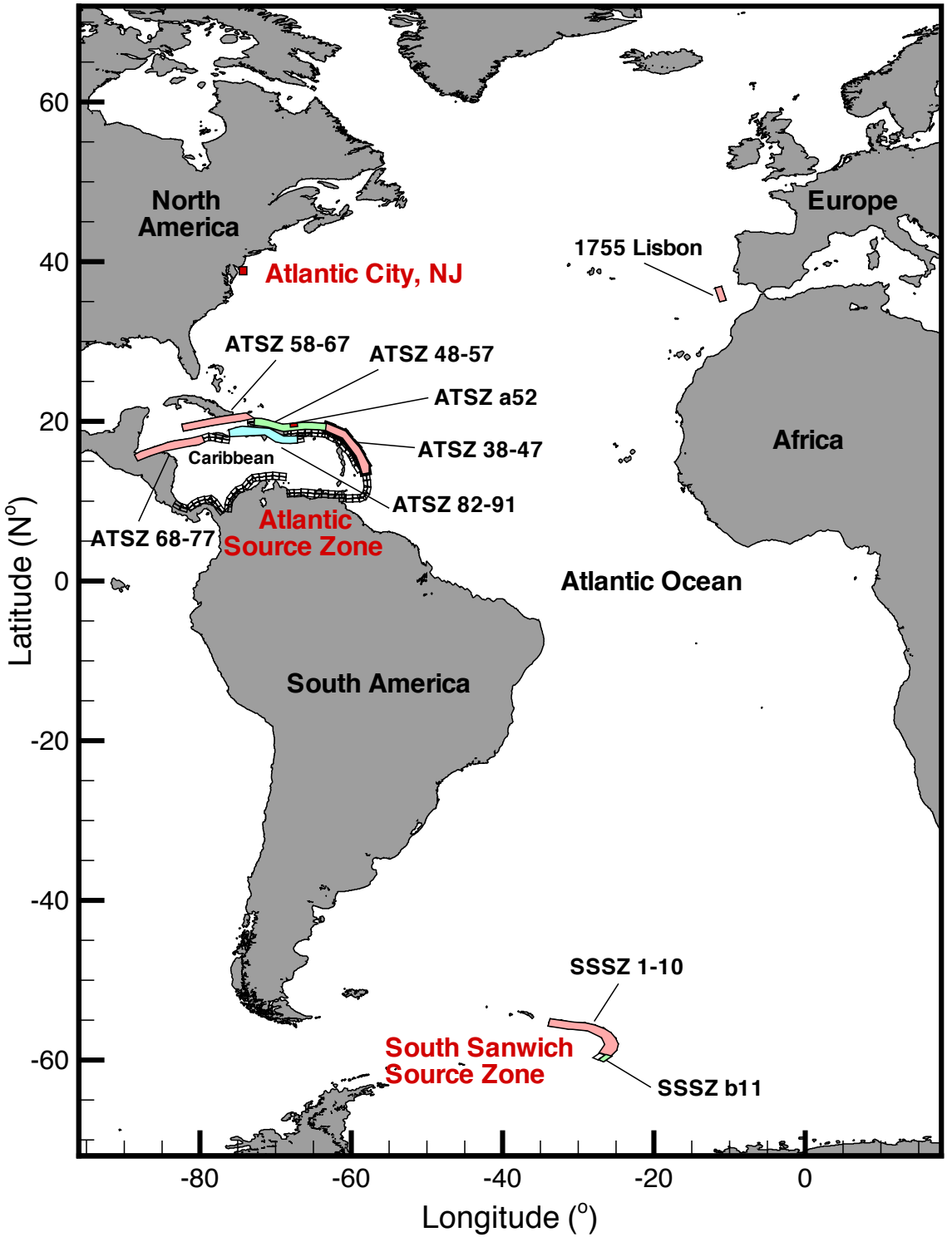
North America
Europe
Africa
South America
Atlantic Ocean
Caribbean
Atlantic City, NJ
1755 Lisbon
ATSZ 58-67
ATSZ 48-57
ATSZ a52
ATSZ 38-47
ATSZ 82-91
ATSZ 68-77
Atlantic Source Zone
SSSZ 1-10
SSSZ b11
South Sanwich Source Zone
60
40
20
0
-20
-40
-60
Latitude (N°)
-80
-60
-40
-20
0
Longitude (°)

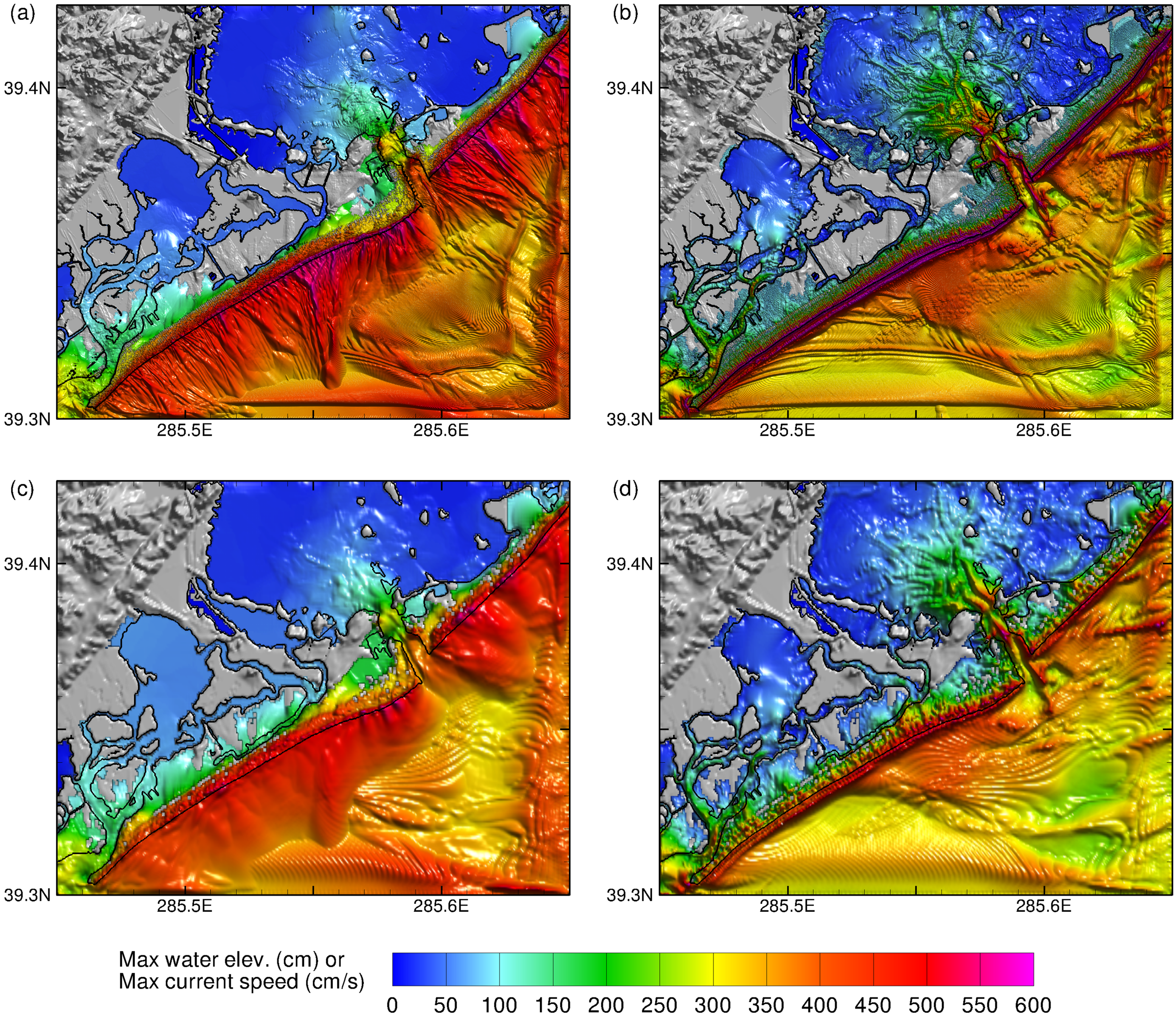
(a)
(b)
(c)
(d)
39.4N
39.3N
285.5E
285.6E
Max water elev. (cm) or
Max current speed (cm/s)
0
50
100
150
200
250
300
350
400
450
500
550
600

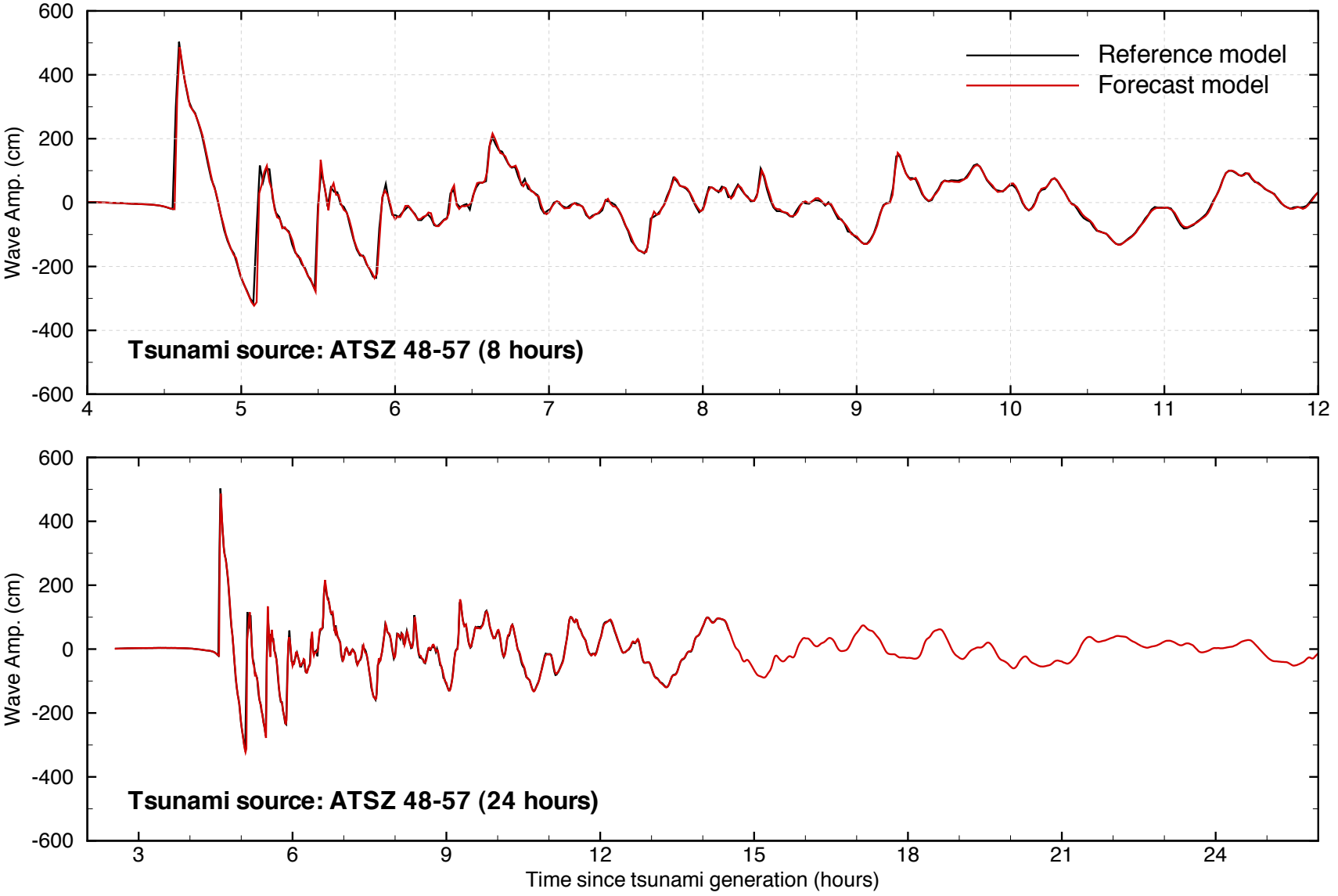
Reference model
Forecast model
Wave Amp. (cm)
Tsunami source: ATSZ 48-57 (8 hours)
Tsunami source: ATSZ 48-57 (24 hours)
Time since tsunami generation (hours)

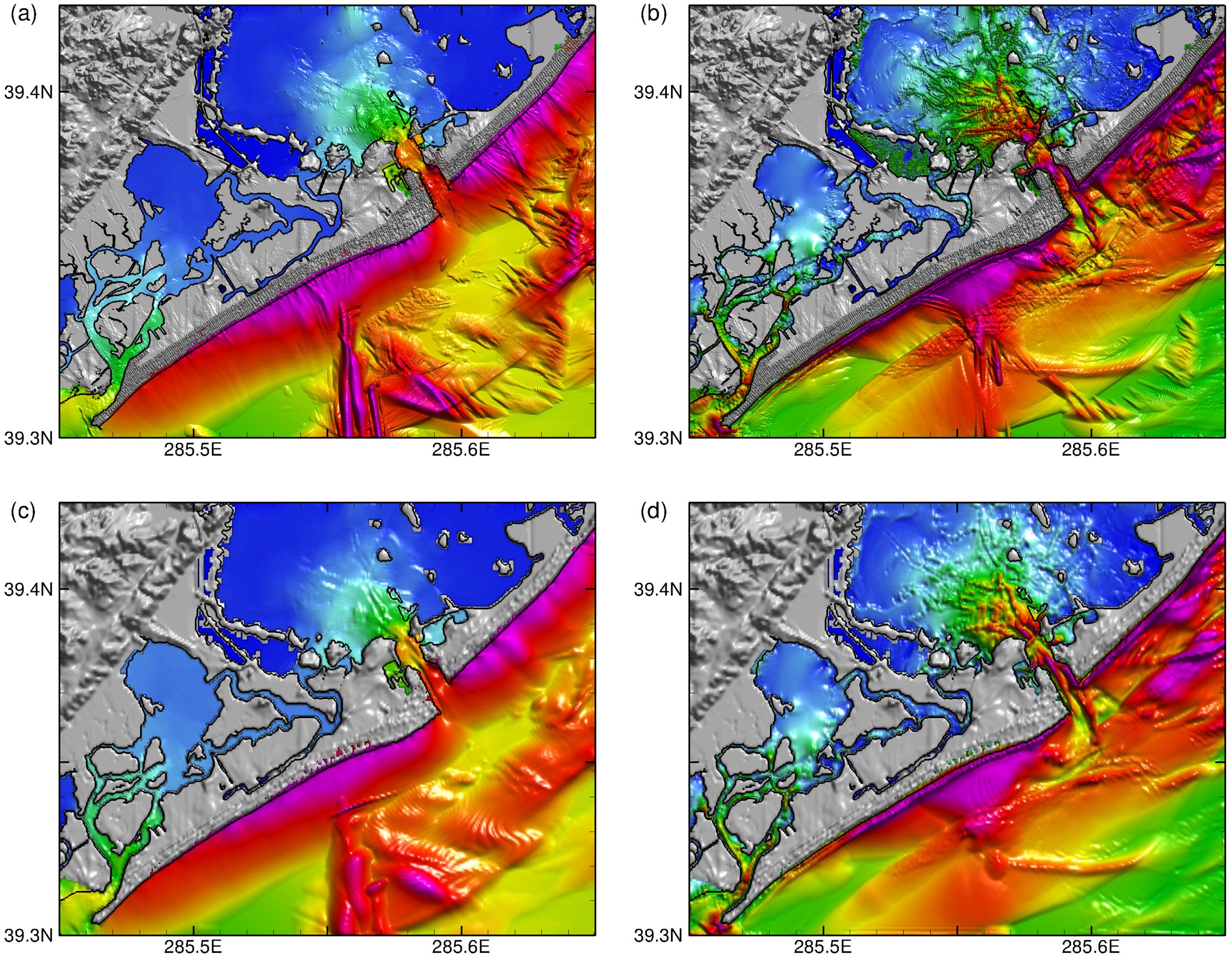
(a)
(b)
(c)
(d)
39.4N
39.3N
285.5E
285.6E
Max water elev. (cm) or
Max current speed (cm/s)
0
50
100
150
200
250
300
350
400

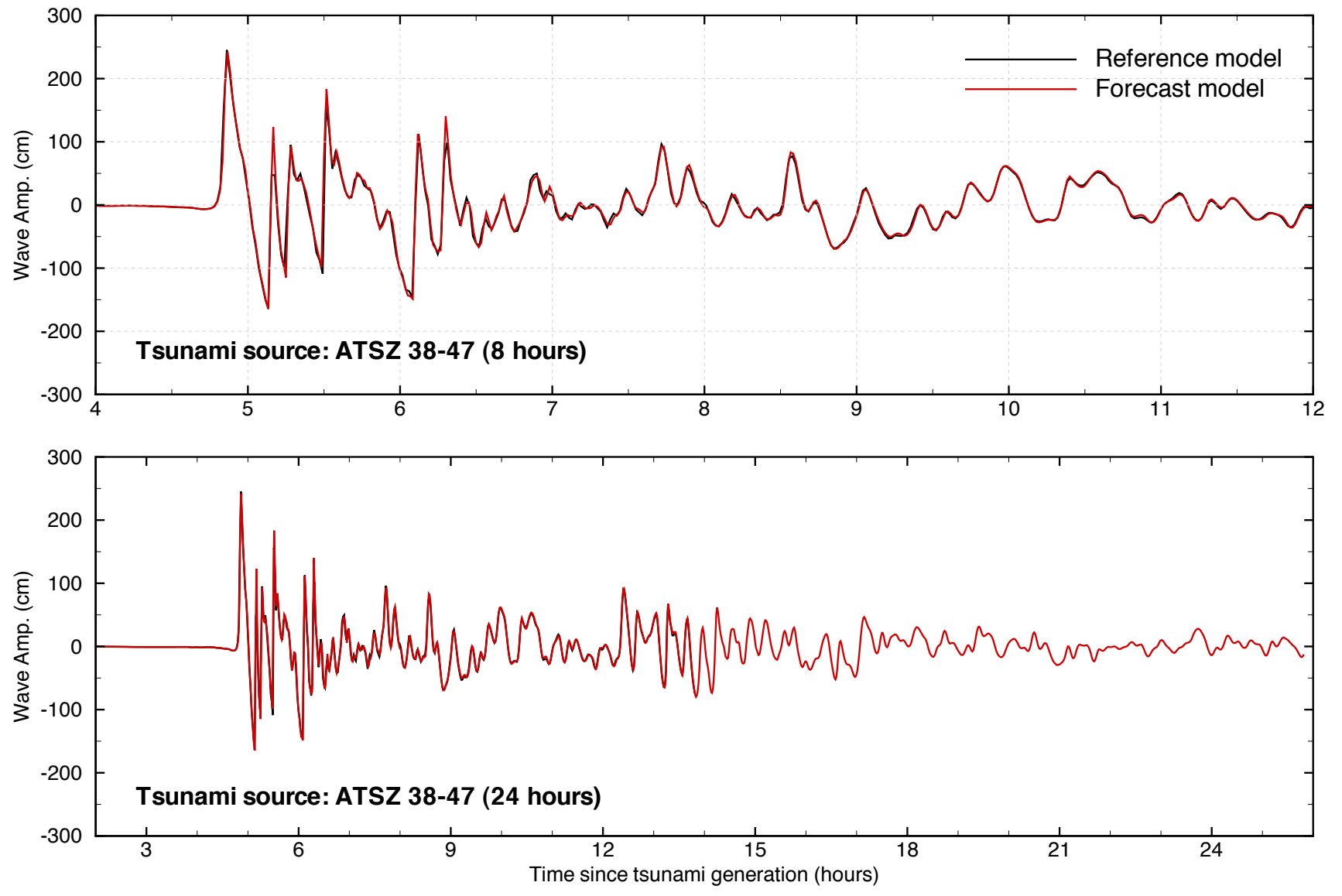
Reference model
Forecast model
Wave Amp. (cm)
Tsunami source: ATSZ 38-47 (8 hours)
Tsunami source: ATSZ 38-47 (24 hours)
Time since tsunami generation (hours)

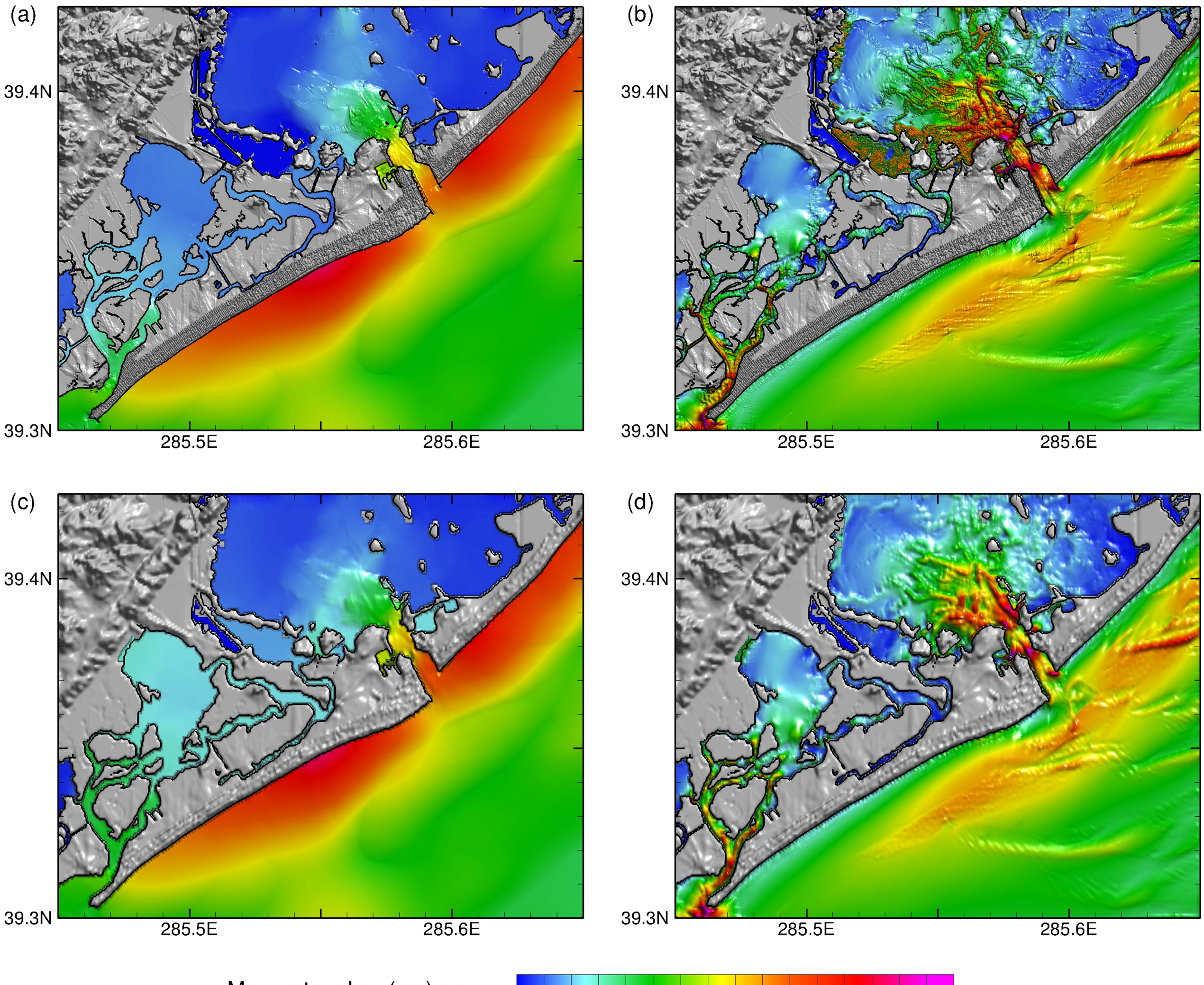
(a)
(b)
(c)
(d)
39.4N
39.3N
285.5E
285.6E
Max water elev. (cm) or
Max current speed (cm/s)
0
20
40
60
80
100
120
140
160

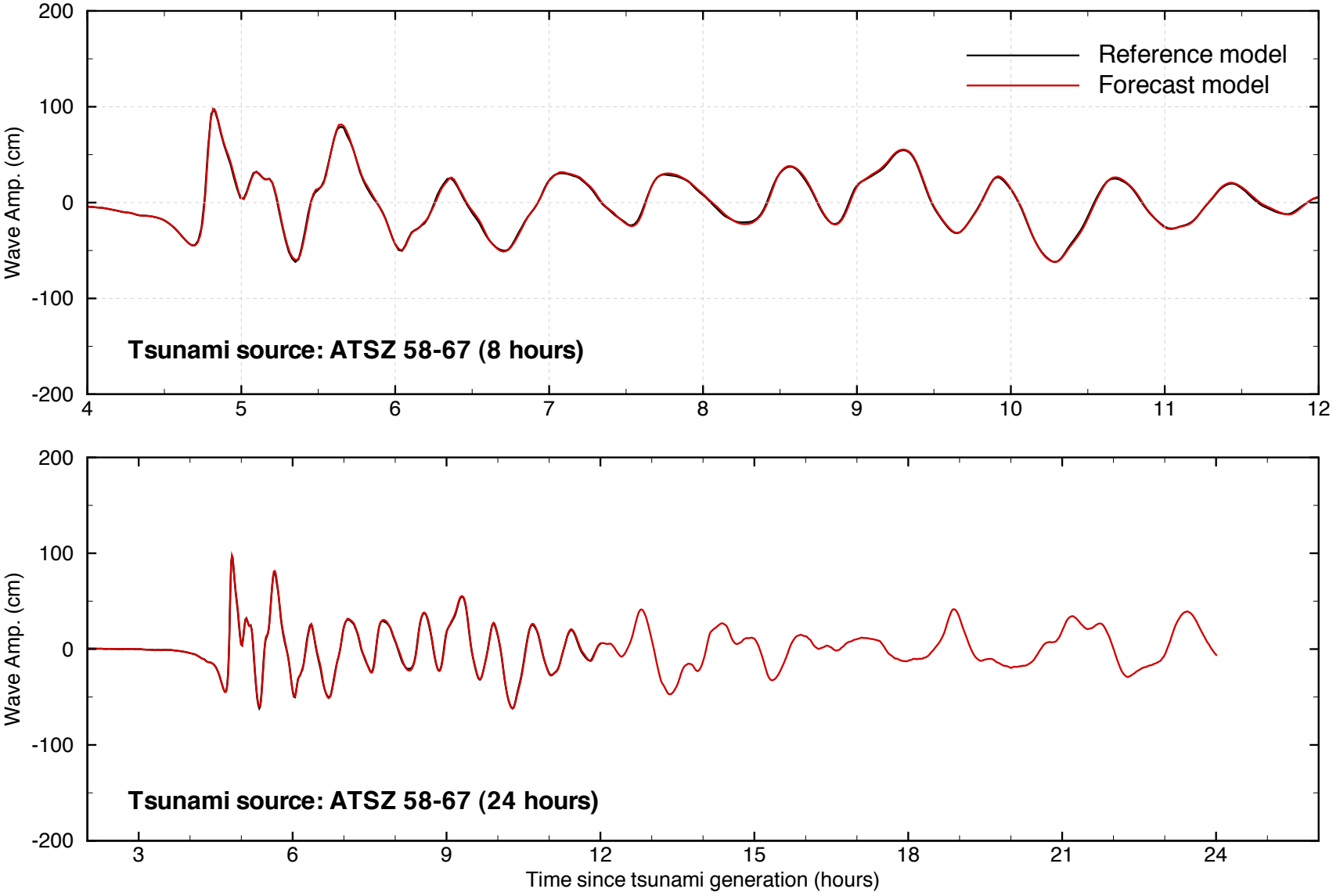
Reference model
Forecast model
Wave Amp. (cm)
Tsunami source: ATSZ 58-67 (8 hours)
Tsunami source: ATSZ 58-67 (24 hours)
Time since tsunami generation (hours)

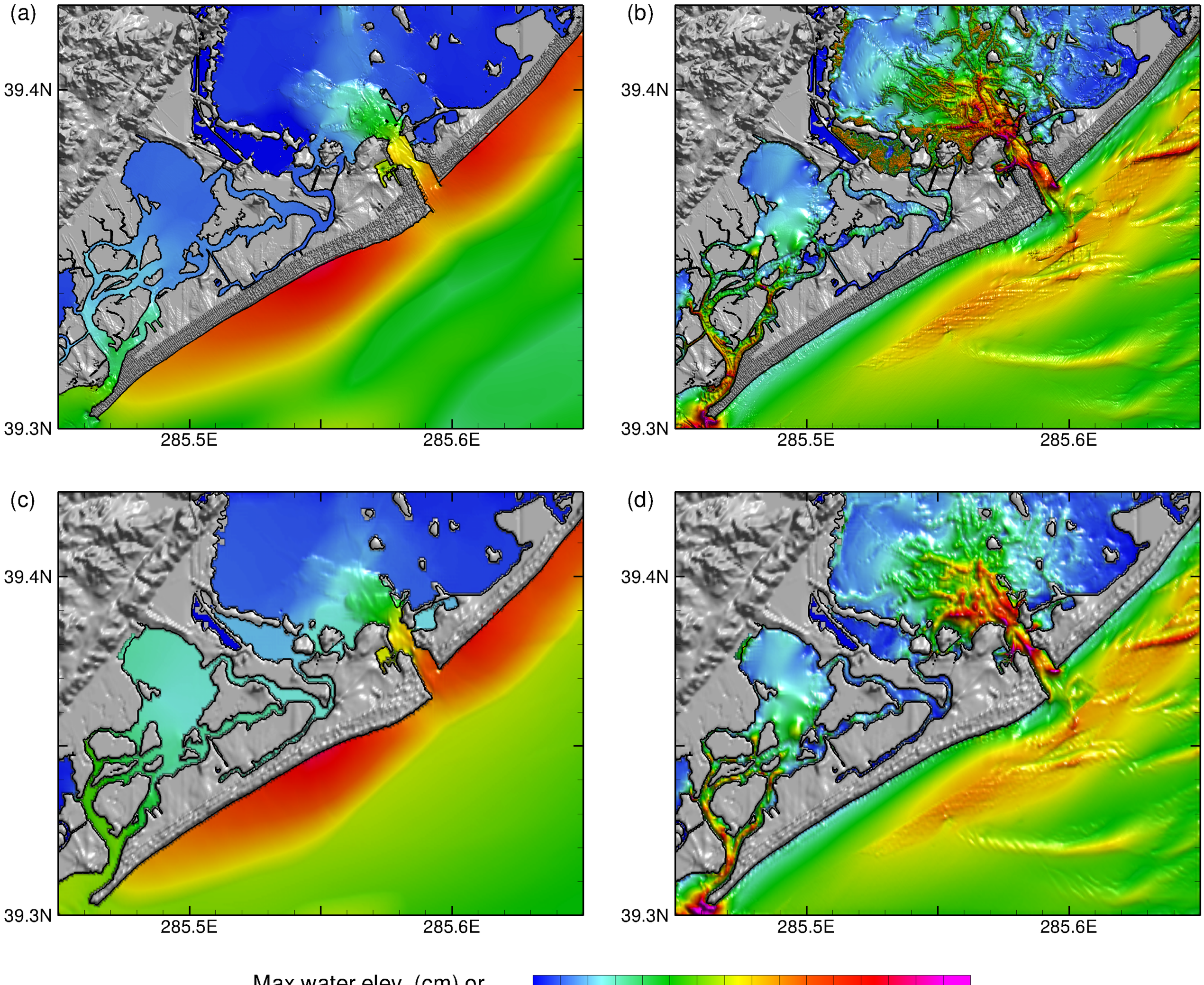
(a)
(b)
(c)
(d)
39.4N
39.3N
285.5E
285.6E
Max water elev. (cm) or
Max current speed (cm/s)
0
20
40
60
80
100
120
140
160

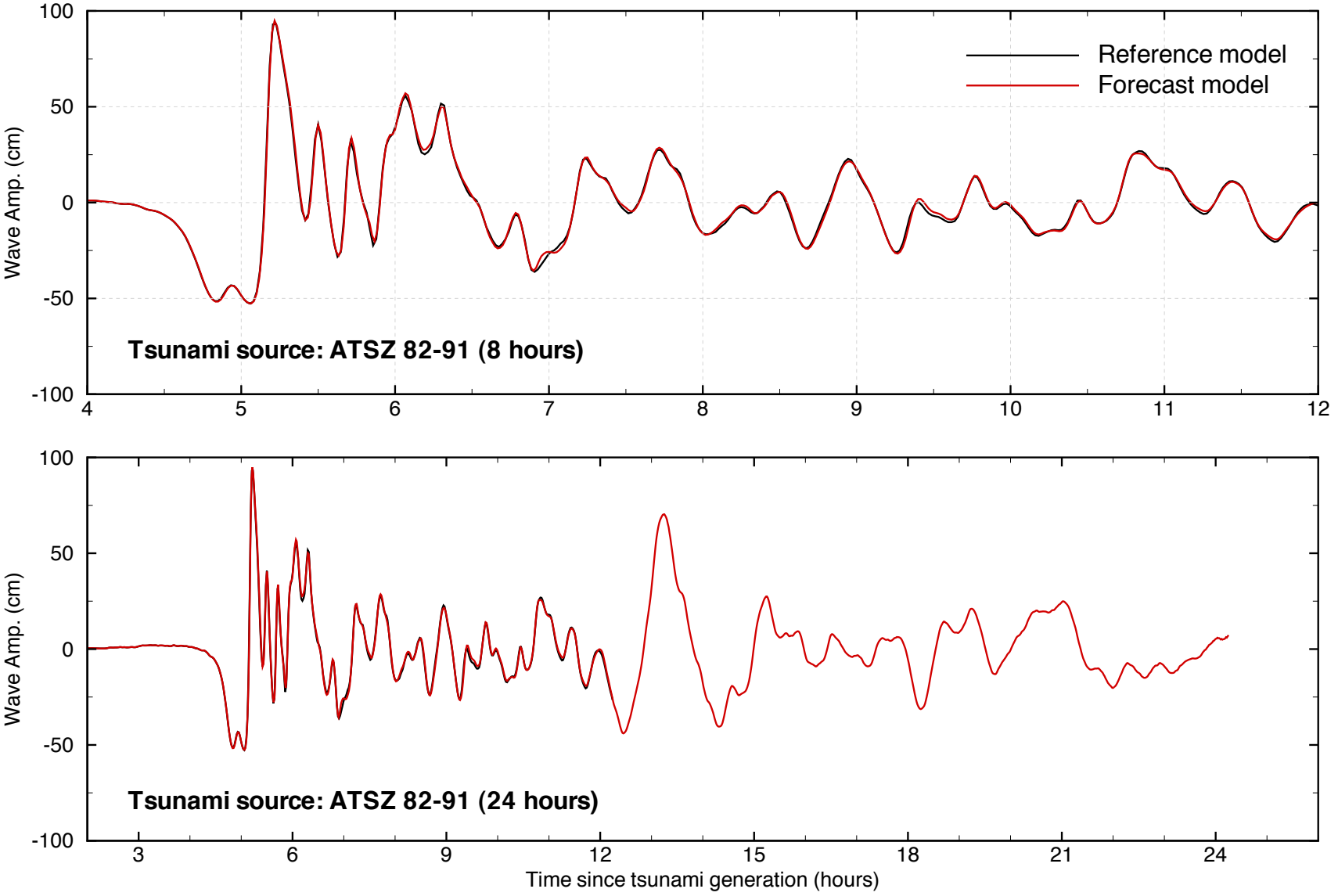
Reference model
Forecast model
Wave Amp. (cm)
Tsunami source: ATSZ 82-91 (8 hours)
Tsunami source: ATSZ 82-91 (24 hours)
Time since tsunami generation (hours)

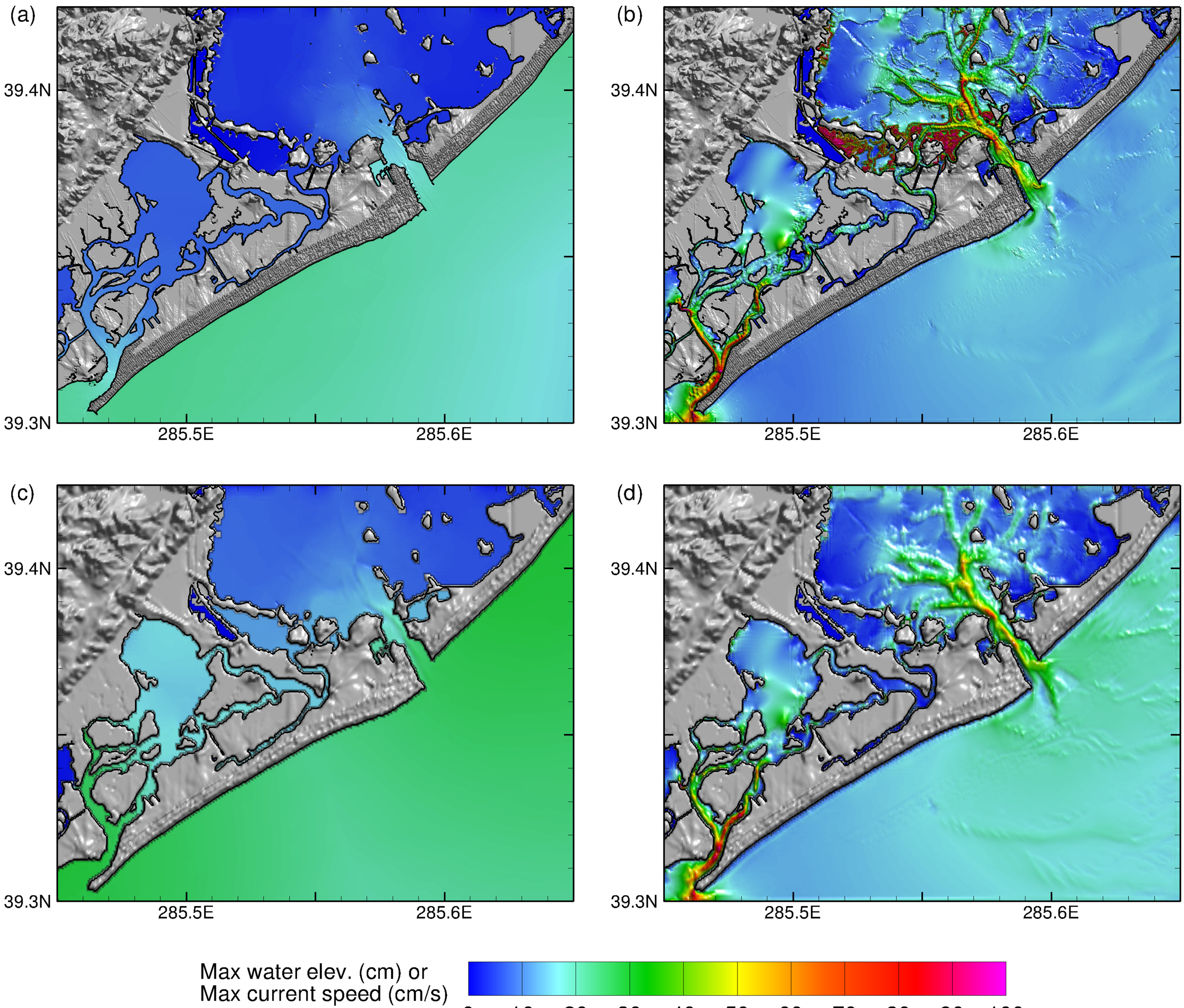
(a)
(b)
(c)
(d)
39.4N
39.3N
285.5E
285.6E
Max water elev. (cm) or
Max current speed (cm/s)
0
10
20
30
40
50
60
70
80
90
100

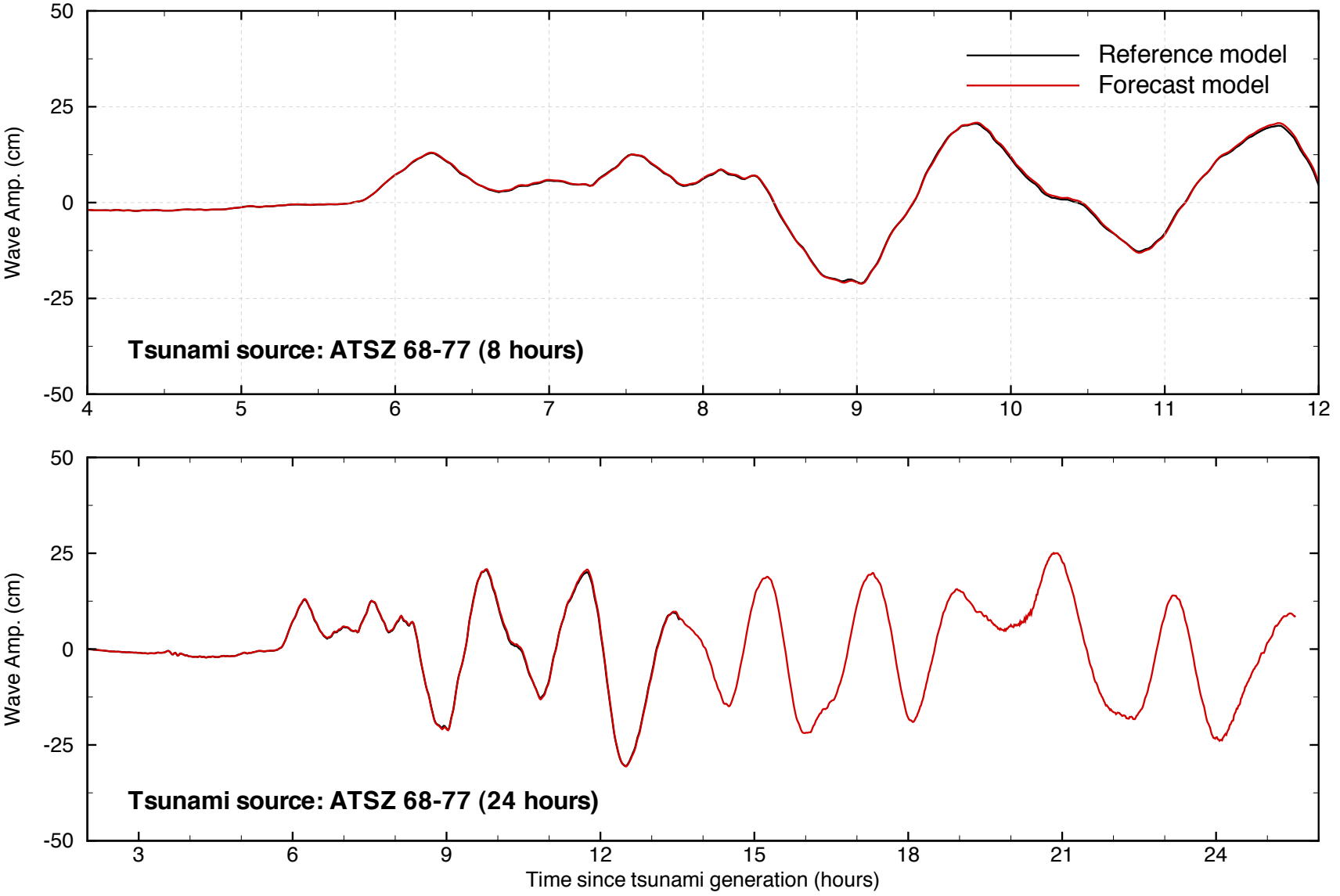
Reference model
Forecast model
Wave Amp. (cm)
Tsunami source: ATSZ 68-77 (8 hours)
Tsunami source: ATSZ 68-77 (24 hours)
Time since tsunami generation (hours)

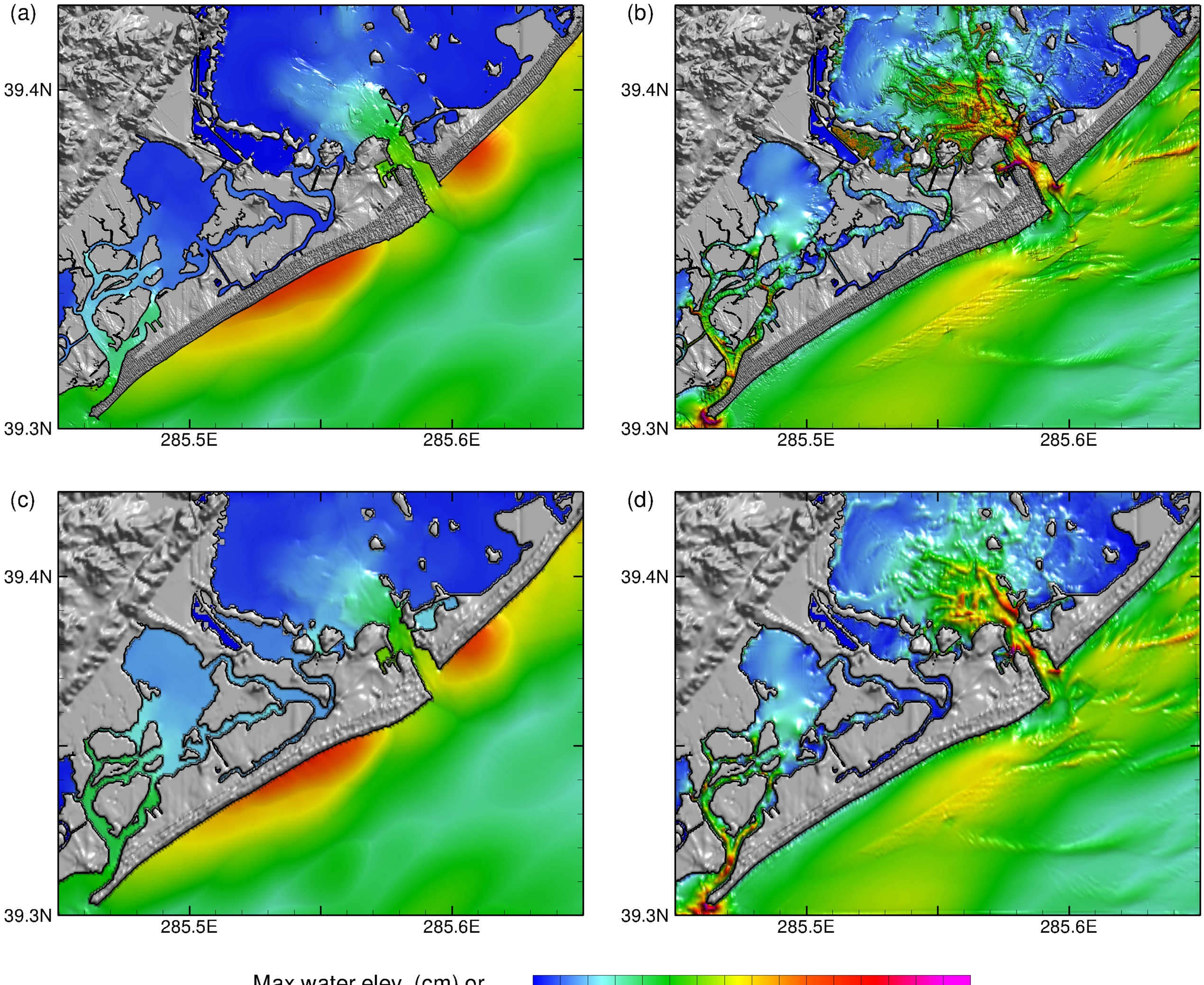
(a)
(b)
(c)
(d)
39.4N
39.3N
285.5E
285.6E
Max water elev. (cm) or
Max current speed (cm/s)
0
20
40
60
80
100
120
140
160

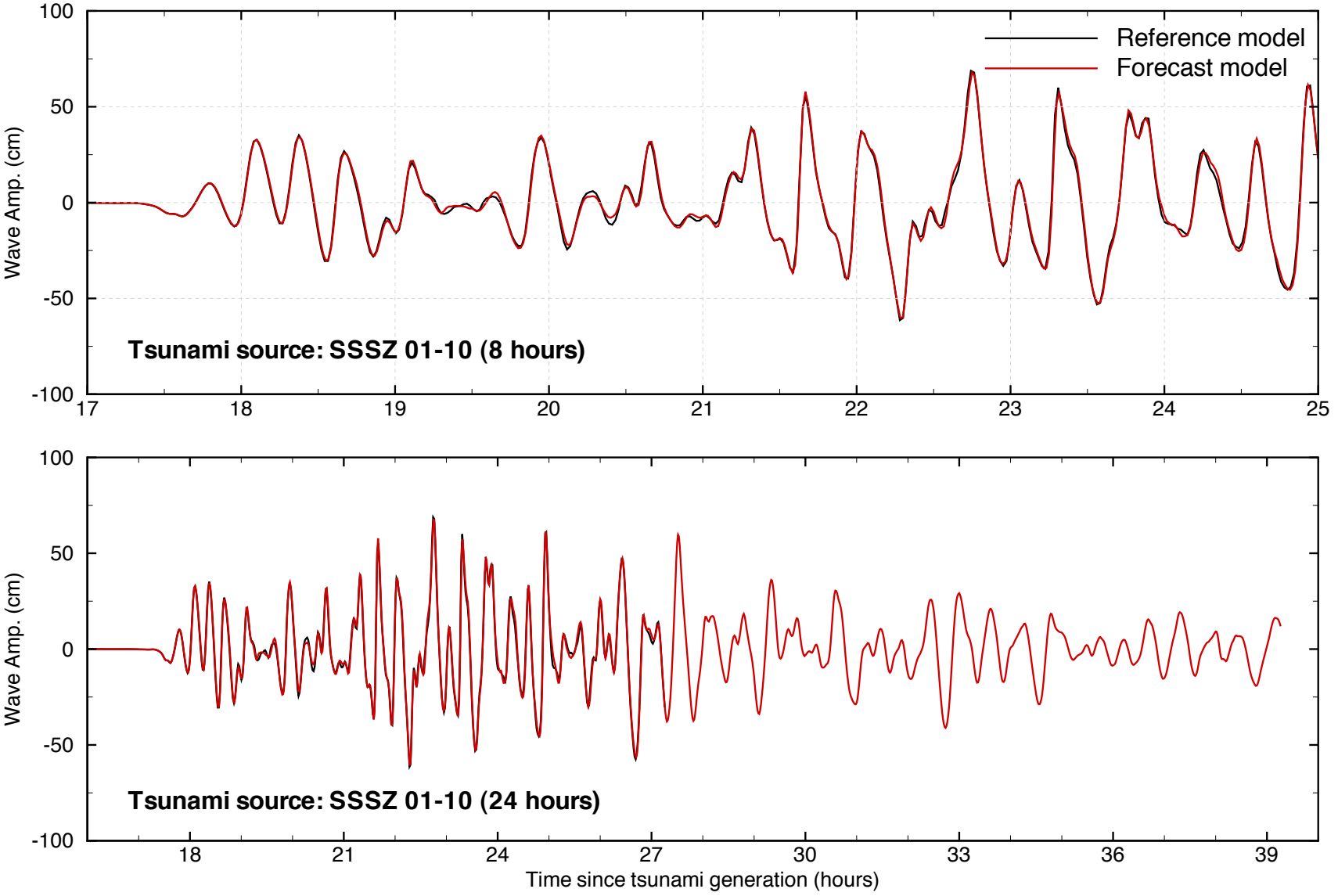
Reference model
Forecast model
Wave Amp. (cm)
Tsunami source: SSSZ 01-10 (8 hours)
100
50
0
-50
-100
17
18
19
20
21
22
23
24
25
Wave Amp. (cm)
Tsunami source: SSSZ 01-10 (24 hours)
100
50
0
-50
-100
18
21
24
27
30
33
36
39
Time since tsunami generation (hours)

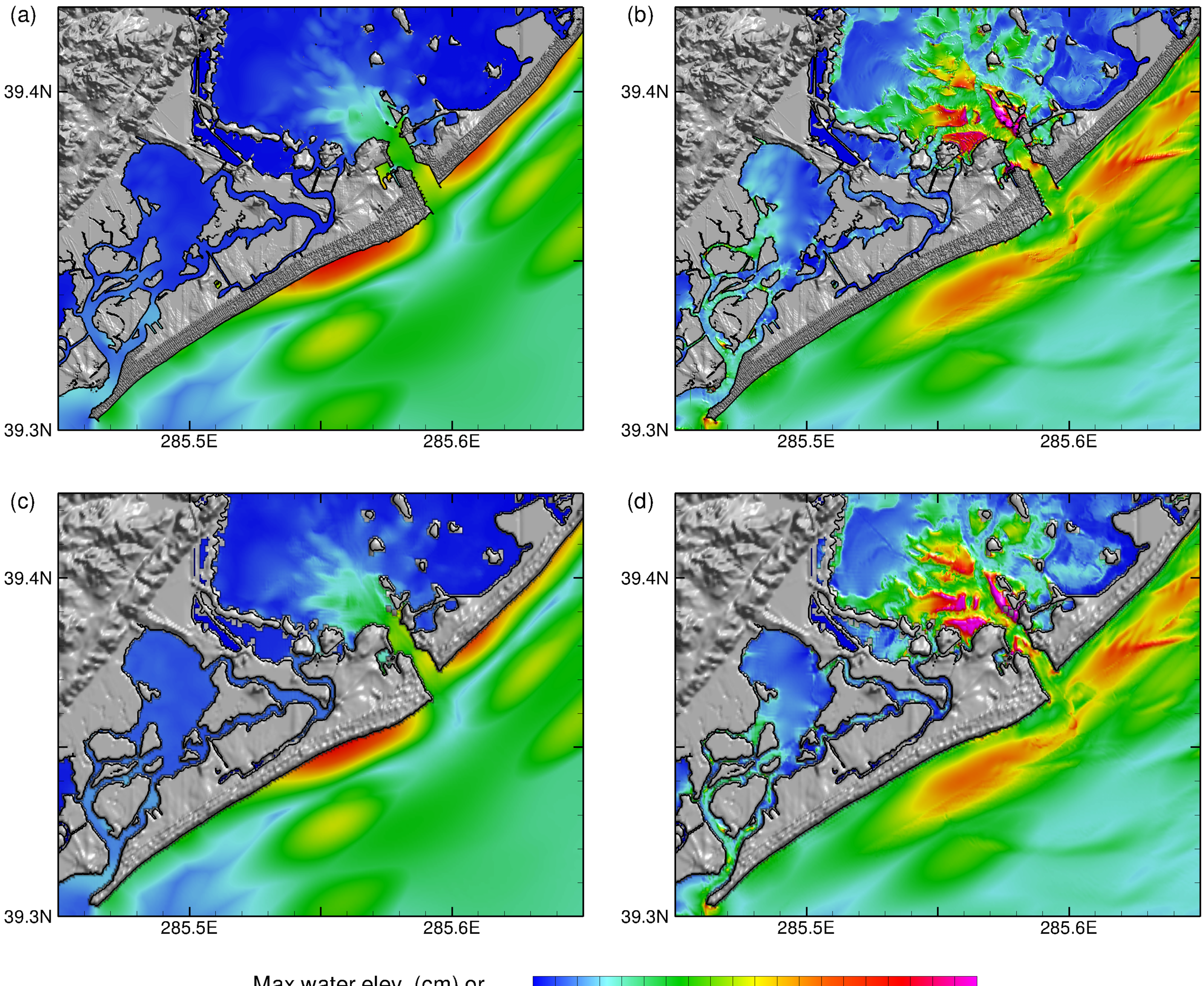
(a)
(b)
(c)
(d)
39.4N
39.3N
285.5E
285.6E
Max water elev. (cm) or
Max current speed (cm/s)
0
2
4
6
8
10
12
14
16
18
20

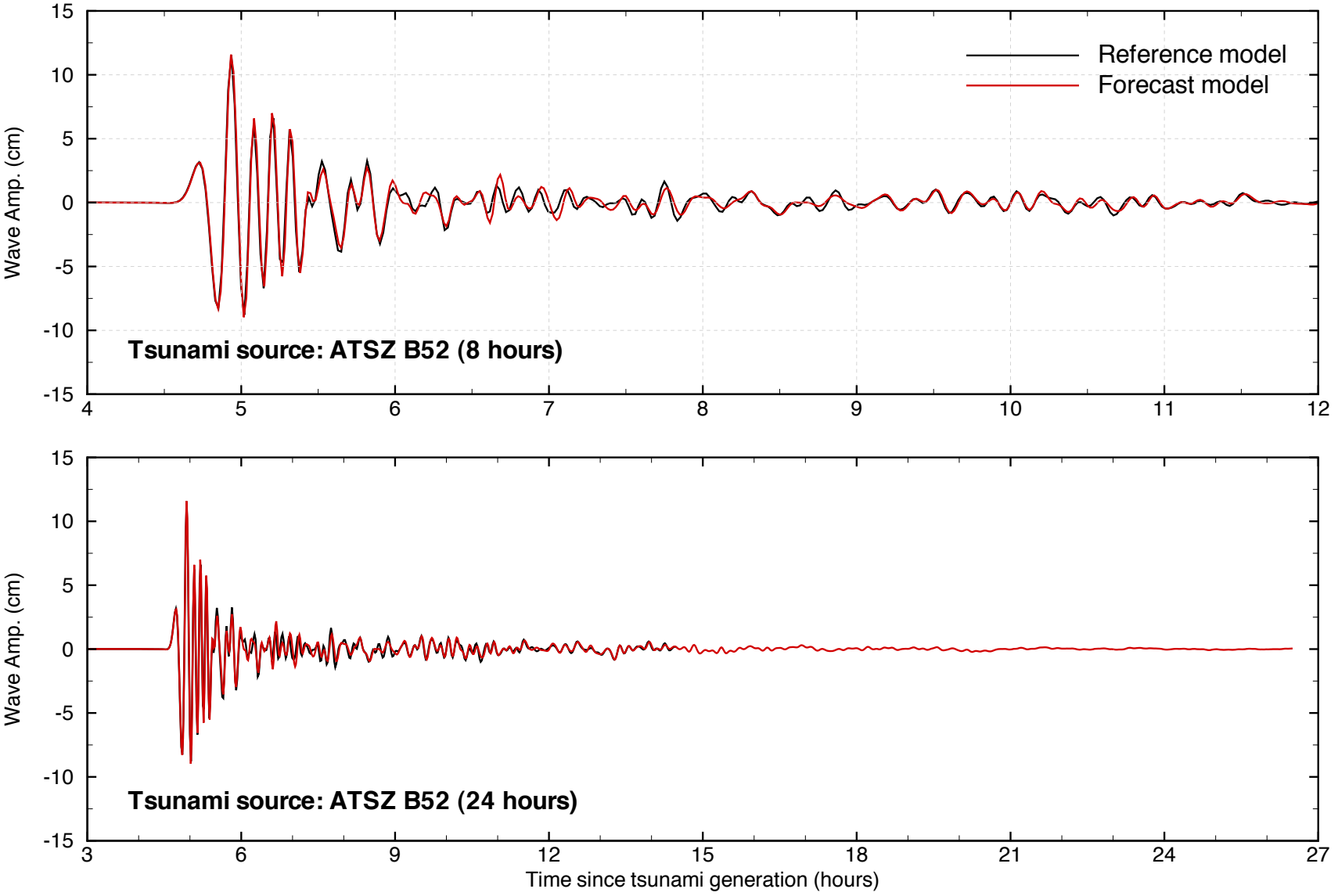
Reference model
Forecast model
Wave Amp. (cm)
Tsunami source: ATSZ B52 (8 hours)
Tsunami source: ATSZ B52 (24 hours)
Time since tsunami generation (hours)

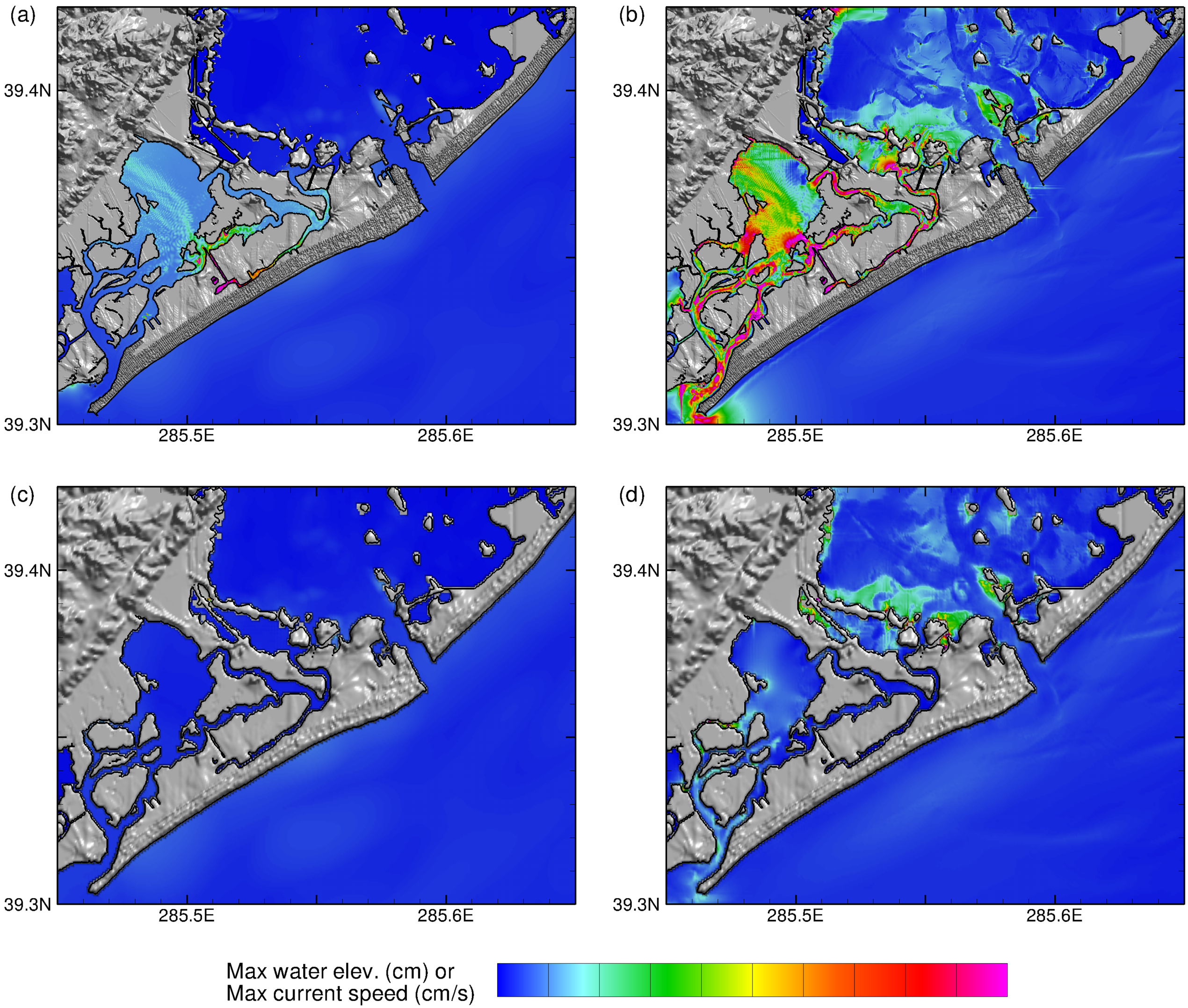
(a)
(b)
(c)
(d)
39.4N
39.3N
285.5E
285.6E
Max water elev. (cm) or
Max current speed (cm/s)
0
0.05
0.1
0.15
0.2
0.25
0.3
0.35
0.4
0.45
0.5

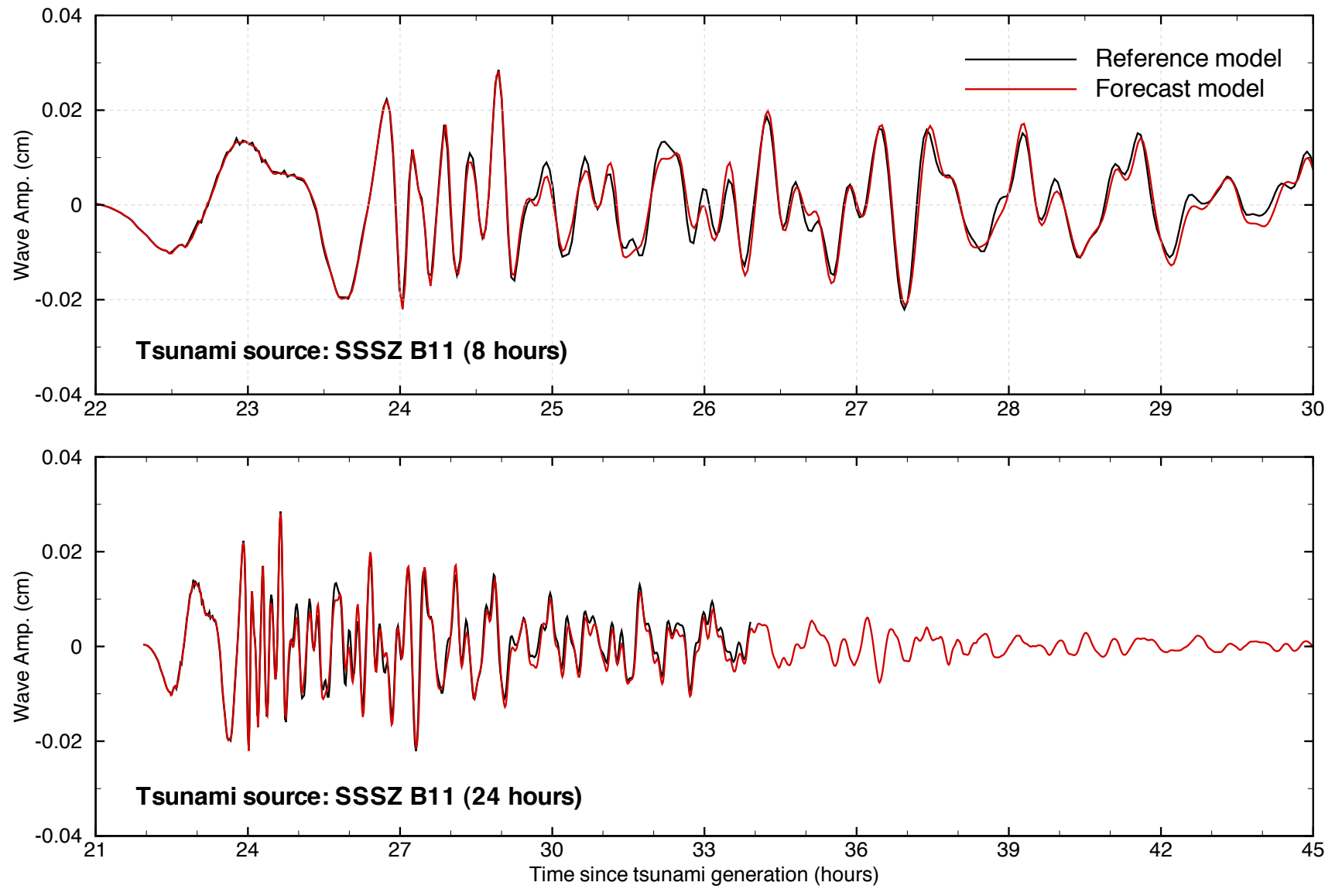
Reference model
Forecast model
Tsunami source: SSSZ B11 (8 hours)
Tsunami source: SSSZ B11 (24 hours)
Wave Amp. (cm)
Wave Amp. (cm)
Time since tsunami generation (hours)
0.04
0.02
0
-0.02
-0.04
22
23
24
25
26
27
28
29
30
21
24
27
30
33
36
39
42
45

Appendix C: Tsunami Forecast System Testing

Jean Newman, Yong Wei

1.0 PURPOSE

Forecast models are tested with synthetic tsunami events covering a range of tsunami source locations. Testing is also done with selected historical tsunami events when available.

The purpose of forecast model testing is three-fold. The first objective is to assure that the results obtained with NOAA's tsunami forecast system, which has been released to the Tsunami Warning Centers for operational use, are identical to those obtained by the researcher during the development of the forecast model. The second objective is to test the forecast model for consistency, accuracy, time efficiency, and quality of results over a range of possible tsunami locations and magnitudes. The third objective is to identify bugs and issues in need of resolution by the researcher who developed the Forecast Model or by the forecast software development team before the next version release to NOAA's two Tsunami Warning Centers.

Local hardware and software applications, and tools familiar to the researcher(s), are used to run the Method of Splitting Tsunamis (MOST) model during the forecast model development. The test results presented in this report lend confidence that the model performs as developed and produces the same results when initiated within the forecast application in an operational setting as those produced by the researcher during the forecast model development. The test results assure those who rely on the Atlantic City tsunami forecast model that consistent results are produced irrespective of system.

2.0 TESTING PROCEDURE

The general procedure for forecast model testing is to run a set of synthetic tsunami scenarios through the forecast system application and compare the results with those obtained by the researcher during the forecast model development and presented in the Tsunami Forecast Model Report. Specific steps taken to test the model include:

1. Identification of testing scenarios, including the standard set of synthetic events and customized synthetic scenarios that may have been used by the researcher(s) in developing the forecast model.
2. Creation of new events to represent customized synthetic scenarios used by the researcher(s) in developing the forecast model, if any.
3. Submission of test model runs with the forecast system, and export of the results from A, B, and C grids, along with time series.
4. Recording applicable metadata, including the specific version of the forecast system used for testing.
5. Examination of forecast model results from the forecast system for instabilities in both time series and plot results.
6. Comparison of forecast model results obtained through the forecast system with those obtained during the forecast model development.
7. Summarization of results with specific mention of quality, consistency, and time efficiency.
8. Reporting of issues identified to modeler and forecast software development team.

9. Retesting the forecast models in the forecast system when reported issues have been addressed or explained.

Synthetic model runs were tested on a DELL PowerEdge R510 computer equipped with two Xeon E5670 processors at 2.93 Ghz, each with 12 MBytes of cache and 32GB memory. The processors are hex core and support hyperthreading, resulting in the computer performing as a 24 processor core machine. Additionally, the testing computer supports 10 Gigabit Ethernet for fast network connections. This computer configuration is similar or the same as the configurations of the computers installed at the Tsunami Warning Centers so the compute times should only vary slightly.

3.0 Results

The Atlantic City forecast model was tested with NOAA's tsunami forecast system version 3.2.

The Atlantic City, New Jersey forecast model was tested with three synthetic scenarios. Test results from the forecast system and comparisons with the results obtained during the forecast model development are shown numerically in Table 2 and graphically in Figures 1 to 3. The results show that the forecast model is stable and robust, with consistent and high quality results across geographically distributed tsunami sources and mega-event tsunami magnitudes. The model run time (wall clock time) was under 38 minutes for 12 hours of simulation time, and under 13 minutes for 4 hours. This run time is just over the 10 minute run time for 4 hours of simulation time that satisfies time efficiency requirements.

Three synthetic events were run on the Atlantic City forecast model. The modeled scenarios were stable for all cases tested, with no instabilities or ringing. Results show that the largest modeled height was 489.88 cm and originated in the Caribbean (ATSZ 48-57) source. Amplitudes greater than 100 cm were recorded for the two test sources. The smallest signal of 48.92 cm was recorded for the far field South Sandwich Islands (SSSZ 1-10) source. Direct comparisons, of output from the forecast tool with results from available development synthetic events, demonstrated that the wave pattern is similar in shape, pattern and amplitude but does not match by eye. These discrepancies are mainly caused by different propagation databases used to provide the boundary conditions for model runs. Developed in April 2011, the forecast model report shows the Atlantic City model results based on an old tsunami propagation database, while the SITF testing results in Appendix C reflect the tsunami propagation database that were updated in December of 2011. It is known that the new propagation database will lead to improvement of the model results.

Source Zone	Tsunami Source	α [m]	SIFT Max (cm)	Development Max (cm)	SIFT Min (cm)	Development Min (cm)
ATSZ	A38-A47, B38-B47	25	271.005	241.7	-171.153	-164.2
ATSZ	A48-A57, B48-B57	25	489.880	486.7	-314.680	-322.7
SSSZ	A1-A10, B1-B10	25	48.919	67.9	-47.050	-60.13

Table 1. Table of maximum and minimum amplitudes (cm) at the Atlantic City, New Jersey warning point for synthetic and historical events tested using SIFT 3.2 and obtained during development.

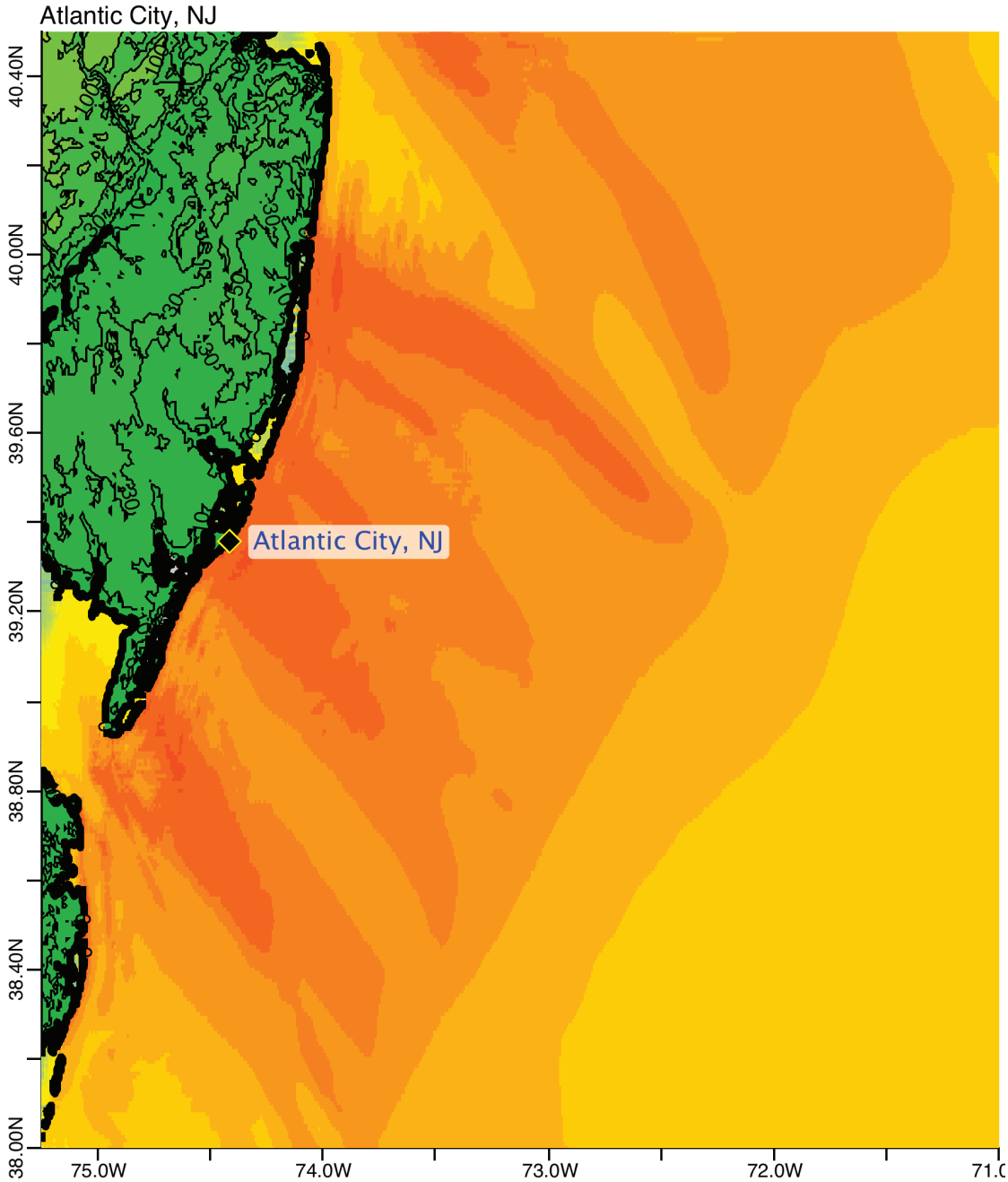

Figure 1. Max computed wave amplitude of A grid, Atlantic City, for synthetic event ATSZ 38-47.

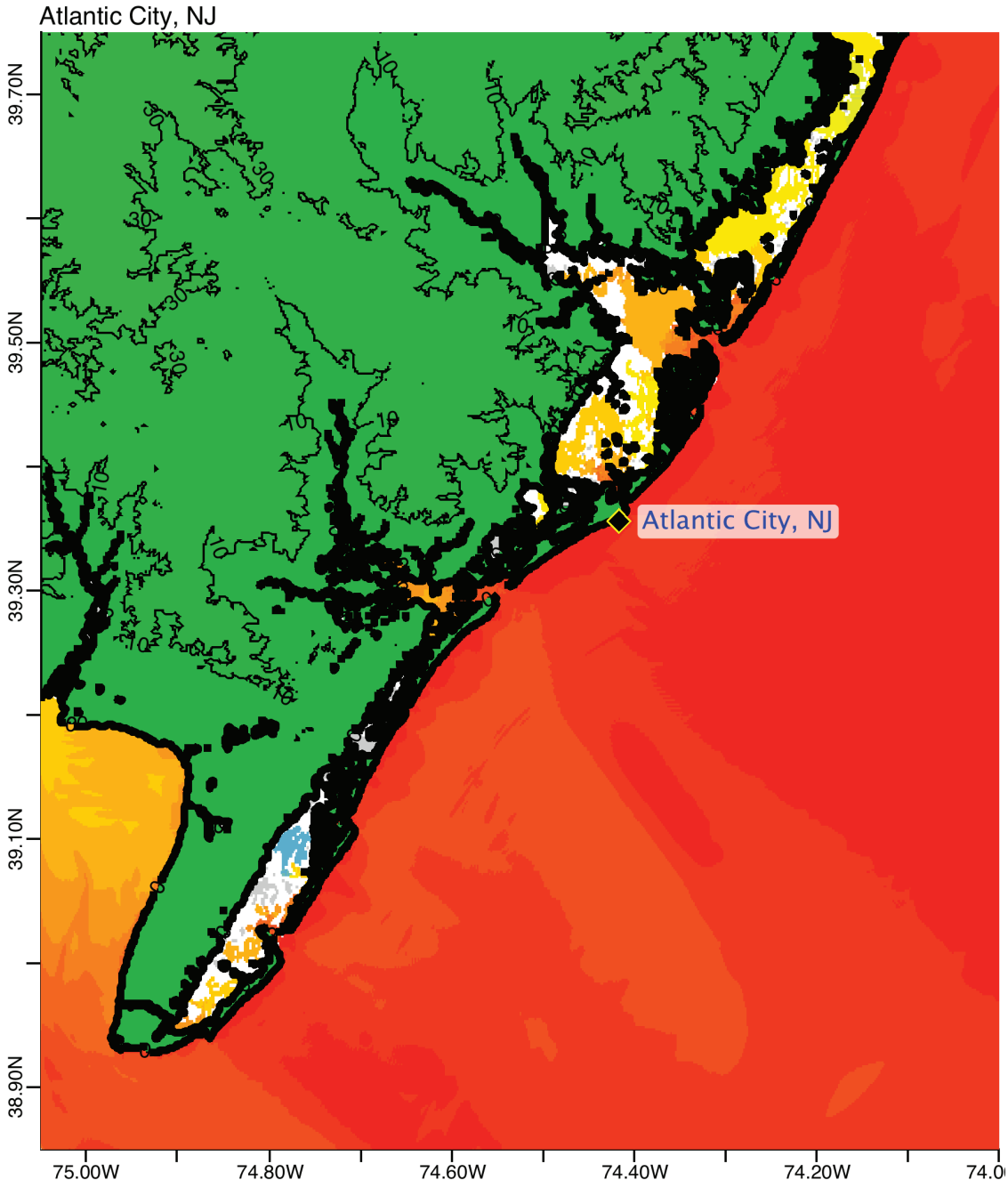

Figure 2. Max computed wave amplitude of B grid, Atlantic City, for synthetic event ATSZ 38-47.

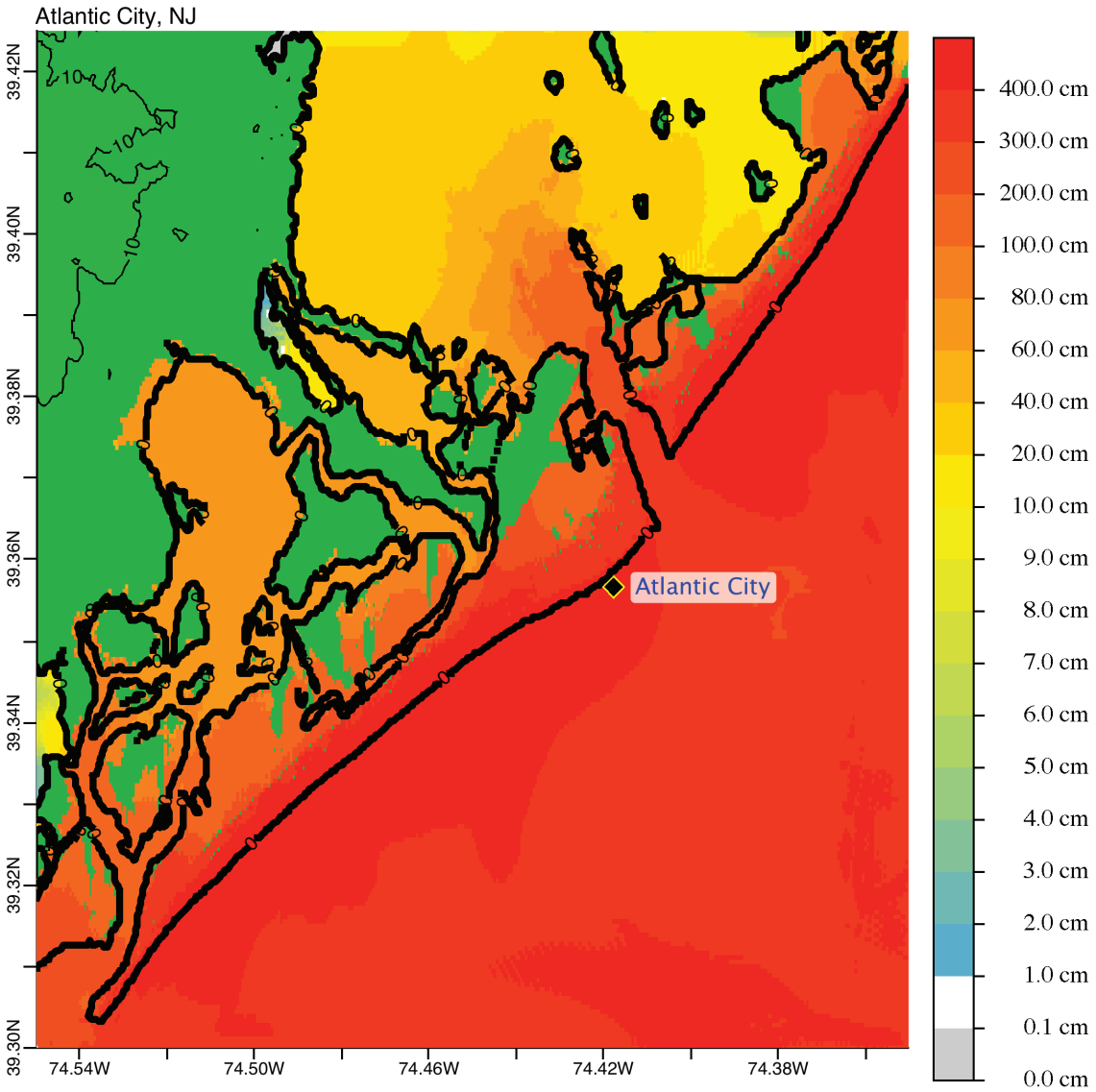

Figure 3. Max computed wave amplitude of C grid, Atlantic City, for synthetic event ATSZ 38-47.

(a)

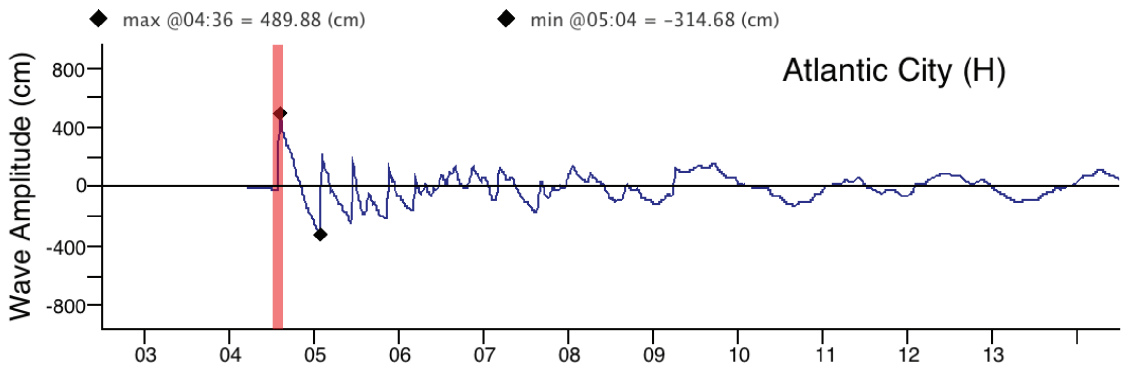

(b)

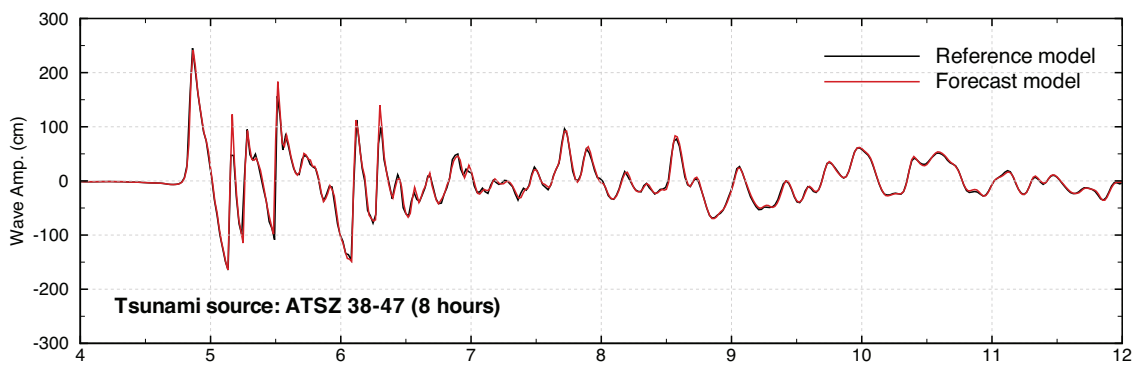

Figure 4. Computed time series at Atlantic City tide gage, for synthetic event ATSZ 38-47: (a) time series computed in the forecast system; (b) time series shown in the forecast model report.

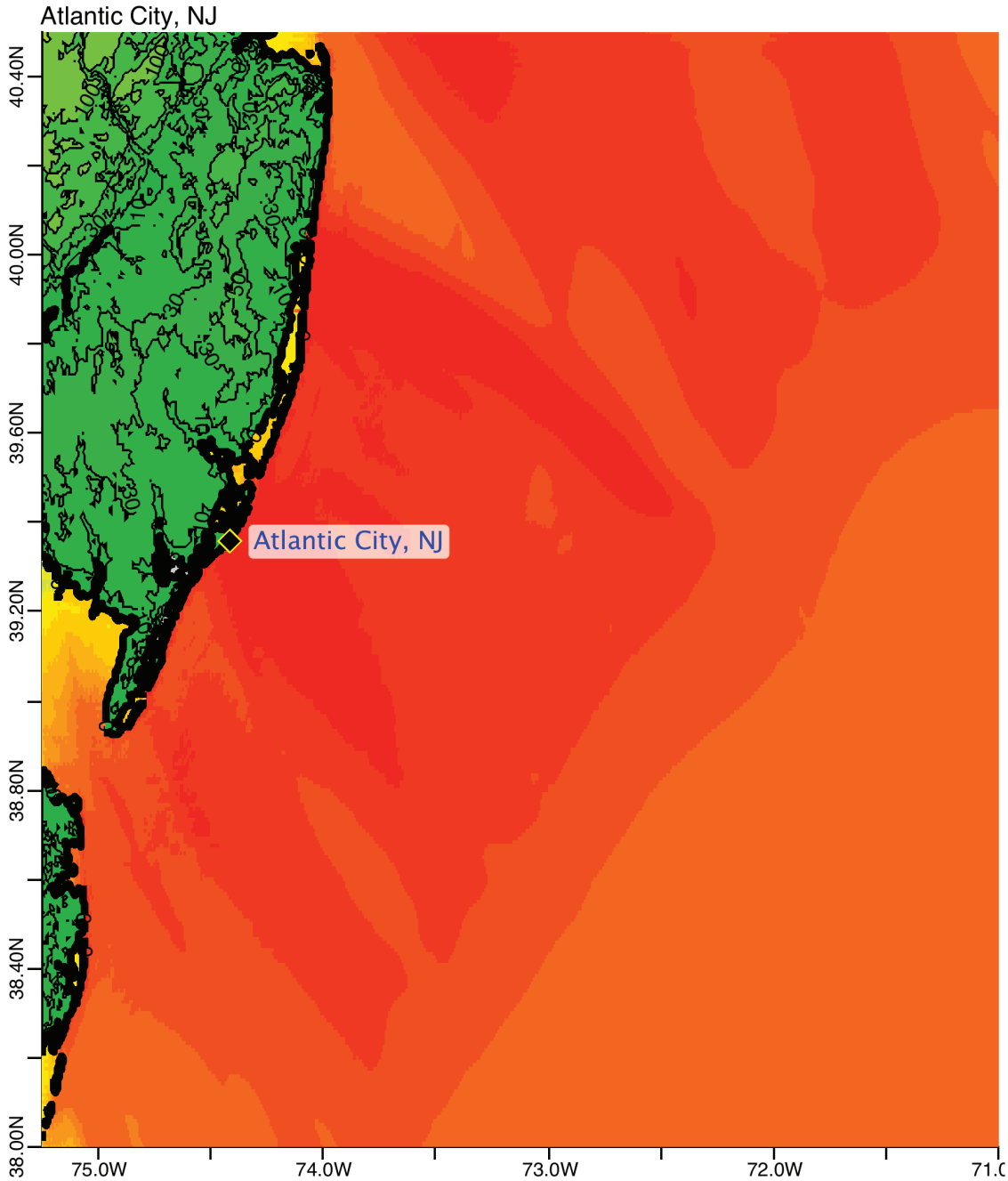

Figure 5. Max computed wave amplitude of A grid, Atlantic City, for synthetic event ATSZ 48-57.

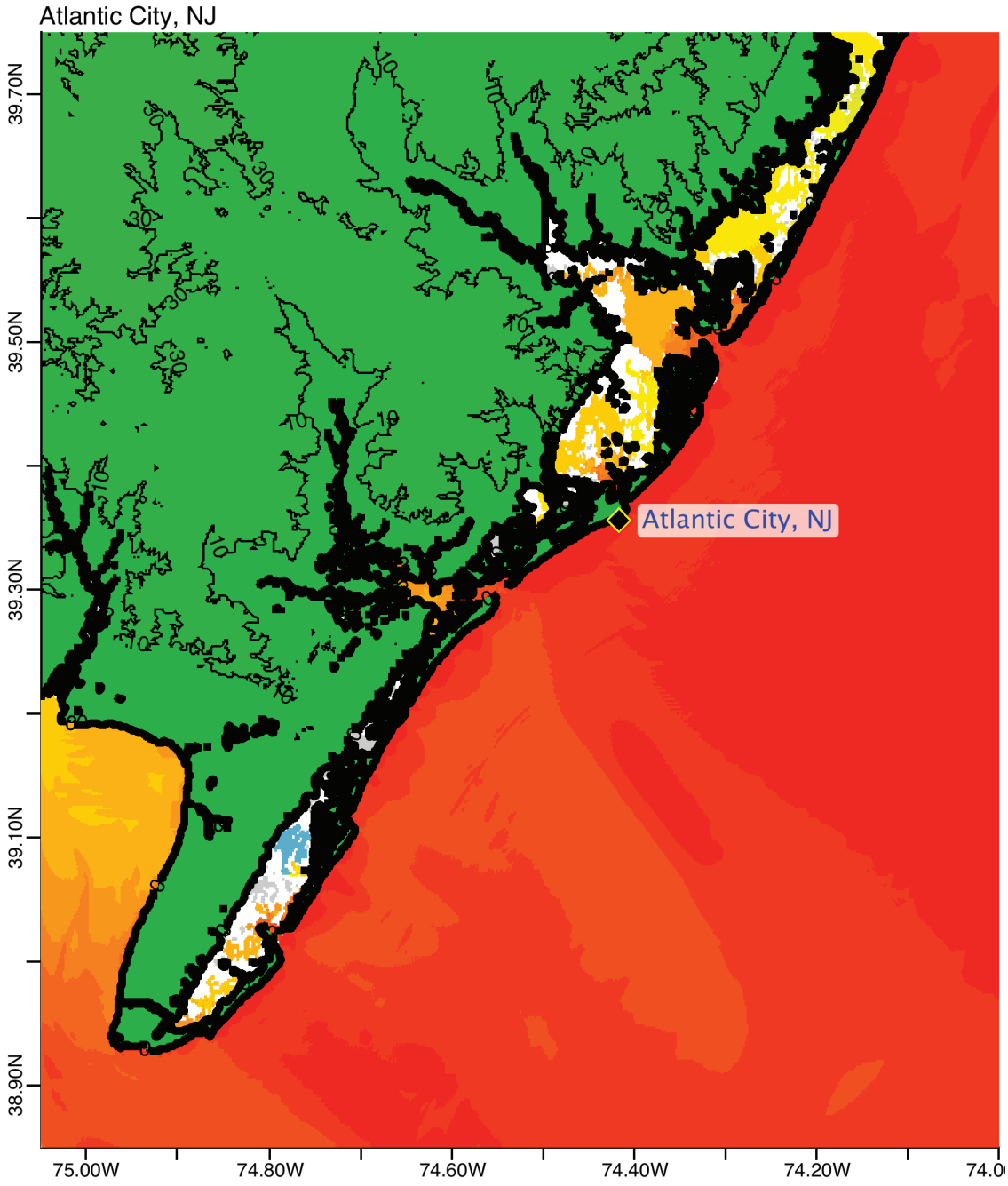

Figure 6. Max computed wave amplitude of B grid, Atlantic City, for synthetic event ATSZ 48-57.

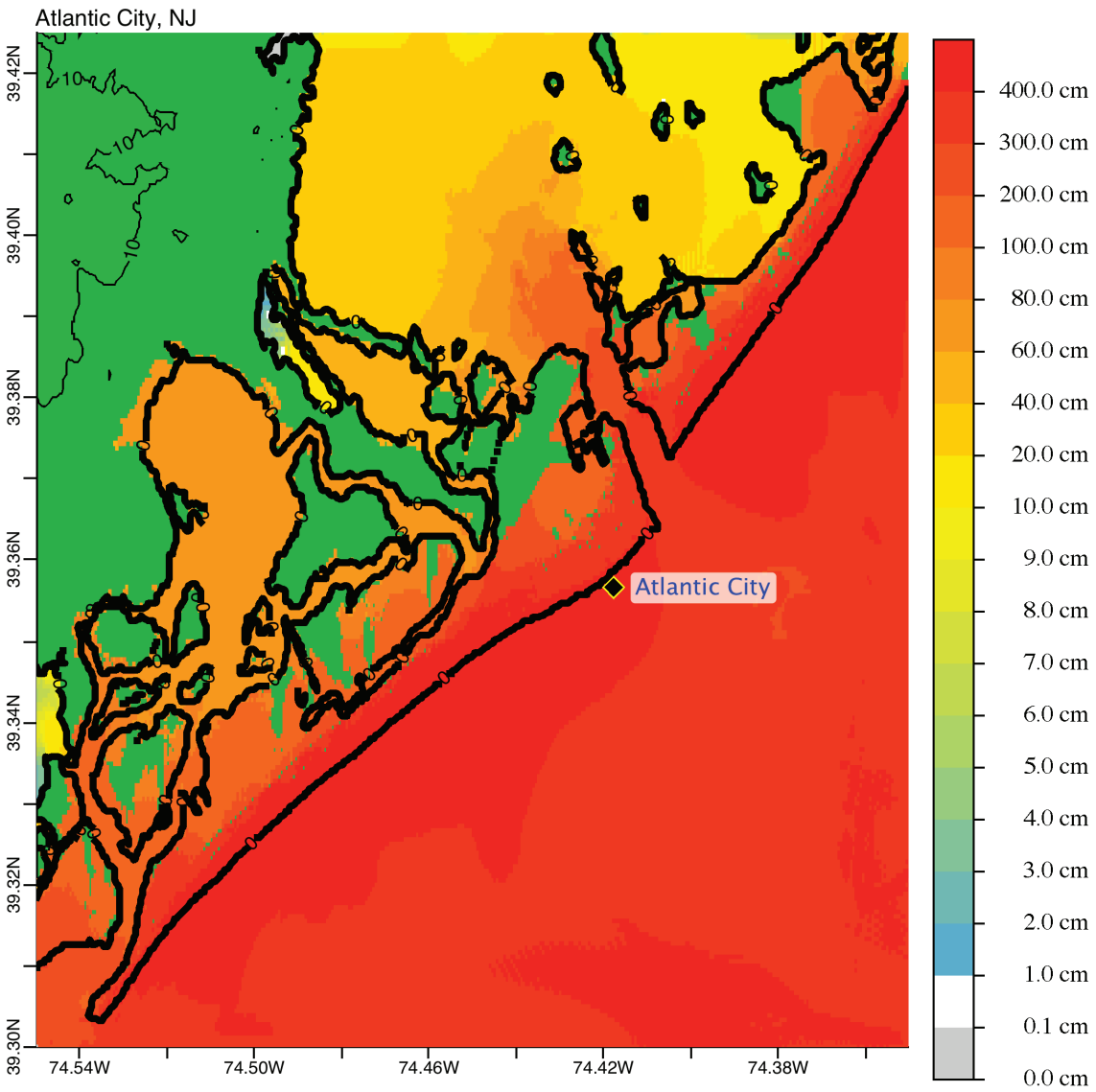

Figure 7. Max computed wave amplitude of C grid, Atlantic City, for synthetic event ATSZ 48-57.

(a)

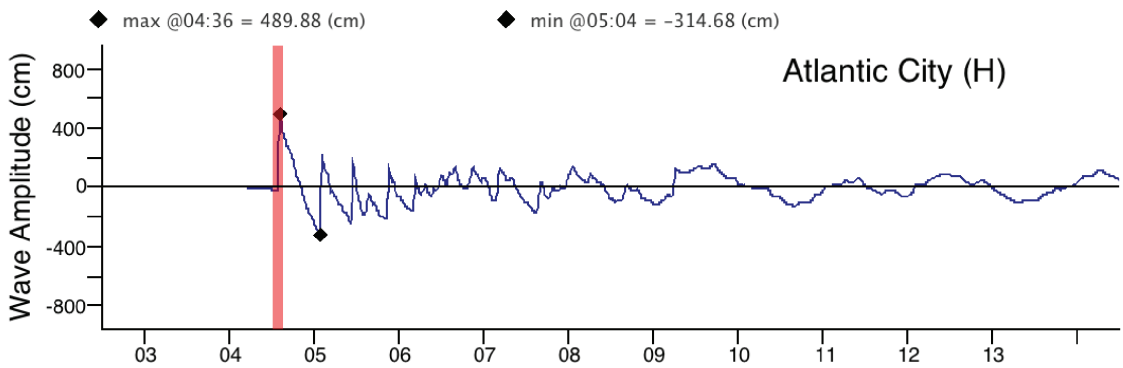

(b)

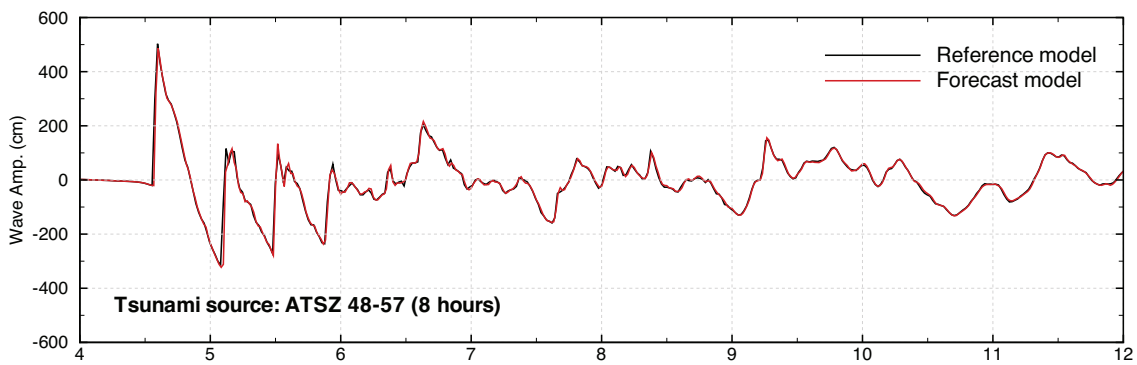

Figure 8. Computed time series at Atlantic City tide gage, for synthetic event ATSZ 48-57: (a) time series computed in the forecast system; (b) time series shown in the forecast model report.

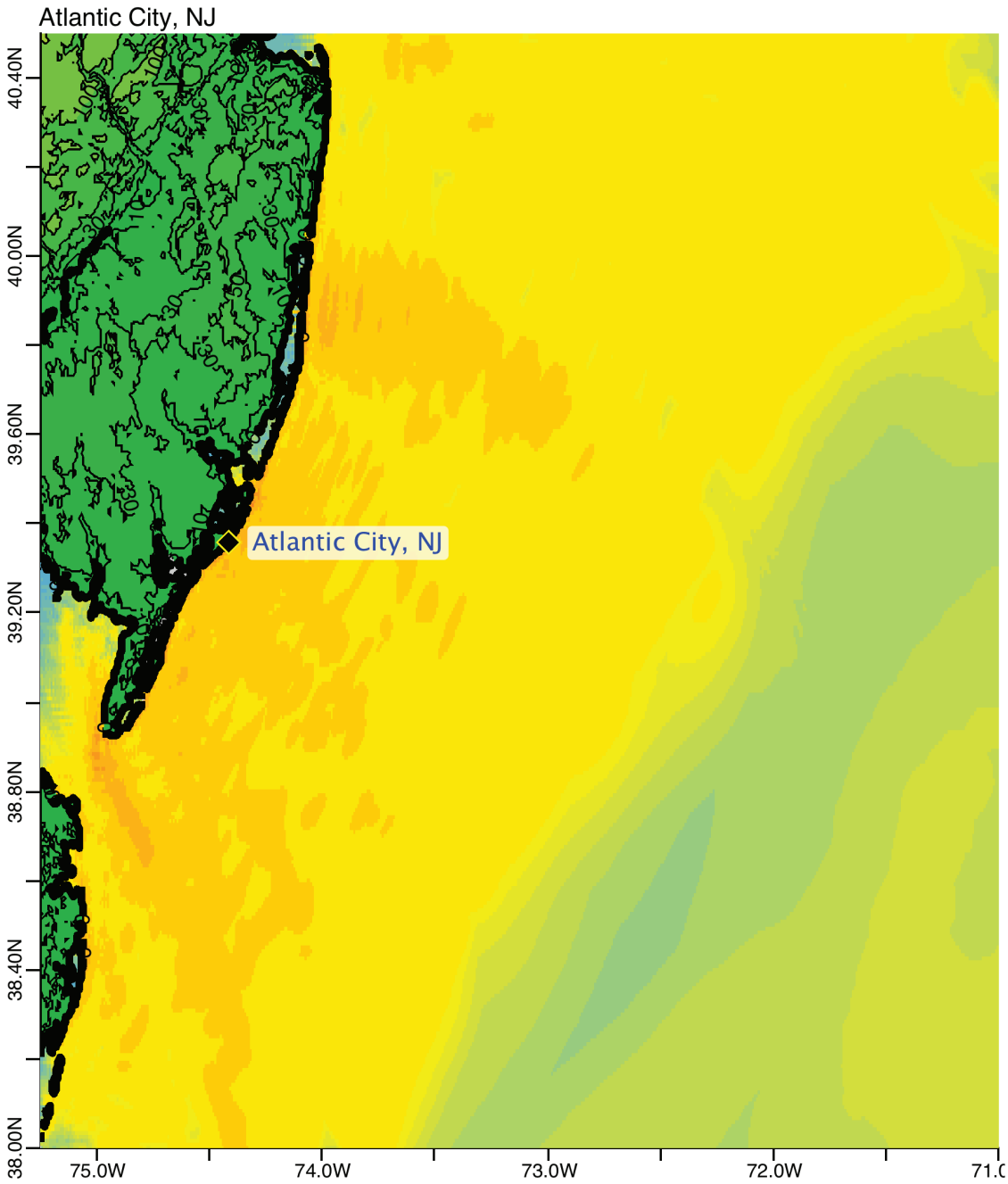

Figure 9. Max computed wave amplitude of A grid, Atlantic City, for synthetic event SSSZ 1-10.

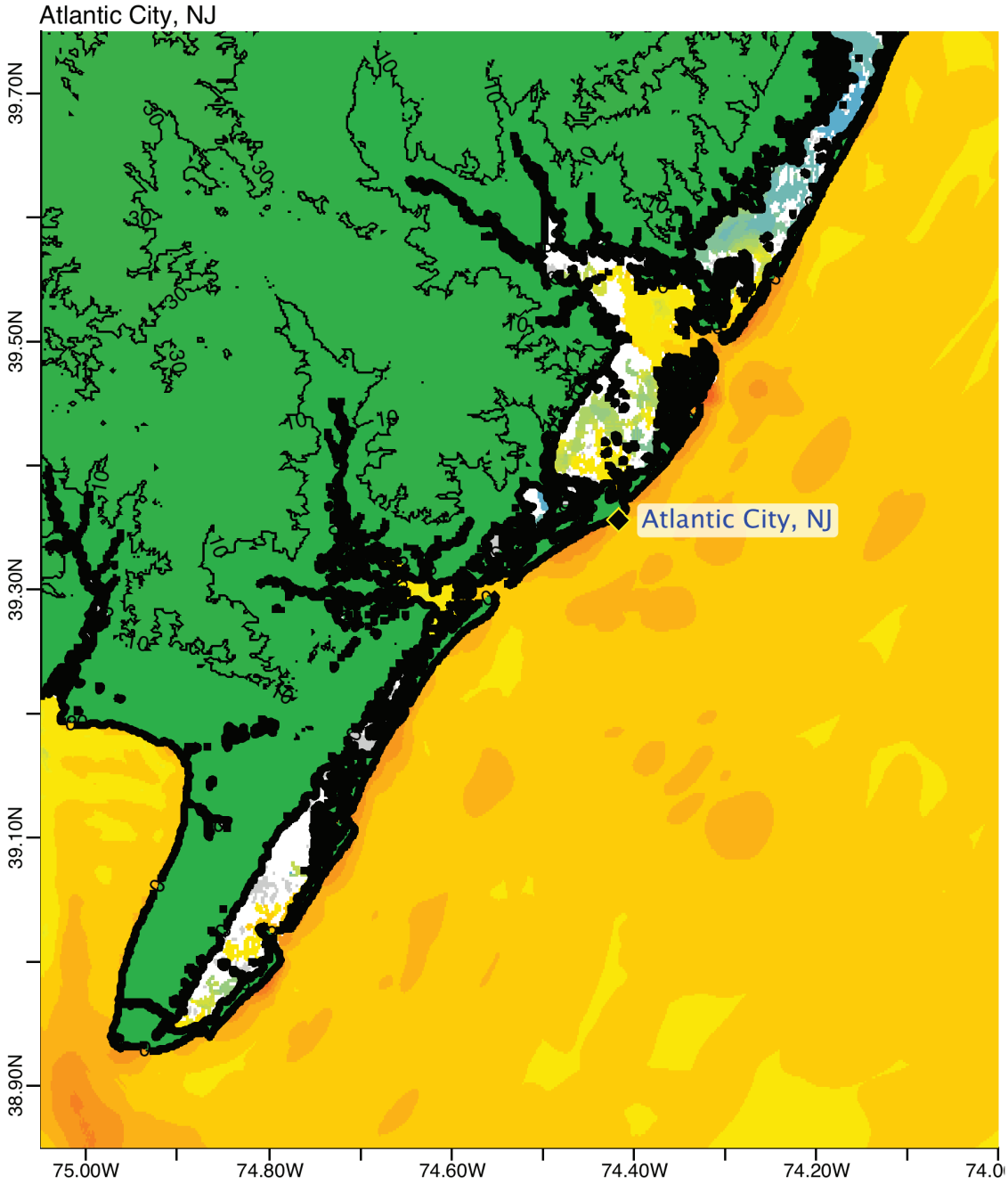

Figure 10. Max computed wave amplitude of B grid, Atlantic City, for synthetic event SSSZ 1-10.

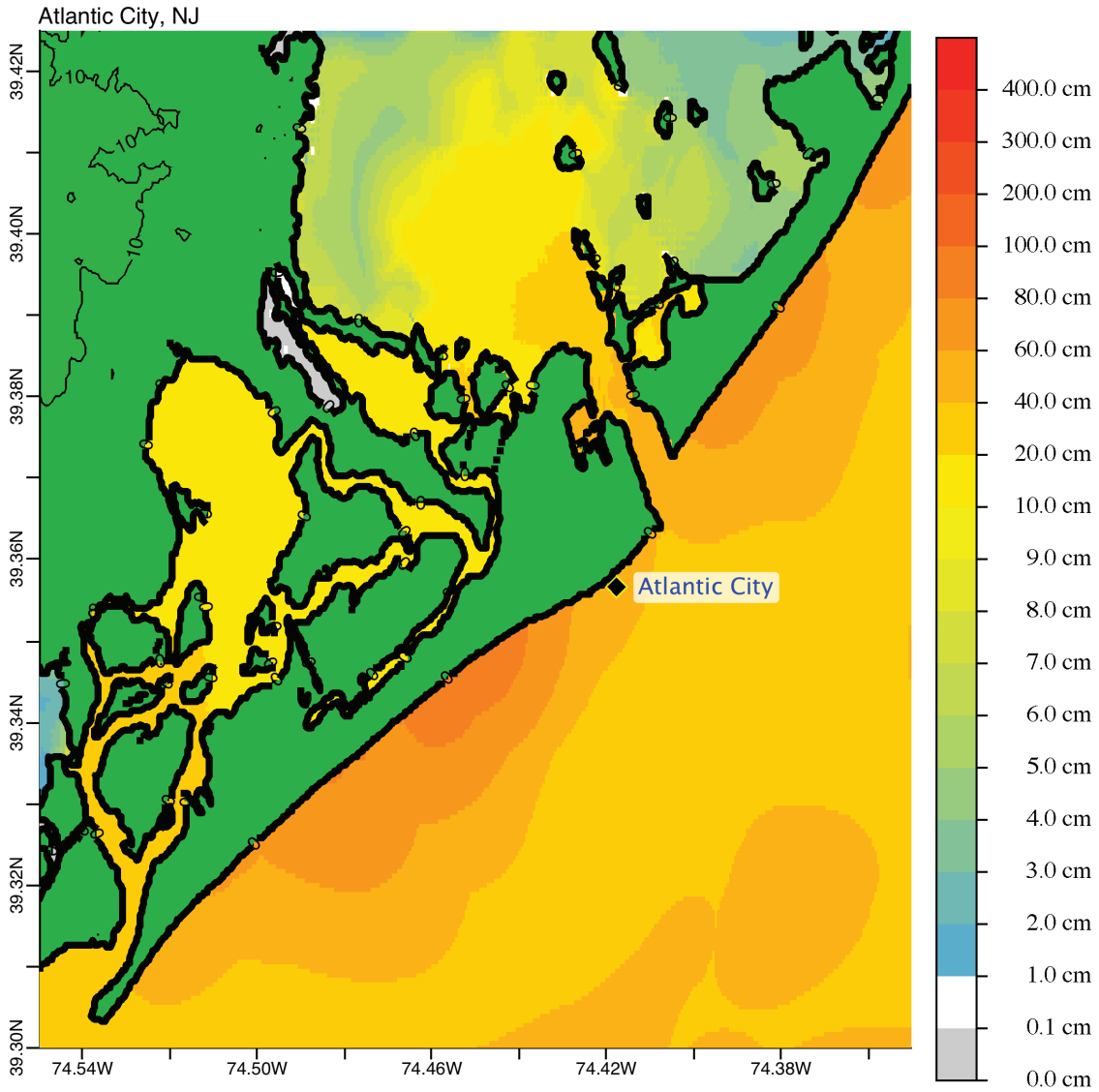

Figure 11. Max computed wave amplitude of C grid, Atlantic City, for synthetic event SSSZ 1-10.

(a)

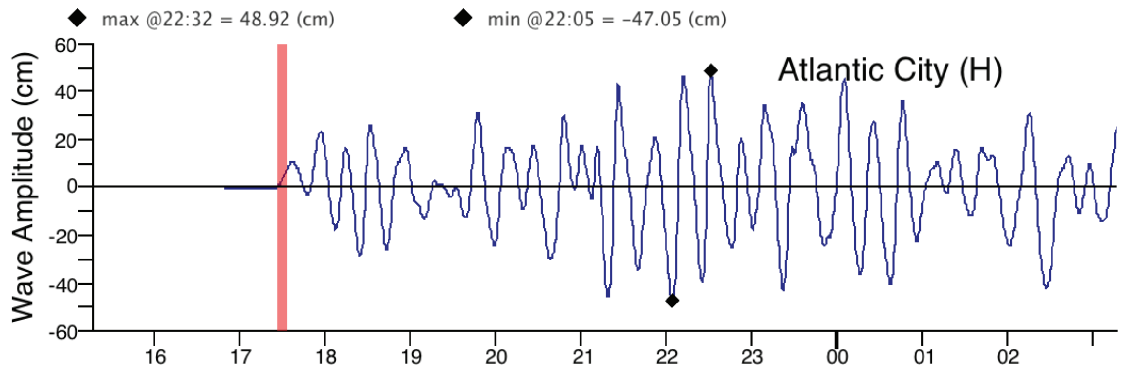

(b)

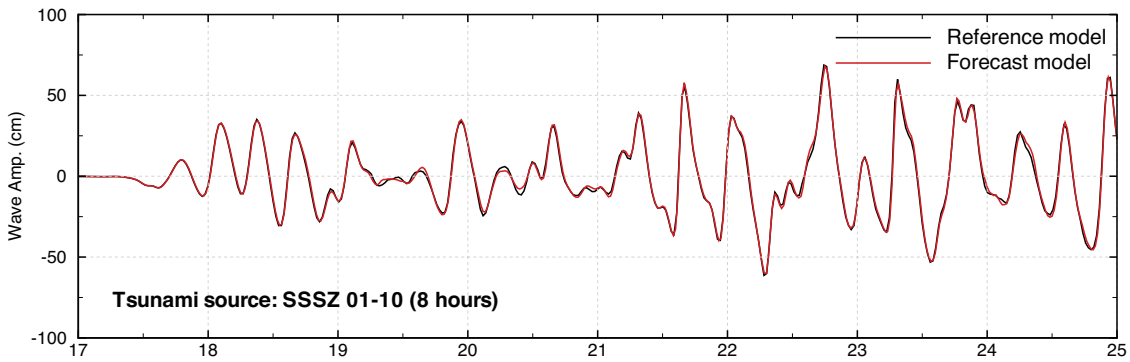

Figure 12. Computed time series at Atlantic City tide gage, for synthetic event SSSZ 1-10: (a) time series computed in the forecast system; (b) time series shown in the forecast model report.

Tables:

Table 1: Historical tsunami events that have affected central north of U.S. East Coast, including Atlantic City, New Jersey.

Table 2: MOST setup parameters for reference and forecast models for Atlantic City, Maryland.

Table 3: Synthetic tsunami events – Atlantic

Table 1. Historical tsunami events that have affected central north of U.S. East Coast, including Atlantic City, New Jersey

Event	Date, Time (UTC), Epicenter	Magnitude	Earthquake source area	Max water elev. at Atlantic City
1755 Lisbon	01 Nov. 10:16:00 36.0ºN 11.0ºW	8.5 – 9.0	Portugal: Lisbon	-
1817 Philadelphia	08 Jan 39.95ºN 75.1ºW	?	Philadelphia	-
1821	03 Sep	-	Meteorological	-
1840 Philadelphia	11 Nov 39.8ºN 75.2ºW	5.2	Philadelphia	-
1871 New York	18 Jun 40.5ºN 73.9ºW	?	New York	-
1884 New York	10 Aug 10:07:00 40.6ºN 73.75ºW	5.5	New York	-
1895 New Jersey	1 Sep 11:09:00 40.667ºN 74.883ºW	4.3	New Jersey	-
1913	9 Jun	-	Unknown	-
1918 Puerto Rico	11 Oct 14:14:00 18.5ºN 67.5ºW	7.3	Atlantic (ATSZ)	0.06 m
1923	6 Aug	-	Unknown	-
1924	8 Aug	-	Unknown	-
1929 Grand Banks	18 Nov 20:32:00 44.69ºN 56.0ºW	7.2	Canada: Grand Banks	0.68 m
1931	19 Aug	-	Meteorological	3.0 m
1932	10 Nov	-	Meteorological	-
1938	21 Sep	-	Meteorological	-
1944	14 Sep	-	Meteorological	-
1946 Dominican Republic	4 Aug 17:51:6.0 19.3ºN 68.9ºW	7.8	Atlantic (ATSZ)	-
1946 Dominican Republic	8 Aug 13:28:0.0 19.71ºN 69.51ºW	7.4	Atlantic (ATSZ)	-
1964	19 May	-	Possibly a submarine landslide	-
2004 Sumatra	26 Dec 00:58:53 4, 3.295ºN 5.982ºE	9.0 - 9.3	Indian Ocean (IOSZ)	0.11 m

Table 2: MOST setup parameters for reference and forecast models for Atlantic City, New Jersey.

		Reference Model				Forecast Model			
Grid	Region	Coverage Lat. [ºN] Lon. [ºW]	Cell Size [“]	nx x ny	Time Step [sec]	Coverage Lat. [ºX] Lon. [ºX]	Cell Size [“]	nx x ny	Time Step [sec]
A	Central north of U.S. East Coast	38.0 – 40.5 75.25 – 71.0	30”	511 × 301	3.15	38.0 – 40.5 75.25 – 71.0	30”	511 × 301	3.0
B	East of New Jersey and Delaware	38.85-39.75 75.05 – 74.0	3”	1261 × 1081	2.7	38.85-39.75 75.05 – 74.0	6”	631 × 541	6.0
C	Atlantic City	39.30 -39.425 74.55 – 74.35	1/3”	2161 × 1351	0.45	39.30 -39.425 74.55 – 74.35	2”	361 × 226	3.0
Minimum offshore depth [m]				1.0				1.0	
Water depth for dry land [m]				0.1				0.1	
Friction coefficient [n^2]				0.0009				0.0009	
CPU time for 4-hr simulation				~ 10 hours				~ 12 minutes	
Reference point at tide gage				74.417778W, 39.356667N (row number I = 239, column number J = 124)					

Computations were performed on a single Intel Xeon processor at 3.6 GHz, Dell PowerEdge 1850.

Table 3. Synthetic tsunami events – Atlantic

Sce. No	Scenario Name	Source Zone	Tsunami Source	α (m)
		Mega-tsunami scenario		
1	ATSZ 38-47	Atlantic	A38-A47, A38-A47	25
2	ATSZ 48-57	Atlantic	A48-A57, B48-B57	25
3	ATSZ 58-67	Atlantic	A58-A67, B58-B67	25
4	ATSZ 68-77	Atlantic	A68-A77, B68-B77	25
5	ATSZ 82-91	Atlantic	A82-A91, B82-B91	25
6	SSSZ 1-10	South Sandwich	A1-A10, B1-B10	25
		Mw 7.5 Scenario		
7	ATSZ B52	Atlantic	B52	1
		Micro-tsunami Scenario		
8	SSSZ B11	South Sandwich	B11	0.01

Appendix A.

Development of the King Cove, Alaska, tsunami forecast model occurred prior to parameters changes that were made to reflect modification to the MOST model code. As a result, the input file for running both the optimized tsunami forecast model and the high-resolution reference inundation model in MOST have been updated accordingly. Appendix A1 and A2 provide the updated files for King Cove, Alaska.

A1. Reference model *.in file for King Cove, Alaska

```
0.001     Minimum amplitude of input offshore wave (m)
1.0       Input minimum depth for offshore (m)
0.1       Input "dry land" depth for inundation (m)
0.0025 Input friction coefficient (n**2)
1         let a and b run up
300.0     blowup limit
0.15      input time step (sec)
216000    input amount of steps
16        Compute "A" arrays every n-th time step, n=
10        Compute "B" arrays every n-th time step, n=
160       Input number of steps between snapshots
0         ...Starting from
1         ...saving grid every n-th node, n=
```

A2. Forecast model *.in file for King Cove, Alaska

```
0.0001    Minimum amplitude of input offshore wave (m)
1.0       Input minimum depth for offshore (m)
0.1       Input "dry land" depth for inundation (m)
0.0016    Input friction coefficient (n**2)
1         let a and b run up
300.0     blowup limit
0.5       input time step (sec)
57600     input amount of steps
5         Compute "A" arrays every n-th time step, n=
10        Compute "B" arrays every n-th time step, n=
60        Input number of steps between snapshots
0         ...Starting from
1         ...saving grid every n-th node, n=
```

Appendix B. Propagation database:

Atlantic Ocean Unit Sources

These propagation source details reflect the database as of January 2010, and there may have been updates in the earthquake source parameters after this date.

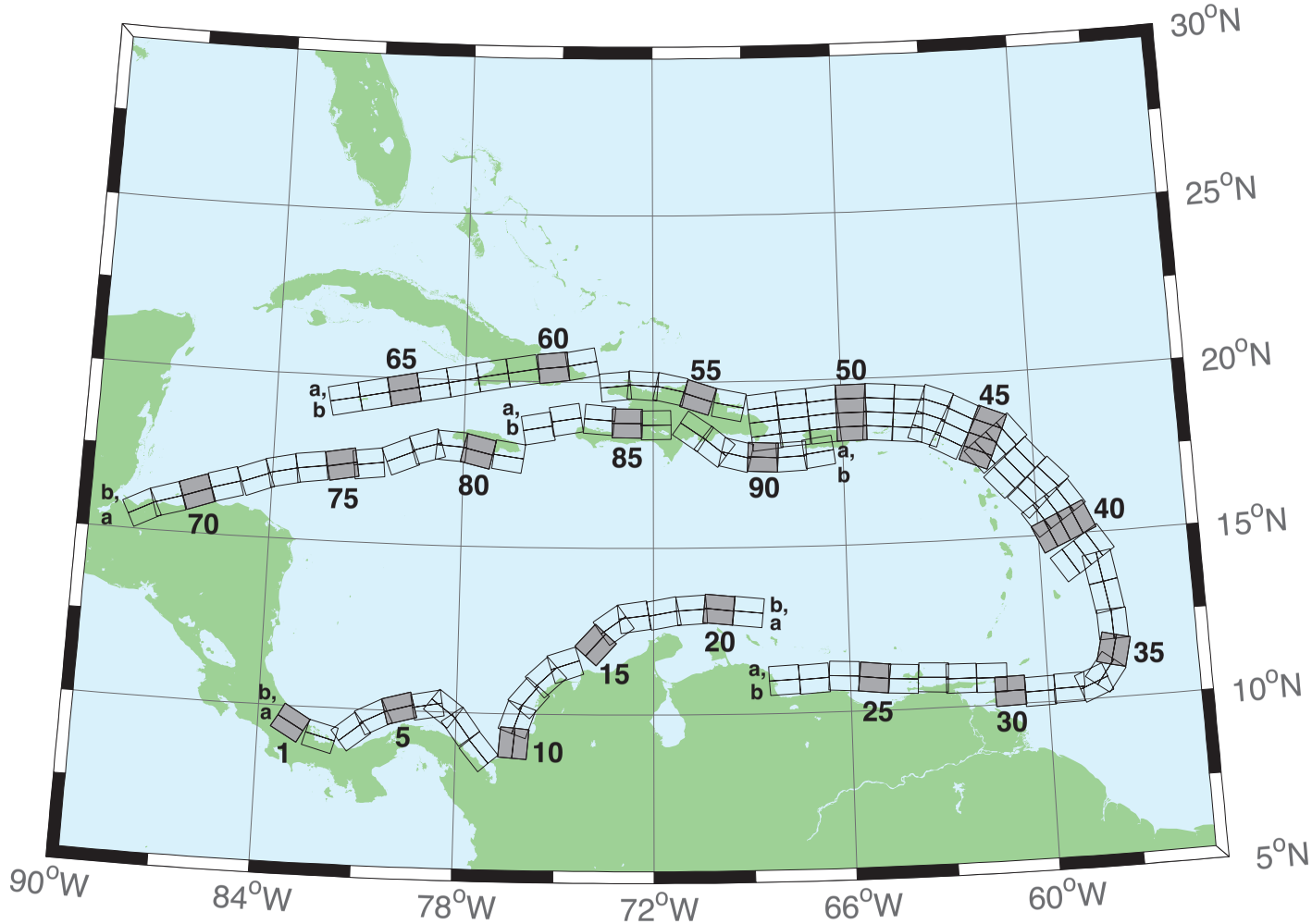

Figure B.1: Atlantic Source Zone unit sources.

Table B.1: Earthquake parameters for Atlantic Source Zone unit sources.

Segment	Description	Longitude(°E)	Latitude(°N)	Strike(°)	Dip(°)	Depth (km)
atsz–1a	Atlantic Source Zone	-83.2020	9.1449	120	27.5	28.09
atsz–1b	Atlantic Source Zone	-83.0000	9.4899	120	27.5	5
atsz–2a	Atlantic Source Zone	-82.1932	8.7408	105.1	27.5	28.09
atsz–2b	Atlantic Source Zone	-82.0880	9.1254	105.1	27.5	5
atsz–3a	Atlantic Source Zone	-80.9172	9.0103	51.31	30	30
atsz–3b	Atlantic Source Zone	-81.1636	9.3139	51.31	30	5
atsz–4a	Atlantic Source Zone	-80.3265	9.4308	63.49	30	30
atsz–4b	Atlantic Source Zone	-80.5027	9.7789	63.49	30	5
atsz–5a	Atlantic Source Zone	-79.6247	9.6961	74.44	30	30
atsz–5b	Atlantic Source Zone	-79.7307	10.0708	74.44	30	5
atsz–6a	Atlantic Source Zone	-78.8069	9.8083	79.71	30	30
atsz–6b	Atlantic Source Zone	-78.8775	10.1910	79.71	30	5
atsz–7a	Atlantic Source Zone	-78.6237	9.7963	127.2	30	30
atsz–7b	Atlantic Source Zone	-78.3845	10.1059	127.2	30	5
atsz–8a	Atlantic Source Zone	-78.1693	9.3544	143.8	30	30
atsz–8b	Atlantic Source Zone	-77.8511	9.5844	143.8	30	5
atsz–9a	Atlantic Source Zone	-77.5913	8.5989	139.9	30	30
atsz–9b	Atlantic Source Zone	-77.2900	8.8493	139.9	30	5
atsz–10a	Atlantic Source Zone	-75.8109	9.0881	4.67	17	19.62
atsz–10b	Atlantic Source Zone	-76.2445	9.1231	4.67	17	5
atsz–11a	Atlantic Source Zone	-75.7406	9.6929	19.67	17	19.62
atsz–11b	Atlantic Source Zone	-76.1511	9.8375	19.67	17	5
atsz–12a	Atlantic Source Zone	-75.4763	10.2042	40.4	17	19.62
atsz–12b	Atlantic Source Zone	-75.8089	10.4826	40.4	17	5
atsz–13a	Atlantic Source Zone	-74.9914	10.7914	47.17	17	19.62
atsz–13b	Atlantic Source Zone	-75.2890	11.1064	47.17	17	5
atsz–14a	Atlantic Source Zone	-74.5666	11.0708	71.68	17	19.62
atsz–14b	Atlantic Source Zone	-74.7043	11.4786	71.68	17	5
atsz–15a	Atlantic Source Zone	-73.4576	11.8012	42.69	17	19.62
atsz–15b	Atlantic Source Zone	-73.7805	12.0924	42.69	17	5
atsz–16a	Atlantic Source Zone	-72.9788	12.3365	54.75	17	19.62
atsz–16b	Atlantic Source Zone	-73.2329	12.6873	54.75	17	5
atsz–17a	Atlantic Source Zone	-72.5454	12.5061	81.96	17	19.62
atsz–17b	Atlantic Source Zone	-72.6071	12.9314	81.96	17	5
atsz–18a	Atlantic Source Zone	-71.6045	12.6174	79.63	17	19.62
atsz–18b	Atlantic Source Zone	-71.6839	13.0399	79.63	17	5
atsz–19a	Atlantic Source Zone	-70.7970	12.7078	86.32	17	19.62
atsz–19b	Atlantic Source Zone	-70.8253	13.1364	86.32	17	5
atsz–20a	Atlantic Source Zone	-70.0246	12.7185	95.94	17	19.62
atsz–20b	Atlantic Source Zone	-69.9789	13.1457	95.94	17	5
atsz–21a	Atlantic Source Zone	-69.1244	12.6320	95.94	17	19.62
atsz–21b	Atlantic Source Zone	-69.0788	13.0592	95.94	17	5
atsz–22a	Atlantic Source Zone	-68.0338	11.4286	266.9	15	17.94
atsz–22b	Atlantic Source Zone	-68.0102	10.9954	266.9	15	5
atsz–23a	Atlantic Source Zone	-67.1246	11.4487	266.9	15	17.94
atsz–23b	Atlantic Source Zone	-67.1010	11.0155	266.9	15	5
atsz–24a	Atlantic Source Zone	-66.1656	11.5055	273.3	15	17.94
atsz–24b	Atlantic Source Zone	-66.1911	11.0724	273.3	15	5
atsz–25a	Atlantic Source Zone	-65.2126	11.4246	276.4	15	17.94
atsz–25b	Atlantic Source Zone	-65.2616	10.9934	276.4	15	5
atsz–26a	Atlantic Source Zone	-64.3641	11.3516	272.9	15	17.94
atsz–26b	Atlantic Source Zone	-64.3862	10.9183	272.9	15	5
atsz–27a	Atlantic Source Zone	-63.4472	11.3516	272.9	15	17.94

Continued on next page

Table B.1 – continued from previous page

Segment	Description	Longitude(°E)	Latitude(°N)	Strike(°)	Dip(°)	Depth (km)
atsz–27b	Atlantic Source Zone	-63.4698	10.9183	272.9	15	5
atsz–28a	Atlantic Source Zone	-62.6104	11.2831	271.1	15	17.94
atsz–28b	Atlantic Source Zone	-62.6189	10.8493	271.1	15	5
atsz–29a	Atlantic Source Zone	-61.6826	11.2518	271.6	15	17.94
atsz–29b	Atlantic Source Zone	-61.6947	10.8181	271.6	15	5
atsz–30a	Atlantic Source Zone	-61.1569	10.8303	269	15	17.94
atsz–30b	Atlantic Source Zone	-61.1493	10.3965	269	15	5
atsz–31a	Atlantic Source Zone	-60.2529	10.7739	269	15	17.94
atsz–31b	Atlantic Source Zone	-60.2453	10.3401	269	15	5
atsz–32a	Atlantic Source Zone	-59.3510	10.8123	269	15	17.94
atsz–32b	Atlantic Source Zone	-59.3734	10.3785	269	15	5
atsz–33a	Atlantic Source Zone	-58.7592	10.8785	248.6	15	17.94
atsz–33b	Atlantic Source Zone	-58.5984	10.4745	248.6	15	5
atsz–34a	Atlantic Source Zone	-58.5699	11.0330	217.2	15	17.94
atsz–34b	Atlantic Source Zone	-58.2179	10.7710	217.2	15	5
atsz–35a	Atlantic Source Zone	-58.3549	11.5300	193.7	15	17.94
atsz–35b	Atlantic Source Zone	-57.9248	11.4274	193.7	15	5
atsz–36a	Atlantic Source Zone	-58.3432	12.1858	177.7	15	17.94
atsz–36b	Atlantic Source Zone	-57.8997	12.2036	177.7	15	5
atsz–37a	Atlantic Source Zone	-58.4490	12.9725	170.7	15	17.94
atsz–37b	Atlantic Source Zone	-58.0095	13.0424	170.7	15	5
atsz–38a	Atlantic Source Zone	-58.6079	13.8503	170.2	15	17.94
atsz–38b	Atlantic Source Zone	-58.1674	13.9240	170.2	15	5
atsz–39a	Atlantic Source Zone	-58.6667	14.3915	146.8	15	17.94
atsz–39b	Atlantic Source Zone	-58.2913	14.6287	146.8	15	5
atsz–39y	Atlantic Source Zone	-59.4168	13.9171	146.8	15	43.82
atsz–39z	Atlantic Source Zone	-59.0415	14.1543	146.8	15	30.88
atsz–40a	Atlantic Source Zone	-59.1899	15.2143	156.2	15	17.94
atsz–40b	Atlantic Source Zone	-58.7781	15.3892	156.2	15	5
atsz–40y	Atlantic Source Zone	-60.0131	14.8646	156.2	15	43.82
atsz–40z	Atlantic Source Zone	-59.6012	15.0395	156.2	15	30.88
atsz–41a	Atlantic Source Zone	-59.4723	15.7987	146.3	15	17.94
atsz–41b	Atlantic Source Zone	-59.0966	16.0392	146.3	15	5
atsz–41y	Atlantic Source Zone	-60.2229	15.3177	146.3	15	43.82
atsz–41z	Atlantic Source Zone	-59.8473	15.5582	146.3	15	30.88
atsz–42a	Atlantic Source Zone	-59.9029	16.4535	137	15	17.94
atsz–42b	Atlantic Source Zone	-59.5716	16.7494	137	15	5
atsz–42y	Atlantic Source Zone	-60.5645	15.8616	137	15	43.82
atsz–42z	Atlantic Source Zone	-60.2334	16.1575	137	15	30.88
atsz–43a	Atlantic Source Zone	-60.5996	17.0903	138.7	15	17.94
atsz–43b	Atlantic Source Zone	-60.2580	17.3766	138.7	15	5
atsz–43y	Atlantic Source Zone	-61.2818	16.5177	138.7	15	43.82
atsz–43z	Atlantic Source Zone	-60.9404	16.8040	138.7	15	30.88
atsz–44a	Atlantic Source Zone	-61.1559	17.8560	141.1	15	17.94
atsz–44b	Atlantic Source Zone	-60.8008	18.1286	141.1	15	5
atsz–44y	Atlantic Source Zone	-61.8651	17.3108	141.1	15	43.82
atsz–44z	Atlantic Source Zone	-61.5102	17.5834	141.1	15	30.88
atsz–45a	Atlantic Source Zone	-61.5491	18.0566	112.8	15	17.94
atsz–45b	Atlantic Source Zone	-61.3716	18.4564	112.8	15	5
atsz–45y	Atlantic Source Zone	-61.9037	17.2569	112.8	15	43.82
atsz–45z	Atlantic Source Zone	-61.7260	17.6567	112.8	15	30.88
atsz–46a	Atlantic Source Zone	-62.4217	18.4149	117.9	15	17.94
atsz–46b	Atlantic Source Zone	-62.2075	18.7985	117.9	15	5
atsz–46y	Atlantic Source Zone	-62.8493	17.6477	117.9	15	43.82
atsz–46z	Atlantic Source Zone	-62.6352	18.0313	117.9	15	30.88

Continued on next page

Table B.1 – continued from previous page

Segment	Description	Longitude(°E)	Latitude(°N)	Strike(°)	Dip(°)	Depth (km)
atsz–47a	Atlantic Source Zone	-63.1649	18.7844	110.5	20	22.1
atsz–47b	Atlantic Source Zone	-63.0087	19.1798	110.5	20	5
atsz–47y	Atlantic Source Zone	-63.4770	17.9936	110.5	20	56.3
atsz–47z	Atlantic Source Zone	-63.3205	18.3890	110.5	20	39.2
atsz–48a	Atlantic Source Zone	-63.8800	18.8870	95.37	20	22.1
atsz–48b	Atlantic Source Zone	-63.8382	19.3072	95.37	20	5
atsz–48y	Atlantic Source Zone	-63.9643	18.0465	95.37	20	56.3
atsz–48z	Atlantic Source Zone	-63.9216	18.4667	95.37	20	39.2
atsz–49a	Atlantic Source Zone	-64.8153	18.9650	94.34	20	22.1
atsz–49b	Atlantic Source Zone	-64.7814	19.3859	94.34	20	5
atsz–49y	Atlantic Source Zone	-64.8840	18.1233	94.34	20	56.3
atsz–49z	Atlantic Source Zone	-64.8492	18.5442	94.34	20	39.2
atsz–50a	Atlantic Source Zone	-65.6921	18.9848	89.59	20	22.1
atsz–50b	Atlantic Source Zone	-65.6953	19.4069	89.59	20	5
atsz–50y	Atlantic Source Zone	-65.6874	18.1407	89.59	20	56.3
atsz–50z	Atlantic Source Zone	-65.6887	18.5628	89.59	20	39.2
atsz–51a	Atlantic Source Zone	-66.5742	18.9484	84.98	20	22.1
atsz–51b	Atlantic Source Zone	-66.6133	19.3688	84.98	20	5
atsz–51y	Atlantic Source Zone	-66.4977	18.1076	84.98	20	56.3
atsz–51z	Atlantic Source Zone	-66.5353	18.5280	84.98	20	39.2
atsz–52a	Atlantic Source Zone	-67.5412	18.8738	85.87	20	22.1
atsz–52b	Atlantic Source Zone	-67.5734	19.2948	85.87	20	5
atsz–52y	Atlantic Source Zone	-67.4781	18.0319	85.87	20	56.3
atsz–52z	Atlantic Source Zone	-67.5090	18.4529	85.87	20	39.2
atsz–53a	Atlantic Source Zone	-68.4547	18.7853	83.64	20	22.1
atsz–53b	Atlantic Source Zone	-68.5042	19.2048	83.64	20	5
atsz–53y	Atlantic Source Zone	-68.3575	17.9463	83.64	20	56.3
atsz–53z	Atlantic Source Zone	-68.4055	18.3658	83.64	20	39.2
atsz–54a	Atlantic Source Zone	-69.6740	18.8841	101.5	20	22.1
atsz–54b	Atlantic Source Zone	-69.5846	19.2976	101.5	20	5
atsz–55a	Atlantic Source Zone	-70.7045	19.1376	108.2	20	22.1
atsz–55b	Atlantic Source Zone	-70.5647	19.5386	108.2	20	5
atsz–56a	Atlantic Source Zone	-71.5368	19.3853	102.6	20	22.1
atsz–56b	Atlantic Source Zone	-71.4386	19.7971	102.6	20	5
atsz–57a	Atlantic Source Zone	-72.3535	19.4838	94.2	20	22.1
atsz–57b	Atlantic Source Zone	-72.3206	19.9047	94.2	20	5
atsz–58a	Atlantic Source Zone	-73.1580	19.4498	84.34	20	22.1
atsz–58b	Atlantic Source Zone	-73.2022	19.8698	84.34	20	5
atsz–59a	Atlantic Source Zone	-74.3567	20.9620	259.7	20	22.1
atsz–59b	Atlantic Source Zone	-74.2764	20.5467	259.7	20	5
atsz–60a	Atlantic Source Zone	-75.2386	20.8622	264.2	15	17.94
atsz–60b	Atlantic Source Zone	-75.1917	20.4306	264.2	15	5
atsz–61a	Atlantic Source Zone	-76.2383	20.7425	260.7	15	17.94
atsz–61b	Atlantic Source Zone	-76.1635	20.3144	260.7	15	5
atsz–62a	Atlantic Source Zone	-77.2021	20.5910	259.9	15	17.94
atsz–62b	Atlantic Source Zone	-77.1214	20.1638	259.9	15	5
atsz–63a	Atlantic Source Zone	-78.1540	20.4189	259	15	17.94
atsz–63b	Atlantic Source Zone	-78.0661	19.9930	259	15	5
atsz–64a	Atlantic Source Zone	-79.0959	20.2498	259.2	15	17.94
atsz–64b	Atlantic Source Zone	-79.0098	19.8236	259.2	15	5
atsz–65a	Atlantic Source Zone	-80.0393	20.0773	258.9	15	17.94
atsz–65b	Atlantic Source Zone	-79.9502	19.6516	258.9	15	5
atsz–66a	Atlantic Source Zone	-80.9675	19.8993	258.6	15	17.94
atsz–66b	Atlantic Source Zone	-80.8766	19.4740	258.6	15	5
atsz–67a	Atlantic Source Zone	-81.9065	19.7214	258.5	15	17.94

Continued on next page

Table B.1 – continued from previous page

Segment	Description	Longitude(°E)	Latitude(°N)	Strike(°)	Dip(°)	Depth (km)
atsz–67b	Atlantic Source Zone	-81.8149	19.2962	258.5	15	5
atsz–68a	Atlantic Source Zone	-87.8003	15.2509	62.69	15	17.94
atsz–68b	Atlantic Source Zone	-88.0070	15.6364	62.69	15	5
atsz–69a	Atlantic Source Zone	-87.0824	15.5331	72.73	15	17.94
atsz–69b	Atlantic Source Zone	-87.2163	15.9474	72.73	15	5
atsz–70a	Atlantic Source Zone	-86.1622	15.8274	70.64	15	17.94
atsz–70b	Atlantic Source Zone	-86.3120	16.2367	70.64	15	5
atsz–71a	Atlantic Source Zone	-85.3117	16.1052	73.7	15	17.94
atsz–71b	Atlantic Source Zone	-85.4387	16.5216	73.7	15	5
atsz–72a	Atlantic Source Zone	-84.3470	16.3820	69.66	15	17.94
atsz–72b	Atlantic Source Zone	-84.5045	16.7888	69.66	15	5
atsz–73a	Atlantic Source Zone	-83.5657	16.6196	77.36	15	17.94
atsz–73b	Atlantic Source Zone	-83.6650	17.0429	77.36	15	5
atsz–74a	Atlantic Source Zone	-82.7104	16.7695	82.35	15	17.94
atsz–74b	Atlantic Source Zone	-82.7709	17.1995	82.35	15	5
atsz–75a	Atlantic Source Zone	-81.7297	16.9003	79.86	15	17.94
atsz–75b	Atlantic Source Zone	-81.8097	17.3274	79.86	15	5
atsz–76a	Atlantic Source Zone	-80.9196	16.9495	82.95	15	17.94
atsz–76b	Atlantic Source Zone	-80.9754	17.3801	82.95	15	5
atsz–77a	Atlantic Source Zone	-79.8086	17.2357	67.95	15	17.94
atsz–77b	Atlantic Source Zone	-79.9795	17.6378	67.95	15	5
atsz–78a	Atlantic Source Zone	-79.0245	17.5415	73.61	15	17.94
atsz–78b	Atlantic Source Zone	-79.1532	17.9577	73.61	15	5
atsz–79a	Atlantic Source Zone	-78.4122	17.5689	94.07	15	17.94
atsz–79b	Atlantic Source Zone	-78.3798	18.0017	94.07	15	5
atsz–80a	Atlantic Source Zone	-77.6403	17.4391	103.3	15	17.94
atsz–80b	Atlantic Source Zone	-77.5352	17.8613	103.3	15	5
atsz–81a	Atlantic Source Zone	-76.6376	17.2984	98.21	15	17.94
atsz–81b	Atlantic Source Zone	-76.5726	17.7278	98.21	15	5
atsz–82a	Atlantic Source Zone	-75.7299	19.0217	260.1	15	17.94
atsz–82b	Atlantic Source Zone	-75.6516	18.5942	260.1	15	5
atsz–83a	Atlantic Source Zone	-74.8351	19.2911	260.8	15	17.94
atsz–83b	Atlantic Source Zone	-74.7621	18.8628	260.8	15	5
atsz–84a	Atlantic Source Zone	-73.6639	19.2991	274.8	15	17.94
atsz–84b	Atlantic Source Zone	-73.7026	18.8668	274.8	15	5
atsz–85a	Atlantic Source Zone	-72.8198	19.2019	270.6	15	17.94
atsz–85b	Atlantic Source Zone	-72.8246	18.7681	270.6	15	5
atsz–86a	Atlantic Source Zone	-71.9143	19.1477	269.1	15	17.94
atsz–86b	Atlantic Source Zone	-71.9068	18.7139	269.1	15	5
atsz–87a	Atlantic Source Zone	-70.4738	18.8821	304.5	15	17.94
atsz–87b	Atlantic Source Zone	-70.7329	18.5245	304.5	15	5
atsz–88a	Atlantic Source Zone	-69.7710	18.3902	308.9	15	17.94
atsz–88b	Atlantic Source Zone	-70.0547	18.0504	308.4	15	5
atsz–89a	Atlantic Source Zone	-69.2635	18.2099	283.9	15	17.94
atsz–89b	Atlantic Source Zone	-69.3728	17.7887	283.9	15	5
atsz–90a	Atlantic Source Zone	-68.5059	18.1443	272.9	15	17.94
atsz–90b	Atlantic Source Zone	-68.5284	17.7110	272.9	15	5
atsz–91a	Atlantic Source Zone	-67.6428	18.1438	267.8	15	17.94
atsz–91b	Atlantic Source Zone	-67.6256	17.7103	267.8	15	5
atsz–92a	Atlantic Source Zone	-66.8261	18.2536	262	15	17.94
atsz–92b	Atlantic Source Zone	-66.7627	17.8240	262	15	5

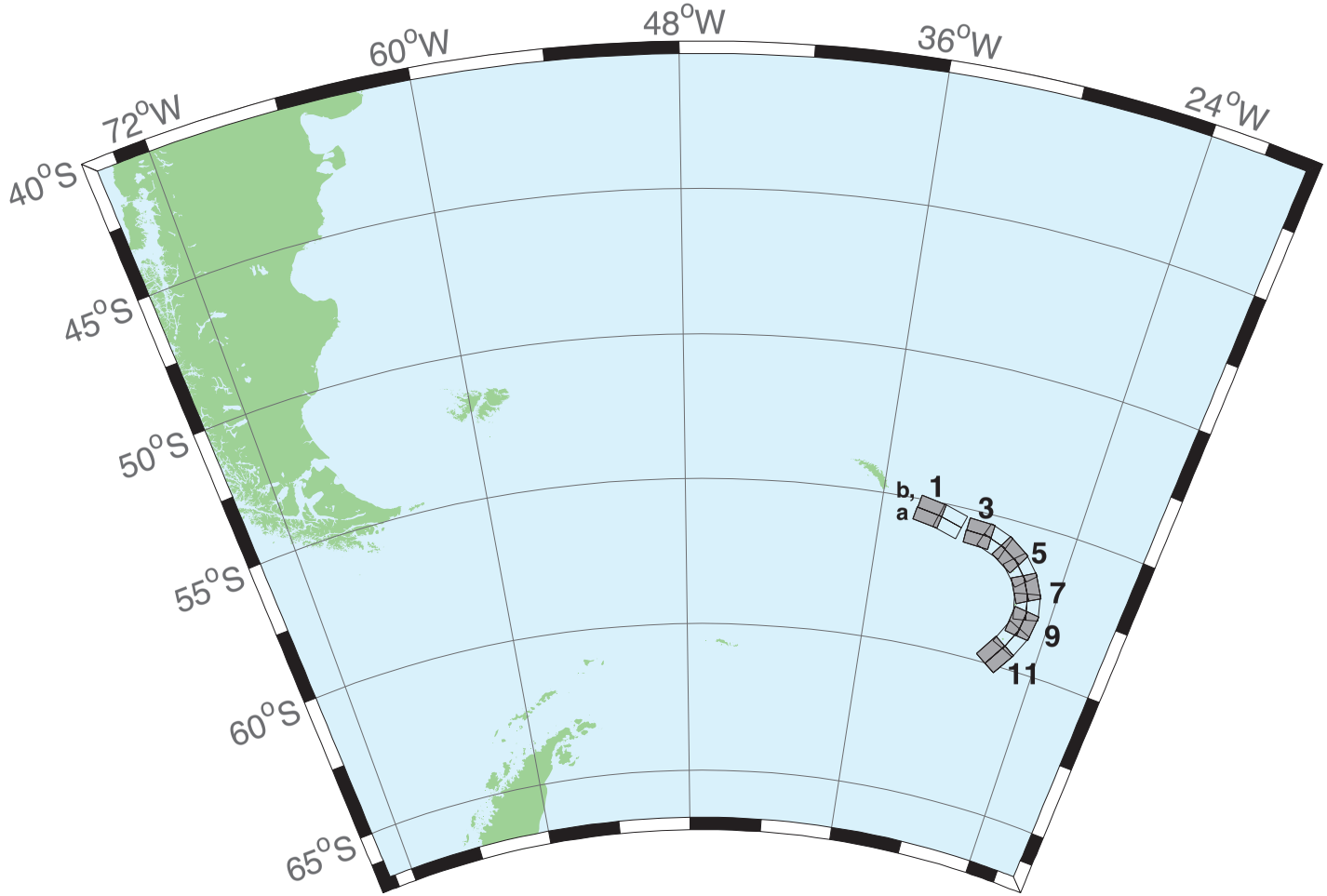

Figure B.2: South Sandwich Islands Subduction Zone.

Table B.2: Earthquake parameters for South Sandwich Islands Subduction Zone unit sources.

Segment	Description	Longitude(°E)	Latitude(°N)	Strike(°)	Dip(°)	Depth (km)
sssz–1a	South Sandwich Islands Subduction Zone	-33.0670	-55.3780	280.2	15	17.94
sssz–1b	South Sandwich Islands Subduction Zone	-32.9242	-54.9510	280.2	15	5
sssz–2a	South Sandwich Islands Subduction Zone	-31.7197	-55.5621	286.3	15	17.94
sssz–2b	South Sandwich Islands Subduction Zone	-31.4969	-55.1457	286.3	15	5
sssz–3a	South Sandwich Islands Subduction Zone	-29.8355	-55.7456	273	15	17.94
sssz–3b	South Sandwich Islands Subduction Zone	-29.7873	-55.3123	273	15	5
sssz–4a	South Sandwich Islands Subduction Zone	-28.7648	-55.8715	290	15	17.94
sssz–4b	South Sandwich Islands Subduction Zone	-28.4930	-55.4638	290	15	5
sssz–5a	South Sandwich Islands Subduction Zone	-27.6356	-56.1844	301.5	15	17.94
sssz–5b	South Sandwich Islands Subduction Zone	-27.2218	-55.8143	301.5	15	5
sssz–6a	South Sandwich Islands Subduction Zone	-26.7655	-56.5959	317.5	15	17.94
sssz–6b	South Sandwich Islands Subduction Zone	-26.1774	-56.3029	317.5	15	5
sssz–7a	South Sandwich Islands Subduction Zone	-26.0921	-57.1441	332.1	15	17.94
sssz–7b	South Sandwich Islands Subduction Zone	-25.3776	-56.9411	332.1	15	5
sssz–8a	South Sandwich Islands Subduction Zone	-25.7129	-57.7563	347.9	15	17.94
sssz–8b	South Sandwich Islands Subduction Zone	-24.9088	-57.6652	347.9	15	5
sssz–9a	South Sandwich Islands Subduction Zone	-25.7003	-58.3505	7.182	15	17.94
sssz–9b	South Sandwich Islands Subduction Zone	-24.8687	-58.4047	7.182	15	5
sssz–10a	South Sandwich Islands Subduction Zone	-26.0673	-58.9577	24.25	15	17.94
sssz–10b	South Sandwich Islands Subduction Zone	-25.2869	-59.1359	24.25	15	5
sssz–11a	South Sandwich Islands Subduction Zone	-26.8279	-59.6329	32.7	15	17.94
sssz–11b	South Sandwich Islands Subduction Zone	-26.0913	-59.8673	32.7	15	5

Appendix C: Tsunami Forecast System Testing

Jean Newman, Yong Wei

1.0 PURPOSE

Forecast models are tested with synthetic tsunami events covering a range of tsunami source locations. Testing is also done with selected historical tsunami events when available.

The purpose of forecast model testing is three-fold. The first objective is to assure that the results obtained with NOAA's tsunami forecast system, which has been released to the Tsunami Warning Centers for operational use, are identical to those obtained by the researcher during the development of the forecast model. The second objective is to test the forecast model for consistency, accuracy, time efficiency, and quality of results over a range of possible tsunami locations and magnitudes. The third objective is to identify bugs and issues in need of resolution by the researcher who developed the Forecast Model or by the forecast software development team before the next version release to NOAA's two Tsunami Warning Centers.

Local hardware and software applications, and tools familiar to the researcher(s), are used to run the Method of Splitting Tsunamis (MOST) model during the forecast model development. The test results presented in this report lend confidence that the model performs as developed and produces the same results when initiated within the forecast application in an operational setting as those produced by the researcher during the forecast model development. The test results assure those who rely on the Atlantic City tsunami forecast model that consistent results are produced irrespective of system.

2.0 TESTING PROCEDURE

The general procedure for forecast model testing is to run a set of synthetic tsunami scenarios through the forecast system application and compare the results with those obtained by the researcher during the forecast model development and presented in the Tsunami Forecast Model Report. Specific steps taken to test the model include:

1. Identification of testing scenarios, including the standard set of synthetic events and customized synthetic scenarios that may have been used by the researcher(s) in developing the forecast model.
2. Creation of new events to represent customized synthetic scenarios used by the researcher(s) in developing the forecast model, if any.
3. Submission of test model runs with the forecast system, and export of the results from A, B, and C grids, along with time series.
4. Recording applicable metadata, including the specific version of the forecast system used for testing.
5. Examination of forecast model results from the forecast system for instabilities in both time series and plot results.
6. Comparison of forecast model results obtained through the forecast system with those obtained during the forecast model development.
7. Summarization of results with specific mention of quality, consistency, and time efficiency.
8. Reporting of issues identified to modeler and forecast software development team.

9. Retesting the forecast models in the forecast system when reported issues have been addressed or explained.

Synthetic model runs were tested on a DELL PowerEdge R510 computer equipped with two Xeon E5670 processors at 2.93 Ghz, each with 12 MBytes of cache and 32GB memory. The processors are hex core and support hyperthreading, resulting in the computer performing as a 24 processor core machine. Additionally, the testing computer supports 10 Gigabit Ethernet for fast network connections. This computer configuration is similar or the same as the configurations of the computers installed at the Tsunami Warning Centers so the compute times should only vary slightly.

3.0 Results

The Atlantic City forecast model was tested with NOAA's tsunami forecast system version 3.2.

The Atlantic City, New Jersey forecast model was tested with three synthetic scenarios. Test results from the forecast system and comparisons with the results obtained during the forecast model development are shown numerically in Table 2 and graphically in Figures 1 to 3. The results show that the forecast model is stable and robust, with consistent and high quality results across geographically distributed tsunami sources and mega-event tsunami magnitudes. The model run time (wall clock time) was under 38 minutes for 12 hours of simulation time, and under 13 minutes for 4 hours. This run time is just over the 10 minute run time for 4 hours of simulation time that satisfies time efficiency requirements.

Three synthetic events were run on the Atlantic City forecast model. The modeled scenarios were stable for all cases tested, with no instabilities or ringing. Results show that the largest modeled height was 489.88 cm and originated in the Caribbean (ATSZ 48-57) source. Amplitudes greater than 100 cm were recorded for the two test sources. The smallest signal of 48.92 cm was recorded for the far field South Sandwich Islands (SSSZ 1-10) source. Direct comparisons, of output from the forecast tool with results from available development synthetic events, demonstrated that the wave pattern is similar in shape, pattern and amplitude but does not match by eye. These discrepancies are mainly caused by different propagation databases used to provide the boundary conditions for model runs. Developed in April 2011, the forecast model report shows the Atlantic City model results based on an old tsunami propagation database, while the SITF testing results in Appendix C reflect the tsunami propagation database that were updated in December of 2011. It is known that the new propagation database will lead to improvement of the model results.

Source Zone	Tsunami Source	α [m]	SIFT Max (cm)	Development Max (cm)	SIFT Min (cm)	Development Min (cm)
ATSZ	A38-A47, B38-B47	25	271.005	241.7	-171.153	-164.2
ATSZ	A48-A57, B48-B57	25	489.880	486.7	-314.680	-322.7
SSSZ	A1-A10, B1-B10	25	48.919	67.9	-47.050	-60.13

Table 1. Table of maximum and minimum amplitudes (cm) at the Atlantic City, New Jersey warning point for synthetic and historical events tested using SIFT 3.2 and obtained during development.

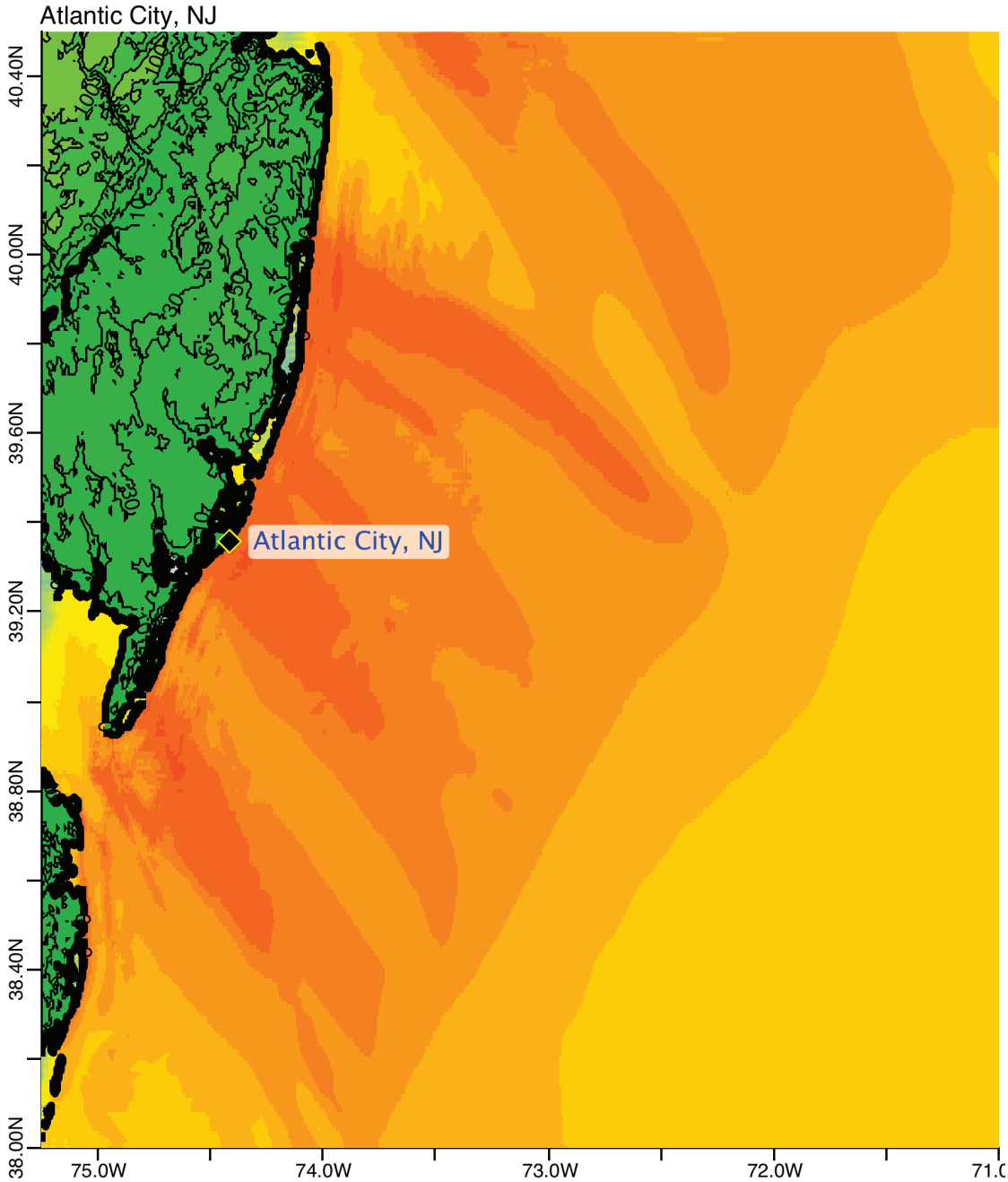

Figure 1. Max computed wave amplitude of A grid, Atlantic City, for synthetic event ATSZ 38-47.

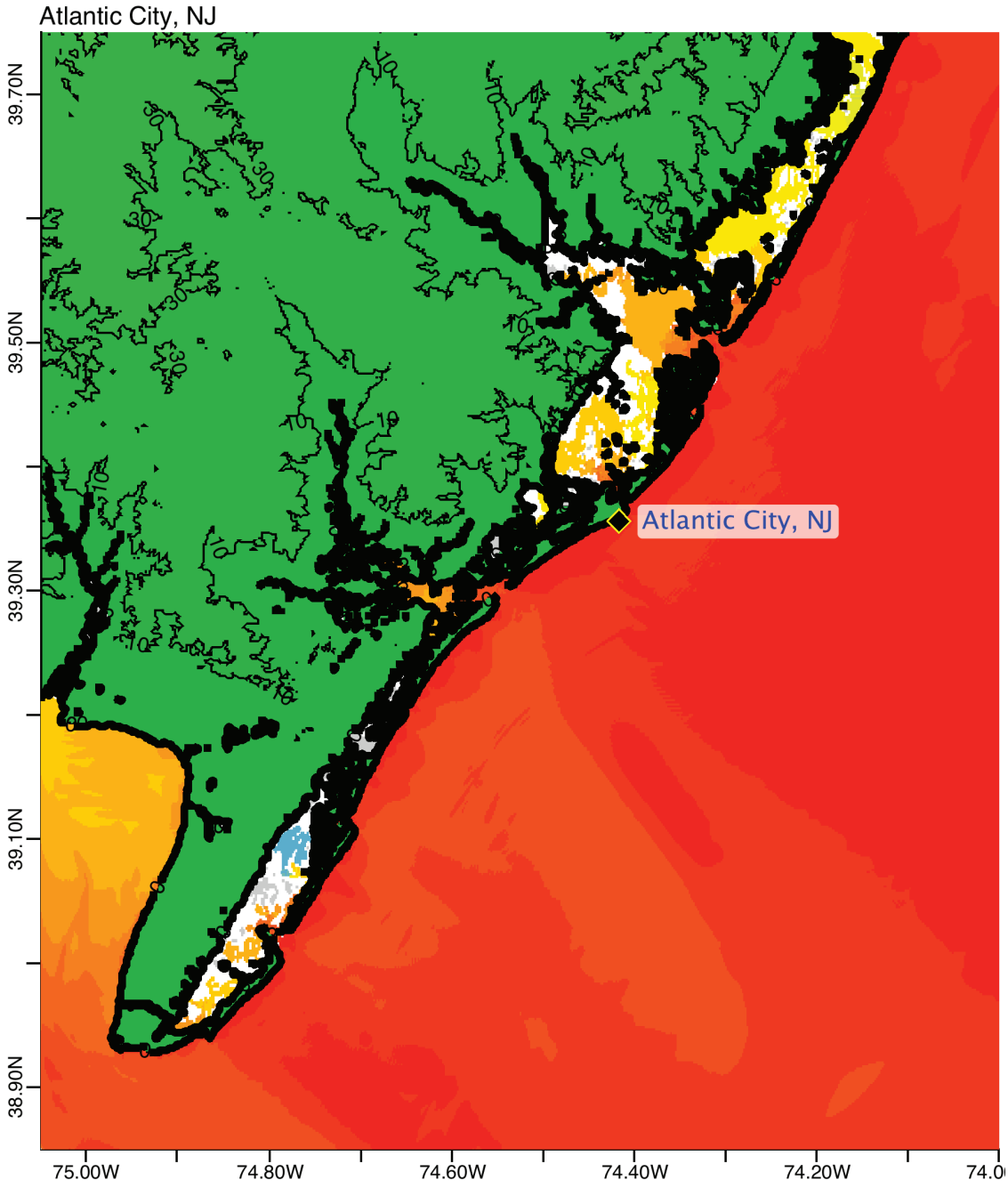

Figure 2. Max computed wave amplitude of B grid, Atlantic City, for synthetic event ATSZ 38-47.

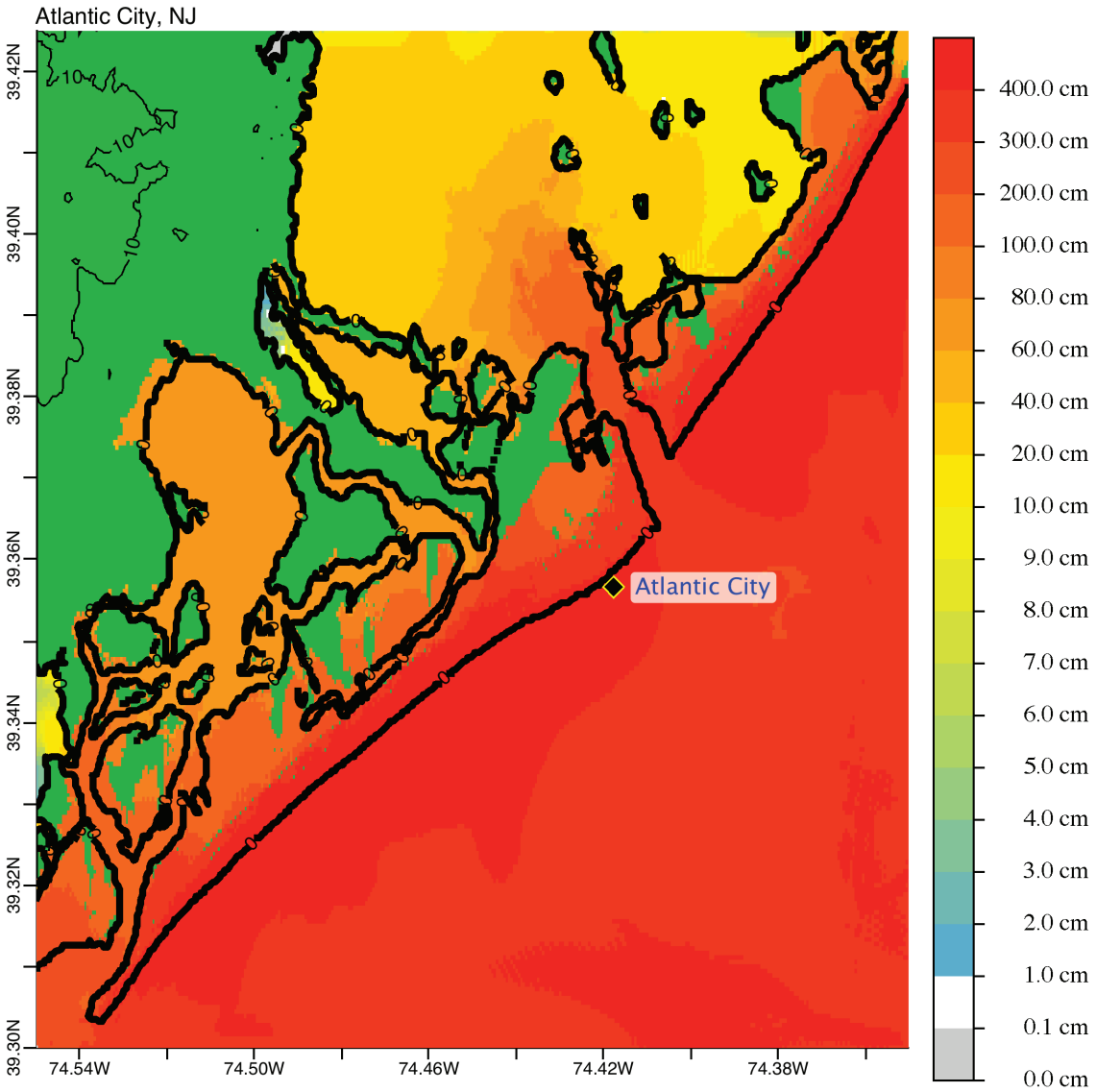

Figure 3. Max computed wave amplitude of C grid, Atlantic City, for synthetic event ATSZ 38-47.

(a)

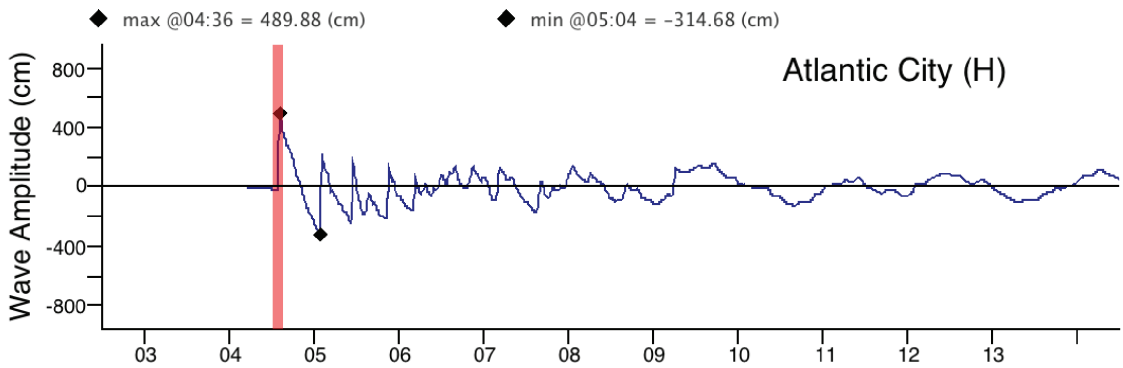

(b)

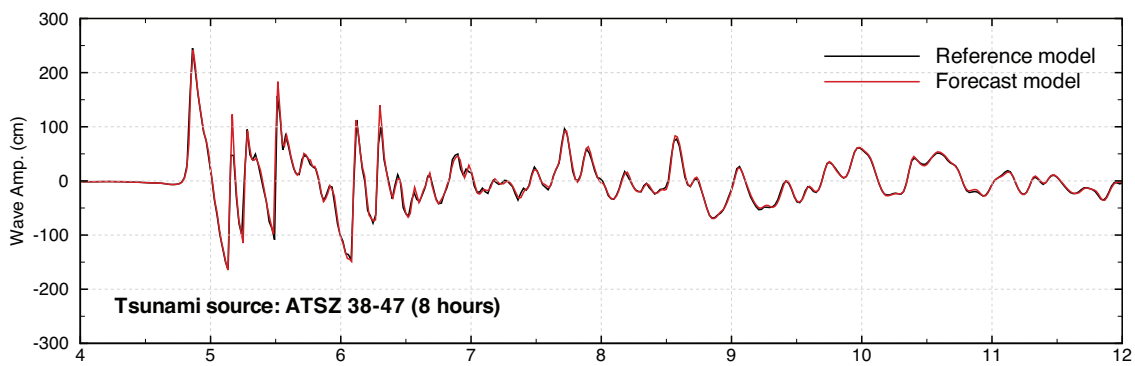

Figure 4. Computed time series at Atlantic City tide gage, for synthetic event ATSZ 38-47: (a) time series computed in the forecast system; (b) time series shown in the forecast model report.

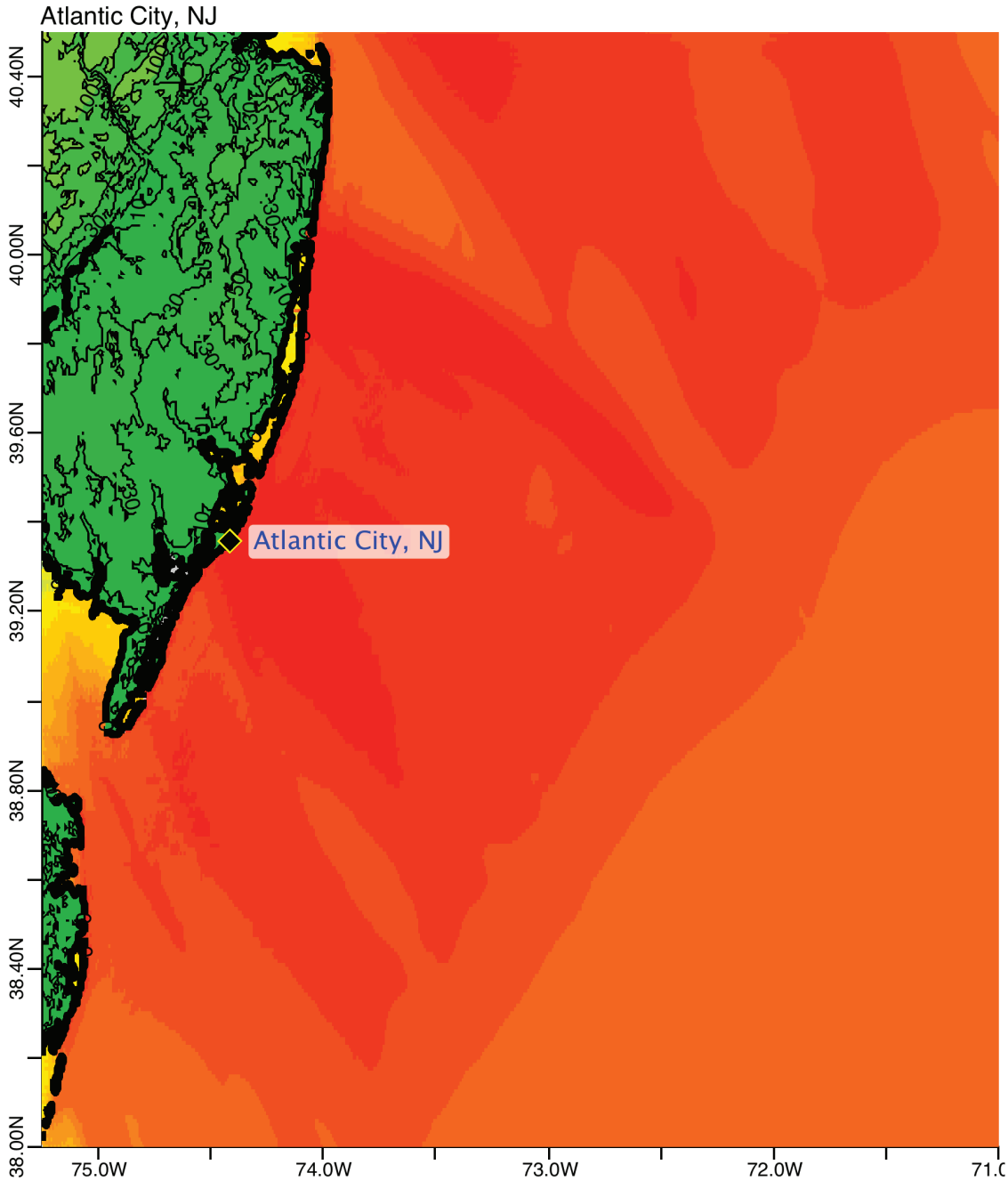

Figure 5. Max computed wave amplitude of A grid, Atlantic City, for synthetic event ATSZ 48-57.

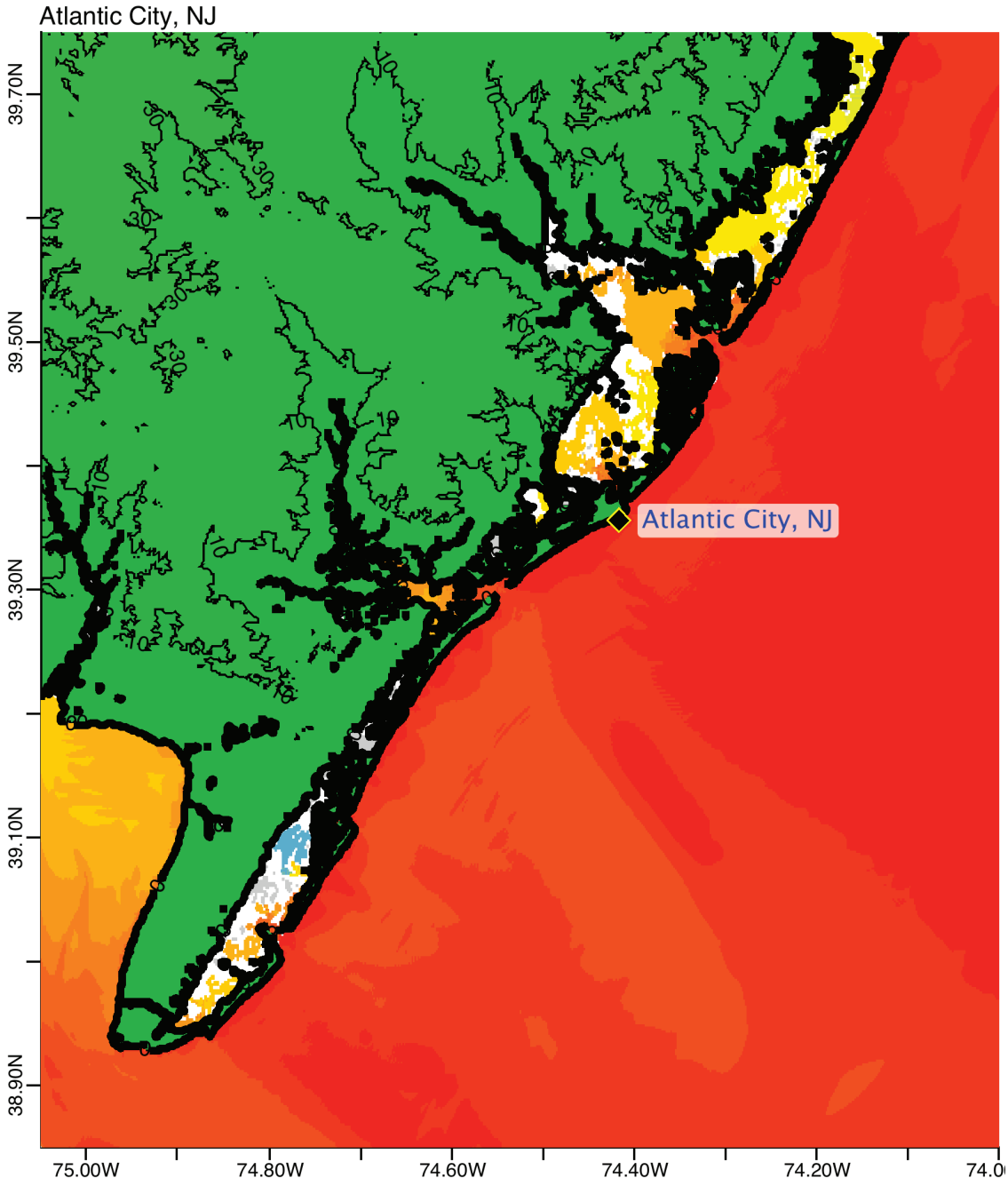

Figure 6. Max computed wave amplitude of B grid, Atlantic City, for synthetic event ATSZ 48-57.

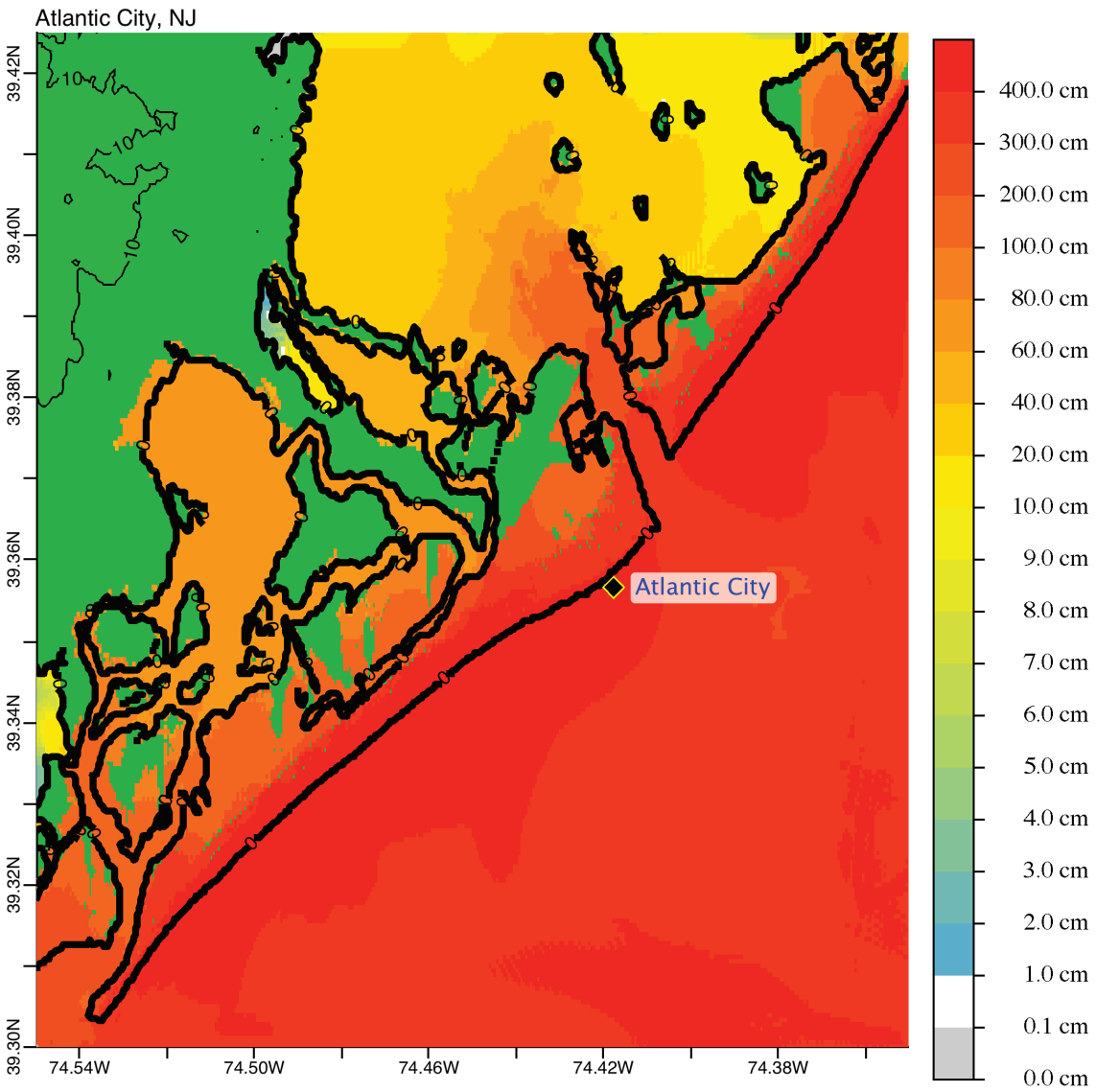

Figure 7. Max computed wave amplitude of C grid, Atlantic City, for synthetic event ATSZ 48-57.

(a)

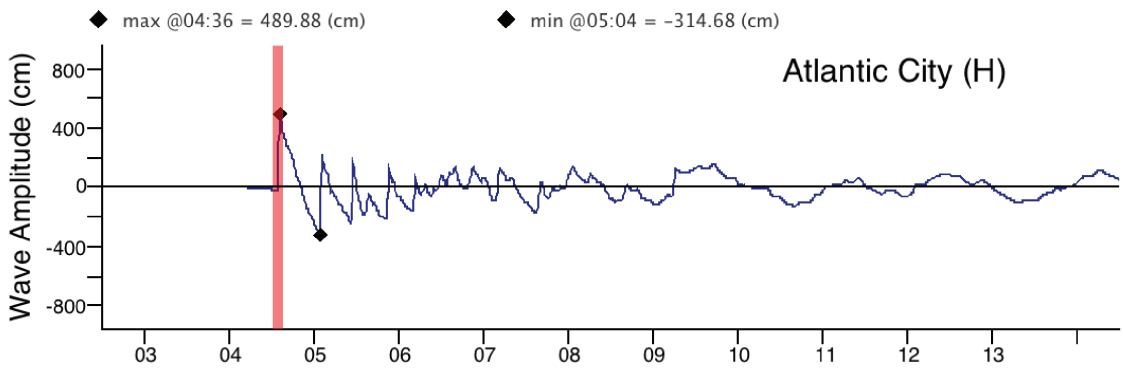

(b)

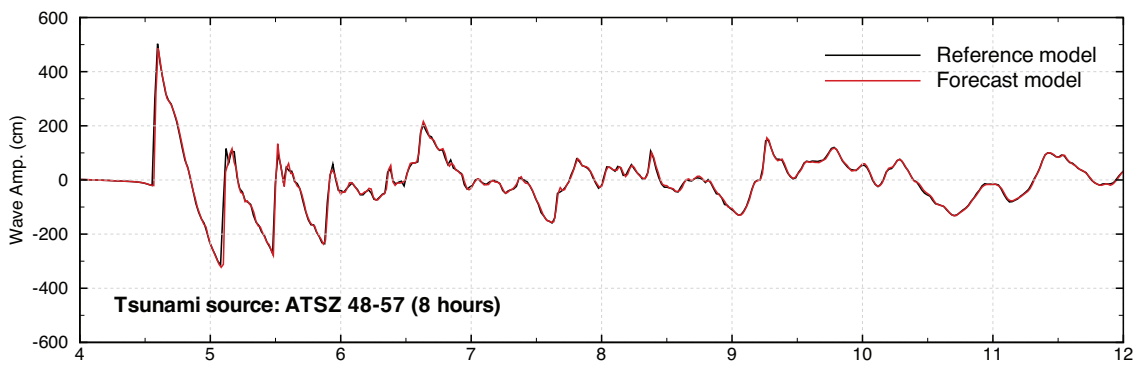

Figure 8. Computed time series at Atlantic City tide gage, for synthetic event ATSZ 48-57: (a) time series computed in the forecast system; (b) time series shown in the forecast model report.

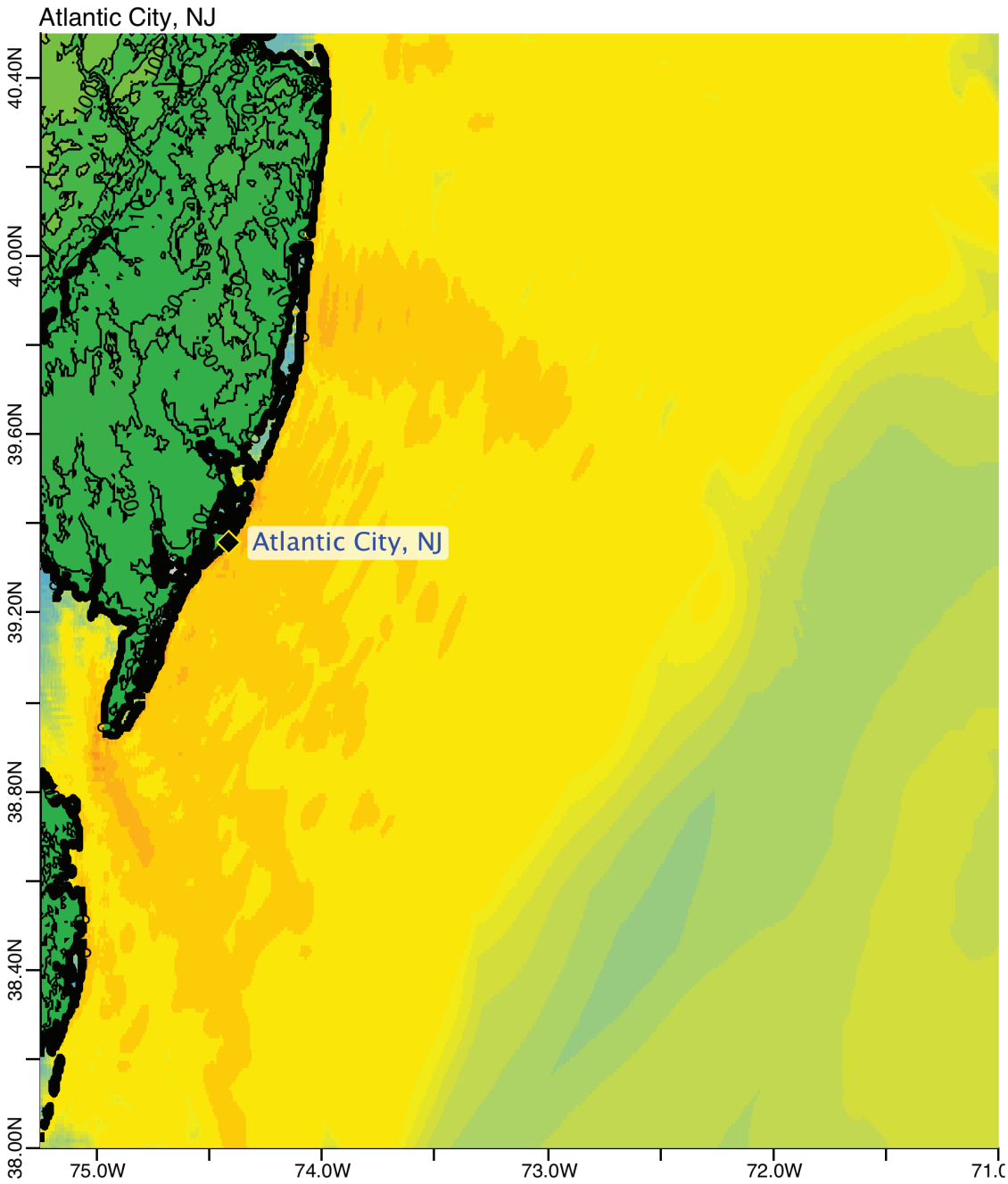

Figure 9. Max computed wave amplitude of A grid, Atlantic City, for synthetic event SSSZ 1-10.

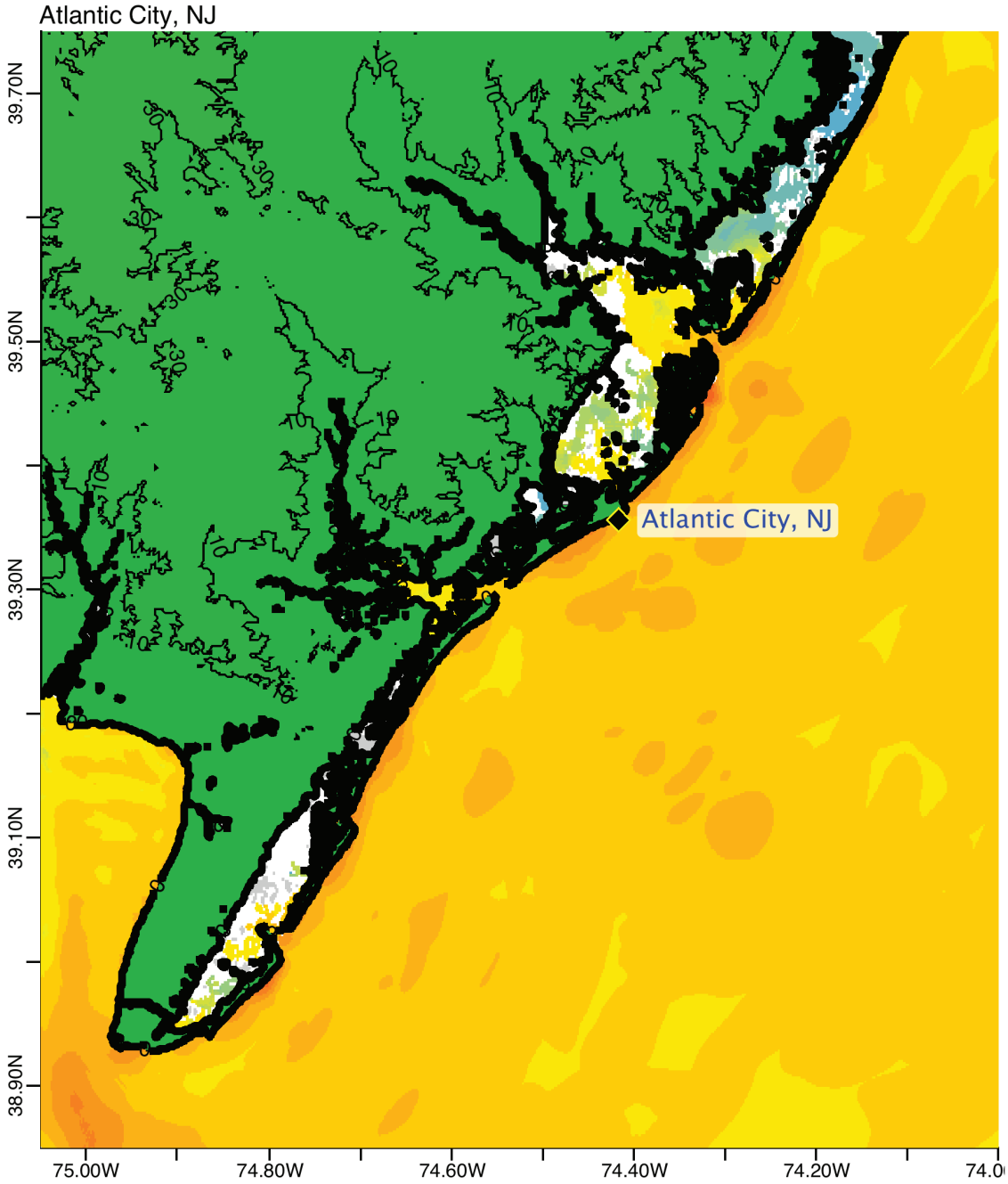

Figure 10. Max computed wave amplitude of B grid, Atlantic City, for synthetic event SSSZ 1-10.

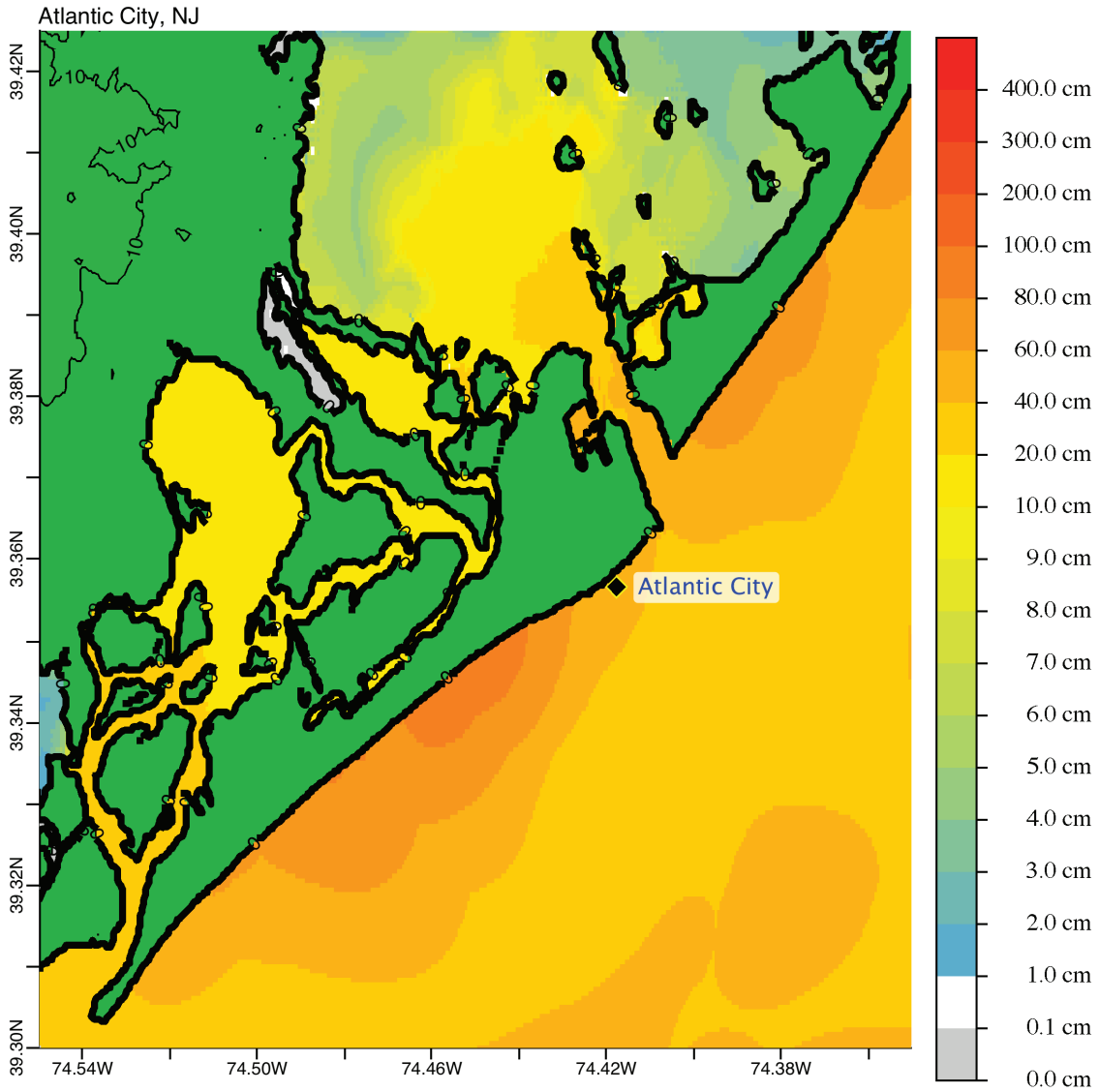

Figure 11. Max computed wave amplitude of C grid, Atlantic City, for synthetic event SSSZ 1-10.

(a)

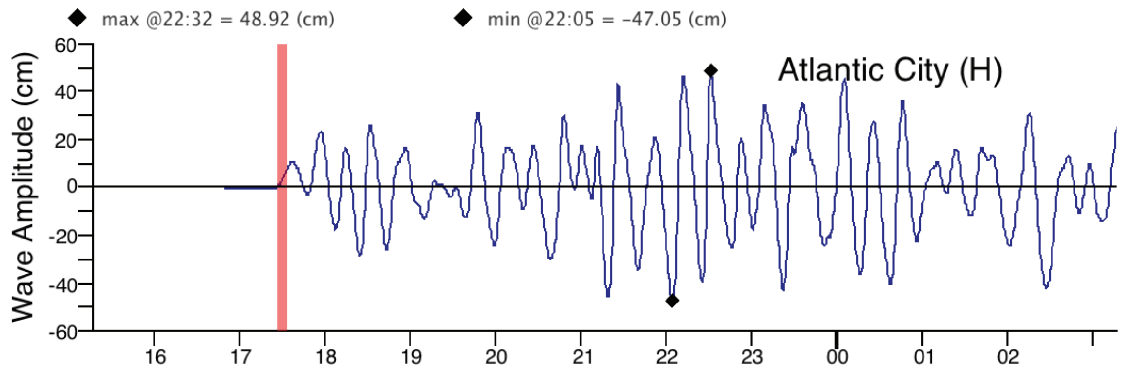

(b)

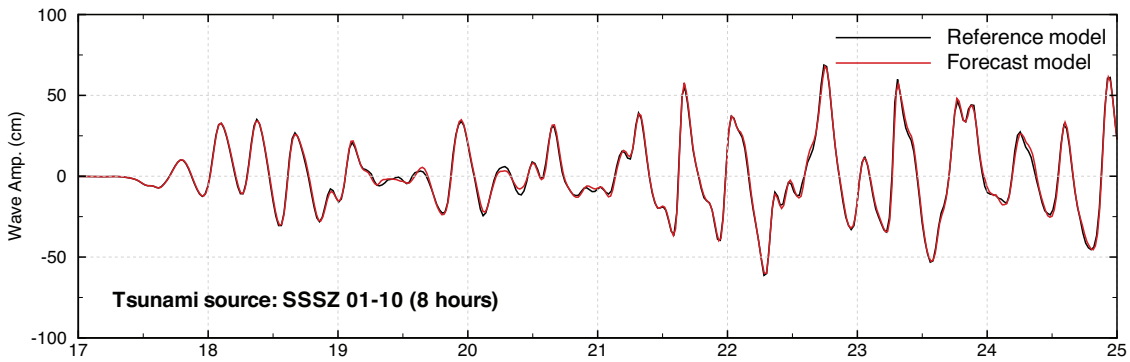

Figure 12. Computed time series at Atlantic City tide gage, for synthetic event SSSZ 1-10: (a) time series computed in the forecast system; (b) time series shown in the forecast model report.